Peer-reviewed version available at *Nanomaterials* **2018**, *8*, 945; doi:10.3390/nano8110945

Hybrid Nanocarbons Reinforced Rubber Nanocomposites: Detailed insights about Mechanical, Dynamical Mechanical Properties, Payne and Mullin Effects

Suneel Kumar Srivastava* (sunill1111954@yahoo.co.uk)

Inorganic Materials and Polymer Nanocomposite Laboratory, Department of Chemistry, Indian Institute of Technology, Kharagpur-72102, India

Yogendra Kumar Mishra* (ykm@tf.uni-kiel.de)

Functional Nanomaterials, Institute for Materials Science, Kiel University, Kaiserstr. D-24143, Kiel, Germany

ABSTRACT

The reinforcing ability of the fillers results in significant improvements in properties of polymer matrix at extremely low filler loadings compared to conventional fillers. In view of this, present review article describes the different methods used in preparation of different rubber nanocomposites reinforced with nanodimensional individual carbonaceous fillers, such as graphene, expanded graphite, single walled carbon nanotubes, multiwalled carbon nanotubes and graphite oxide, graphene oxide and hybrid fillers consisting combination of individual fillers. This is followed by review of mechanical properties (tensile strength, elongation at break, Young modulus, and fracture toughness) and dynamic mechanical properties (glass transition temperature, crystallization temperature, melting point) of these rubber nanocomposites. Finally, Payne and Mullin Effects have also been reviewed in rubber filled with different carbon based nanofillers.

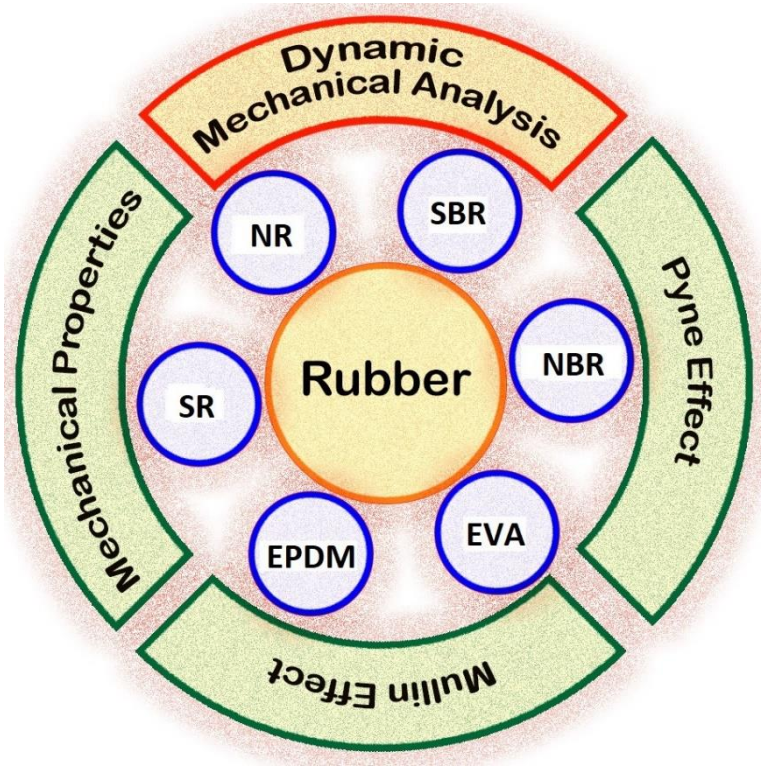

Keywords: Rubber nanocomposites, Mechanical properties, Dynamical mechanical properties, Payne effect, Mullin effect.

Peer-reviewed version available at Nanomaterials 2018, 8, 945; doi:10.3390/nano8110945

1. Introduction

Recently, one-dimensional (1D) carbon nanotubes (CNTs) and two-dimensional (2D) graphite oxide and graphene constitute proven graphitic materials receiving considerable attention[1–10]. This is mainly attributed to their outstanding properties, such as larger surface area, excellent thermal, mechanical, electrical and optical properties. In spite of their identical chemical composition, graphene exhibit added advantage due to the abundant availability of graphite as a naturally occurring precursor and its production cost compared to CNTs. These graphitic materials find applications in the field of sensors, batteries, solar cells, actuators, supercapacitors, catalysis, organic light-emitting diodes, field emission transistors, and optical/electrochemical devices, etc. Recent study has shown that these graphitic materials can be successfully used as effective nanofillers in polymer even at very small loadings in order to significantly improve properties of polymers. However, agglomeration remains one of the most common problems with CNTs as well as graphene due to the presence of inter-tubular interaction and restacking of graphene sheets, respectively. In addition, their poor dispersion in many common organic solvents as well as in polymer matrices remains another issue. Such restacking tendency of these graphitic fillers could be overcome through their surface leading to better dispersion of filler and polymer through strong filler filler-polymer interaction. Graphite oxide[5,11] and carbon nanofibre[7] are other carbon material investigated in development of polymer nanocomposites. Recently, (3D) materials obtained by the hybridization of 1D and 2D graphene have also been employed as hybrid fillers due to enhanced dispersion compared to the dispersion problem faced by the individual fillers in polymers[12,13].

Elastomers, according to the general IUPAC definition, are polymers that exhibit rubber-like elasticity. They find extensive applications in a variety of commercial as well as domestic

products[14-19]. The most common examples of these elastomers are natural rubber (NR). In addition, other important rubbers include silicone rubber (SR), styrene butadiene rubber (SBR), acrylonitrile butadiene rubber (NBR), butyl rubber (BR), ethylene vinyl acetate copolymer (EVA) and ethylene propylene diene rubber (EPDM) etc. Among these, different rubber types available, NR is largest single type produced from latex, whereas others are synthetic polymers manufactured either to replace or to be used together with NR or to make polymers with properties superior of NR. The high deformability (viscoelastic behavior) of these elastomers remained one of most desirable properties for their industrial applications. However, their low elastic modulus and durability makes it mandatory to use of carbon black (CB), clay, graphite and silica etc. as fillers. The unique properties of the composites with carbon nanofillers are probably in rubber industry and essentially in modern tire technology. In view of this, these carbon containing fillers has been receiving considerable amount of attention as filers in rubber nanocomposites due to their superior properties. Considering all these aspects, present chapter review mechanical properties, dynamical mechanical properties, Payne and Mullin Effects effect of NR, SBR, NBR, EPDM, and EVA rubbers filled with graphitic fillers anticipating their superior applications in multifaceted fields. [20-209]**.**

Preparation and Methodology of Rubber Nanocomposites

Rubber nanocomposites have been invariably prepared by solution blending and melt blending. The solution blending method of preparation is not eco-friendly and cost-effective due to the use of excess amount of organic solvents. On the contrary, melt-mixing of polymer with nanofiller is the most effective way to obtain the nanocomposites for commercial application. The method is totally environmentally friendly and does not require solvent. Any kind of polymers such as

thermoplastic or thermosetting can be used to prepare nanocomposites by these techniques. **Table 1-4** records the carbon-based fillers, methodology and morphology for NR, SBR, NBR and SR rubber nanocomposites.

3. Mechanical Properties of Rubber Nanocomposites of Carbon based Fillers

The performance of a composite generally depends on the various filler parameters including geometry, stiffness and orientation. In addition, dispersion of CNT, CNF, graphite oxide, graphene within the rubber matrix account for enhanced properties of rubber. The effect of carbon based nanofiller incorporated rubber nanocomposites are described as below:

3.1 Mechanical Properties of Carbon Filler incorporated NR and its Blend Nanocomposites

NR is an important unsaturated elastomer and a polymer of isoprene. It possesses high strength, high tear resistance, low heat build-up, high resilience, and retention of strength at elevated temperature, excellent dynamic properties and general fatigue resistance. It demonstrated excellent chemical and physical properties including high elasticity and flexibility, corrosion resistance, antivirus permeation and biodegradability and biodegradability[14]. NR finds extensive applications either alone or in combination with other materials in the transportation (e.g. tyres), industrial (sealants), consumer (sports materials), hygienic and medical sectors. Despite its extreme flexibility and stretchable properties, it is subject to weathering and has a poor resistance to heat oil and ozone despite being generally waterproof. Therefore, it is anticipated that carbon nanofillers and their nanohybrids reinforced NR and NR blend nanocomposites could find better applications in tires, adhesives, surgical gloves and sealing materials etc. due to their superior properties.

Peer-reviewed version available at *Nanomaterials* **2018**, *8*, 945; doi:10.3390/nano8110945

Mechanical properties of different carbon filler based natural rubber nanocomposites has been studied by many workers[20-63,168-189, 203-205]. Tarawneh and others[22] investigated the mechanical properties of thermoplastic natural rubber (TPNR) nanocomposites reinforced by MWCNTs which showed that 3 wt% of MWCNTs loading in TPNR resulted in increase of ~ 39% and 30% in tensile strength and Young's modulus respectively. Also, it was noted that elongation at break decreased with increase in the percentage of MWCNTs. The maximum impact strength was recorded at 5 wt% of MWCNTs which was increased by 74% as compared with a pristine TPNR. Thomas *et al.*,[23] reported stress–strain curves for pure NR and NR/MWCNT composites as shown in **Figure** 1. It is noted that NR exhibits a large increase in stress at higher deformations due to strain-induced crystallization, whereas, the strain at rupture is reduced for its MWCNT composites. The corresponding mechanical data of NR/MWCNT nanocomposites shows increase in Young's modulus of NR (~0.50 MPa) with MWCNT loadings. It was found to attain highest value of ~1.10 MPa at 5 wt% of maximum MWCNT loading. This is attributed to the anisometry of the filler structures, its nucleating effect, and dispersion of filler and polymer-filler interactions. They also observed maximum improvement in tensile strength at around 1 wt% loading of MWCNT in NR, whereas, elongation at break showed no improvement on MWCNT loading in NR. Tarawnch *et al.*,[24] studied effect of sonication on the mechanical properties of TPNR nanocomposites reinforced by 1 wt % of MWCNT. The Young's modulus, tensile strength, elongation at break and impact strength increased by almost 11%, 21%, 43% and 50%, respectively as compared with a pristine due to good dispersion achieved after optimal sonication time of 1 hour.

Nakaramontri *et al.*,[26] used *ex-situ* and *in-situ* surface functionalized MWCNT as filler in NR and study their mechanical properties. **Table 5** shows the tensile strength, elongation at break and 100% modulus data of NR gums and MWCNT composites of melt and latex-based samples. Addition of CNTs resulted in an increase of 100% modulus and a decreasing elongation at break due to reinforcement effect of MWCNTs. Tensile strength decreased on adding either raw MWCNTs or *ex-situ* functionalized MWCNTs to the NR. In contrast, *in-situ* functionalization exhibited higher tensile strength compared to neat rubbers. Elongation at break values of NR composites filled with raw or ex situ-functionalized MWCNTs were found to be lower than unfilled rubbers. **Table 5** also revealed the superior tensile tests performance of composites prepared by in situ method. Ali *et al.*,[27] studied mechanical properties of polylactic acid (PLA)/liquid natural rubber (LNR) filled with MWCNT prepared by melt blending method. This result has shown that PLA/LNR nanocomposite filled with 3.5 wt % of MWCNTs exhibited 22 and 20 % higher tensile strength and Young's modulus respectively. Such improvements could be directed to good dispersion of MWCNTs inside the PLA/LNR matrix. Their study also indicated that elongation at break of PLA/LNR with MWCNTs decreased with increasing amount of MWCNTs indicating its flexibility. The impact strength also increased to ~42% in PLA/LNR/MWCNTs (3.5 wt%) due to the better dispersion of MWCNTs in the matrix generating significant toughening effect. Anoop *et al.*,[30] observed significantly improved mechanical properties in NR/SWCNTs nanocomposites prepared through a latex stage mixing method. NR/SWNTs (2.0 phr) in relation to pure NR containing SWCNTs showed tensile strength and modulus higher by 56% and 63% respectively. The modulus at 100% and 300% and tensile strength of vulcanizates at loadings up to 15 phr were unaffected by sample prepared by the ultrasonic method[31]. Kueseng and Jacob [33] also studied mechanical properties of single-

walled carbon nanotubes (SWCNT) filled NR nanocomposites prepared by solvent method. The corresponding mechanical test results show an increase in the initial modulus for up to 50% in relation to pure NR. Young's Modulus also increased with increasing SWCNT contents. Tarawneh *et al.*,[38] also determined the optimum mechanical properties of different percentages of MWCNTs-OMMT (1%wt MWCNTs+3%wt OMMT, 2%wt MWCNTs+2%wt OMMT and 3%wt MWCNTs+1% wt OMMT) hybrid filled TPNR nanocomposites. These findings showed increase in tensile strength and Young's modulus in the presence of nanotubes and maximum value were obtained for the nanocomposites with highest nanotubes (3%wt) which increased about 33% and 36%, respectively compared with pure TPNR matrix. Such significant improvement in these mechanical properties was assigned to interfacial adhesion between fillers and the matrix due to aspect ratio and fillers orientation in the TPNR matrix. In contrast, elongation at break considerably decreased with increasing the percentage of MWCNTs.

Mechanical property of melt blended ENR/MWCNT and the ENR/MWCNT modified by bis(triethoxysilylpropyl) tetrasulfide (TESPT) composites exhibit improved tensile properties and modulus than pristine ENR[41]. Azira *et al.*,[42] prepared MWCNT/ENR nanocomposite through latex technology and observed considerable increase in its mechanical comparison to either neat ENR and its CB filled ENR composite. Natural rubber composites with different contents of 1, 3, 10, and 20 wt% vapor-grown carbon nanofibers (VGCFs) were synthesized using a solvent casting method[43]. Their mechanical property investigations showed NR/3 wt% VGCF composite had the greatest tensile strength. The stress–strain curves of NR/TRG composites clearly indicate that there is a dramatic improvement (282%) in modulus at low loading (3% wt./wt.) of TRG [203].

Hybrid nanomaterials, such as MWCNT/Silica,[20] MWCNT/CB,[32,35,54], CNT-clay,[38] CNT-Graphene[39] have also been used in reinforcing of natural rubbers. Fritzsche *et al.*,[20] incorporated MWCNTs in highly silica filled NR by applying melt mixing techniques. To distinguish between properties based on silica and MWCNT, the amount of silica has been successively exchanged by the same amount of MWCNTs upto 10 phr of MWCNT. The resulting samples show an increased mechanical stiffness and tensile strength. The tensile strength increases from 14 to 17 MPa when part of the silica is exchanged by 10 phr of MWCNT, though the elongation at break is successively reduced. Stress–strain behavior of NR composites with silica and CNT (dry mixing) showed mechanical reinforcement of the CNT/silica hybrid system at strains below 100% mainly results from the CNT[24]. Xu *et al.*,[32] prepared NR/MWCNTs (1-5 phr) master batch by latex compounding assisted by anionic surfactants containing phenyl ring moieties and co-coagulated process and measured their mechanical properties. It is noted that tensile strength, stress at 300 % strain and tear strength of NR/CB/MWCNTs and composite with 4 phr MWNTs loading were increased by 12.36, 26.02 and 16.95 %, respectively. Such improvement in mechanical properties is ascribed to the homogenous dispersion of MWNTs, interfacial adhesion between MWNTs and NR polymer chains. Alternatively, possibility synergistic reinforcing effect of CB and MWNTs in NR matrix also cannot be ruled out. Dong and others[35] studied mechanical properties of natural rubber composites reinforced with hybrid fillers consisting of carbon nanotube bundles (CNTB)/CB (0/25,1/22,3/16,5/10 phr) and findings are displayed in **Table 6**. It is noted that CNTB)/CB(5/10 phr) hybrid filled NR composite showed remarkable increments in the stress at 100 and 300% corresponding to 64% and 57% increase in stress compared to neat natural rubber. The tensile strength and tear strength were also improved indicating an enhanced fracture resistance with increasing content of CNTBs. They ascribed such

Peer-reviewed version available at *Nanomaterials* **2018**, *8*, 945; doi:10.3390/nano8110945

reinforcement of the CNTBs its high aspect ratio and surface area. In another study, stress-strain plots of NR filled with hybrid consisting of MWCNT (2 phr) and expanded (0-20 phr) organically modified montmorillonite (EOMt) were studied as shown in **Figure** 2[44]. They noted significant improvement of the tensile modulus for all nanocomposites due to the strong interaction of MWCNT with the elastomeric matrix. Further, tensile strength attained maximum improvements in NR/MWCNT-2 phr (25.84 MPa) compared to that of neat NR (22.38 MPa). The addition of EOMt further increases tensile strengths of NR/MWCNT-2 phr/EOMT-16 phr (31.15 MPa) followed by a slight decrease in NR/MWCNT-2phr/20phr-/EOMT nanocomposite (29.12 MPa). Further, the nanocomposites consisting 16 and 20 phr/EOMt exhibit not only higher modulus but also a slightly higher elongation at break (EB). Ismail *et al.*,[34] studied effects of SiO_2/MWCNT hybrid filler (total loading fixed at 30 phr) on the mechanical properties of NR nanocomposites and findings are displayed in **Figure 3** (a,b). It is seen that silica/MWCNT hybrid loading (29/1) exhibits highest tensile strength and EB due to the good dispersion and lower agglomeration of both fillers. However, tensile strength and EB decrease at further higher MWCNT loading ratio due to poor filler- rubber interaction in the silica/MWCNT hybrid. This study also indicated steady increase in both M100 and M300 with MWCNT loading ratio increased in the silica/MWCNT hybrid. Such observation indicated that the addition of MWCNTs improved the stiffness of the nanocomposites. Tensile properties of ENR-CNT composites prepared by in situ functionalization with various APTES silane concentrations were investigated[40]. **Figure 4** show stress–strain curves of ENR vulcanizate and ENR-CNT composites without and with APTES at concentrations from 0.06 to 0.01 mL/(g of CNTs). It is clearly seen that Young's and the tensile strength rapidly increased with the addition of CNTs in the ENR matrix. This is due to the chemical interactions

Peer-reviewed version available at Nanomaterials 2018, 8, 945; doi:10.3390/nano8110945

of polar functional groups in ENR with the CNT surfaces. In contrast, the tensile strengths of the ENR-CNT composites with APTES were lower than without APTES.

Wipatkrut and Poompradub[177] studied effect of graphite oxide reduced by L-ascorbic acid in NR on the mechanical properties of resulting composites. It was noted that tensile strength and hardness were comparable with those of conductive carbon black filled NR.NR/PVP (5 phr) nanocomposites exhibited enhanced mechanical properties: tensile strength (81 %), tear strength (159 %) compared with pristine NR[178]. The enhanced mechanical properties were also achieved in NR/GO,[83–85] NR/TRGO (thermally reduced graphite oxide)[182,183]. Yan *et al.*,[184] reported that tensile strength and tensile modulus at 300% strain of NR/HDPE/GO (1.5 phr) compared to neat blend were increased by ~ 27% and ~ 24%, respectively. The effects of GO content on the mechanical properties) of NR-g-GMA/GO nanocomposites were investigated[185]. The tensile strength and tear strength of the 3 phr GO loaded in NR-g-GMA with showed maximum improvements compared with NR/GO nanocomposites. Wu *et al.*,[186] reported that maleic anhydride grafted liquid polybutadiene functionalized graphene oxide (MLPB-GO) filled NR composites prepared by co-coagulation process composites are obviously superior to those of NR/GO composites and neat NR. They found that tensile strength, modulus at 300% strain and tear strength of NR composite containing 2.12 phr MLPB-GO compared with neat NR are increased by 40.5%, 109.1% and 85.0% respectively. The significant reinforcement of MLPB-GO in NR is ascribed to the good dispersion of GO and the strong interface interaction in the composites.

Graphene has also been used as reinforcing filler in natural rubber as evident from its mechanical properties[5,33,34,48,49]. Galimberti *et al.*,[36] recorded nominal stress–nominal strain curves on nanocomposites of synthetic poly(1,4-cis-isoprene) filled with organoclay, CB, MWCNT and graphene. They concluded that elongation at break of MWCNT filled nanocomposites superior in graphene filled NR compared to other composites. Recently, investigations related to mechanical properties of the unfilled NR, graphene filled NR, CNT filled NR and NR/MWCNT/graphene has been made[39]. It is observed that 0.5 phr graphene filled NR remarkably increases the tensile strength of NR compared to unfilled NR (17.8 MPa). Interestingly, hybridizing MWCNTs with graphene contributed significant reinforcement effect in NR.

Thomas *et al.*, [62] studied effect of phenol functionalization of carbon nanotubes on properties of natural rubber nanocomposites on stress–strain behavior as displayed in **Figure 5.** It is noted that tensile strength of the composites increases on incorporating of 1 phr of CNT, while higher loading of CNT causes a decrease in tensile strength. Incorporation of CNT causes an increase in Young's modulus of the composites at all loadings, while the elongation at break decreases at higher filler loadings. When CNT is functionalized with phenol and used as filler in NR, increase in modulus is observed at at all loadings. Further, it is noted that tensile strength attains a maximum value at a 5 phr loading and beyond which it decreases, while the elongation at break shows a gradual decrease with increase in CNT loading. The tensile strength, modulus at 300%, and tear strength for NR composites containing 0.9 phr of reduced graphene compared to NR increased by 50.2%, 154.9% and 65.2%, respectively[187]. The incorporation of ZnO nanoparticles doped graphene (5 phr) in NR matrix showed significantly improved mechanical properties over that of NR composite filled with of conventional-ZnO[188]. The incorporation of 0.5 phr of graphene in NR were used

Peer-reviewed version available at *Nanomaterials* **2018**, *8*, 945; doi:10.3390/nano8110945

to prepare corresponding nanocomposites by a modified latex mixing method combined with in situ chemical reduction[189]. The 48% increase in the tensile strength and an 80% increase in the initial tensile modulus are achieved without sacrificing the ultimate strain. But further increasing the GE loading degrades the tensile strength and the ultimate strain.

3.2 Mechanical Properties of Carbon Filler incorporated SBR and its Blend Nanocomposites

SBR exhibit better processability, heat aging and abrasion resistance but is inferior in terms of elongation, hot tear strength, hysteresis, resilience and tensile strength. NBR is widely used due to great oil resistance, heat and plasticizer, and low gas permeability, high shear strength. The varying ratio of nitrile within the polymer can change these characteristics. The addition of carbon containing fillers could enhance processability and mechanical and many `other properties of SBR[64-90,190-194, 206,207].

The composite of SBR loaded with ionic modified MWCNT (10 phr) exhibited impressive enhancements in tensile strength (381% increase) and hardness (34% increase as outcome of the extremely fine dispersion[63]. Falco *et al.*,[66] recorded stress–strain curves at room temperature for SBR compound, SBR/CB composite and SBR/MWCNT composite. It is inferred that nanotubes in the SBR matrix showed remarkable improvement in the tensile strength and strain to failure compared with the sample of SBR/carbon black composite. The higher aspect ratio of MWCNT and better interface between the two phases composites accounted for such improvements in SBR/MWCNT. Girun and others[67] attempted in increasing mechanical properties of SBR/MWCNT (1 to 10 wt%) nanocomposites fabricated by solvent casting method. Their findings showed that Young's modulus of 1 and 10 wt% filled CNTs in SBR compared to SBR without CNTs increased by ~10 and 200 % respectively. The spray drying method followed

Peer-reviewed version available at *Nanomaterials* **2018**, *8*, 945; doi:10.3390/nano8110945

by subsequent mechanical mixing has been used to prepare styrene-butadiene rubber/carbon nanotubes nanocomposites and study their mechanical properties[68]. In compared to pure SBR composites, mechanical properties such as tensile strength, tear strength and hardness of the composites filled with CNTs at certain contents were dramatically improved almost by 600%, 250% and 70%, respectively. Tensile strength of SBR also increased by 21 to 70 % for the corresponding CNT contents. Peddini *et al.*,[69] used master batches of discreet well-dispersed MWCNTs in a SBR matrix using and subsequently, it was diluted it with SBR to prepare sample containing lower MWCNT (1 to 12.3 wt. %) loadings and studied its tensile stress-strain behavior. **Figure** 6 (a,b) show variation of tensile stress at break and elongation at break as a function of MWCNT loading in SBR. It is noted that tensile stress at break increases with increasing MWCNT loading up to 10 wt. % and then decrease at higher loadings. This increase reflects the reinforcing effect of filler with high modulus and strength and good SBR-MWCNT surface bonding between the MWCNT and SBR. A change in response of the elongation at break around 6-8 wt. % is also evident. The average elongation at break values for the composites are very close to that of SBR (~450%) up to the loading level of the proposed threshold. It is remarkable to see essentially no decrease in elongation at break with addition of MWCNT below this threshold. The high elongation at break could be ascribed to a strong interfacial bonding between SBR and tube surface. Alternatively, possibility straightening of the curved or coiled tubes in the stretch direction along with the matrix as schematically shown in **Figure 7**(a b) also cannot be ruled out. At higher MWCNT loadings, the elongation at break shows a modest decrease. These workers also investigated mechanical properties of SBS/CB and compared with SBR/MWCNTs composites of similar compositions composites. The corresponding Young's Modulus data at 100%, 200% and 300% of deformation for these composites[70]. This study revealed no significant influence of CB

on SBR on the Young's Modulus in contrast to SBR/MWCNT composites. On the other hand, increase in MWCNT content causes a significant increase, mainly at higher strain levels. MWCNT act as reinforcement agents, however this effect does not comprise the strain capability of the elastomer, resulting in materials with higher tenacity in comparison with SBS. Atieh[71] employed MWCNTs functionalized with carboxylic group disperse it homogeneously in SBR in an attempt to enhance the mechanical properties of these resulting nanocomposites. It was seen that Young's Modulus of the rubber nanocomposites at 10 wt% of MWCNTs loading is ~6 times higher than SBR. Further, tensile strength of nanocomposites also increased due to the compatibility between MWCNTs and SBR. They also extended their work and used amine functionalized MWCNTs to evaluate the extent of reinforcement[72]. The tensile strength of the SBR/functionalized MWCNT (10 wt%) rubber nanocomposites is found to be ~ 2 (181%) times that of pure SBR. This is ascribed to well-dispersed MWCNT and a good interface between the MWCNT and SBR matrix. An increase of 175% in Young's modulus was observed in 10% loaded filer in SBR nanocomposite.

Laoui[74] investigated effect of reinforcing SBR with phenol functionalized carbon nanotubes on the mechanical properties of the resulting nanocomposite. It is noted that mechanical properties are substantially improves for the small filler loading. The higher increase in tensile strength is also observed at higher MWCNT loadings in SBR. Stress-strain curve also showed strength of the SBR/MWCNT (10 wt%) almost three times (282 %) than that of pure SBR, while the strain is decreased from 21 to 7 due to dispersed of CNTs and a good interfacial bond between the functionalized CNT and SBR matrix. It is also noted that Young modulus increases by 40 % and 240 % corresponding to 1 and 10wt% of functionalized MWCNT. Das and others[78] used mixing method to incorporate MWCNTs in a rubber blend in a 50:50 blend of solution-styrene–butadiene

rubber and butadiene rubber. It is noted that stress increases with the incorporation of the CNTs with a sharp rise of the initial modulus.

Schopp *et al.*,[79] prepared SBR nanocomposites containing different carbon-based fillers using an aqueous dispersion blend technique and carried out stress/strain tests of these SBR nanocomposites a displayed in **Figure 8**. The elongation at break and tensile strength for SBR/C (2, 5, 10, 25 phr) filler composites relative to neat SBR are displayed in **Figure 9**. It is noted that addition of all these carbon fillers affords higher tensile strength, which increases with increasing filler content. Carbon filler performance improves with the following filler ranking: Expanded graphite<Rubber carbon black<CNT<Multilayer Graphene<Chemically reduced graphite oxide <Thermally reduced graphite oxide. The highest tensile strength increases (240%) is found for SBR/25 phr TRGO. Among the carbon fillers, only the CRGO addition simultaneously increases elongation at break and tensile strength. **Figure 10** show stress at 50 and 300% strain of SBR/C based fillers as relative values compared to neat SBR. This clearly reveals that all fillers show increasing filler content in SBR increase tensile stress. It is noted highest stress at 300% strain is observed for SBR containing 25 phr CRGO (260%).Das and others[73] reported solution styrene butadiene rubber composites reinforced with EG, grapheme nanoplatelets and MWCNTs. It was concluded that SBR/MWCNT showed significant improvement in mechanical properties compared to other composites. The high aspect ratio of MWCNT enabled to form a network at low filler loading and, consequently, good reinforcement effect was observed.

The formation of hybrid fillers (MWCNT and EG) showed improvements in mechanical properties due to the synergistic effect. The hardness of SBR composites filled with graphene showed sharp

Peer-reviewed version available at *Nanomaterials* **2018**, *8*, 945; doi:10.3390/nano8110945

increase in hardness and 300%-modulus[77]. Bhowmick *et al.*,[81] filled SBR with modified and unmodified carbon nanofiber and expanded graphite. The comparison of mechanical properties of their nanocomposites compared to the gum on the basis of illustrates that carbon nanofiber increased the modulus by 101%, while tear strength increased by 79% at 6 phr loading. On modification, carbon nanofiber showed 150% increment in modulus and 113% in tensile strength of the nanocomposite, over the gum control. Xing *et al.*,[83] fabricated graphene/SBR nanocomposites by a modified latex compounding method and measured tensile strength and strain at break and strength at 300% strain. It is noted that 260% increase in the tensile strength and a 140% improvement in the strain at break are achieved even at the graphene loading as low as 0.3 phr. At 7 phr of GE in SBR, the tensile strength of the nanocomposite increased to ~11 times higher than that of SBR. At the same time, the strain at break of the nanocomposite remains the same as that of pure SBR. Expanded graphite and. modified expanded graphite filled SBR/BR nanocomposites were also styrene butadiene rubber investigated for mechanical properties[85].

Several other studies are reported on investigating mechanical properties of SBR filled with hybrid fillers. Organically functionalized MWCNTs (O-MWCNTs) showed improved mechanical properties of NR/SBR composites[55]. These findings showed that elongation at break of NR/SBR composites filled with 1.5 phr O-MWCNTs under optimized conditions, was found to be 450% compared to 376% for pristine NR/SBR composites. Nanocomposites based on NR/EPDM/MWCNT were prepared. in an internal and a two roll-mill mixer in two steps and effect of carbon nanotubes (MWCNTs) and mechanical properties of the vulcanized NR/EPDM/MWCNT nanocomposites[56].

Peer-reviewed version available at *Nanomaterials* **2018**, *8*, 945; doi:10.3390/nano8110945

Chen *et al.*,[190] used graphene oxide exhibiting various oxidation degrees and studied its reinforcing performance in SBR. Tensile strength and tear strength of SBR/GO nanocomposites increased by 271.3% and 112.3%, respectively compared with neat SBR. The tensile strength and tear strength of ionic liquid functionalized GO (GO-IL)/SBR nanocomposites with 5 phr of GO-IL increased by 505 and 362,%, respectively compared with neat SBR[191]. SBR/3D segregated graphene (IL-3DGE) dramatically enhanced its mechanical properties[192]. The incorporation of 1.66 vol% IL-3DGE significantly increased tensile strength by 516 % compared to neat SBR. The excellent properties of the composites were attributed to the strong interfacial interactions. GO has also been used as reinforcing filler in immiscible XNBR/SBR blends[193]. The incorporation of only 0.3 phr GO as a reinforcing filler significantly improved tensile strength (71%) and tear strength (94%) of XNBR/SBR blend. XNBR)/GO nanocomposites fabricated by aqueous phase mixing of GO colloidal dispersion with SBR latex and a small loading of XNBR latex, followed by coagulation were thoroughly investigated for mechanical properties[194]. The results showed enhancement in mechanical strength of nanocomposites with the increase of oxidation degree of GO. The tensile strength and tear strength. of SBR/XNBR/GO filled with 3 phr GO increased by 255.3% and 141.5% respectively compared to neat blend. The mechanical properties of the SBR filled with 5 phr of PVP modified graphene oxide (PGO) significantly improved 517 and 387 % increase in tensile strength and tear strength, respectively[206]. It was suggested that PVP molecules could have strong interaction with GO via hydrogen bond and account for this.

Zhang *et al.*,[87] reported tensile curves of SBR/CB and SBR/CB/RG composites fabricated via two-roll mill mixing and corresponding mechanical data is represented in **Table 7**. SBR/CB (100/10 and 100/13 phr) blends showed limited improvements on the tensile properties were

observed in contrast to SBR/CB/reduced grapheme (RG) (100/10/1, 100/10/2,100/2/3 phr composites exhibiting significant improvements. The moduli at 200% elongation (M200) of the SBR/CB-RG blends were found to be higher than those of the SBR/CB blends at no expense of elongation. The elongation at break-even increased from 260% to 300% when 1 phr of RG was applied compared to the SBR/CB blend filled with 10 phr CB. The tensile strength of the blends was enhanced from 3.5 to 4.9 MPa, increased as much as 40% after addition of 1 phr RG. The enhancement of the tensile properties after the application of CB-RG hybrid filler compared to single CB filler can be attributed to the better reinforcement effect of RG on SBR matrix. At higher loadings of RG (2 and 3 phr), M200 of the SBR/CB-RG composites increased without pronounced improvements on tensile strength and elongation at break. In another study, introduction of thermally reduced graphene (0.25 phr) to SBR/MWCNT (1 phr) increased tensile strength of the resulting composites by 49.5% compared to SBR/MWCNT (1 phr)[88]. Such improvement in mechanical and properties was ascribed to the synergistic dispersion between thermally reduced graphene and MWCNTs and the strong interfacial interaction between the hybrid fillers and the rubber matrix. However, further addition of thermally reduced graphene (0.5 phr) reduced the tensile strength of the SBR/MWCNT/composites due to the formation of agglomeration of graphene. Tang *et al.*,[89] used continuous 3D hybrid (HG) consisting of halloysite tubular clay, HNT (referred as H) and tannic acid functionalized graphene, TAG (referred as G) as reinforcing filler in SBR and studied their mechanical properties. It is noted that HG ternary composites exhibit relatively much larger modulus, tensile strength and tear strength compared to SBR-H and SBR-G binary composites. This is in all probability due to extraordinary synergistic effects of halloysite tubular clay and functionalized graphene. The combination of hydroxyl-functionalized exfoliated montmorillonite (Fe-MMT) and cetyltrimethylammoniumbromide-modified MWNT hybrids has

Peer-reviewed version available at Nanomaterials 2018, 8, 945; doi:10.3390/nano8110945

been used to prepare SBR composites by solution method[90]. A remarkable improvement in modulus and tensile strength at low loadings were observed due to homogenous dispersion of the hybrid nanofillers in the SBR matrix. Bhuyan *et al.*,[207] measured mechanical properties of MWCNT/hectorite hybrid (HMH) hybrid filler reinforced styrene SBR. These findings show significant improvement in tensile strength (210%) and elongation at break (42%) of SBR/HMH nanocomposite at 0.7 wt.% HMH. Such superior reinforcing of hybrid filler compared to individual fillers is ascribed to synergistic effect. Alternatively, extraordinary improvement in mechanical properties at such low filler contents could also be attributed to the enhanced level of MWCNTs dispersion in SBR matrix due to the simultaneous presence of hectorite layers.

3.3 Mechanical Properties of Carbon Filler incorporated NBR and its Blend Nanocomposites

NBR is high resistance to hydrocarbon oil required in fuel hoses, o-rings, gaskets, and industrial rolls. However, it is susceptible to ultraviolet light and ozone attack and has been overcome by hydrogenating to HNBR[17]. These are high performance rubbers exhibit excellent abrasion/ adhesion resistance and superior mechanical properties for their widely range applications. NBR is not crystallizable under high strain, and therefore the reinforcing fillers are generally incorporated to yield sufficiently high mechanical properties[91-114,192-196]. Chougule and Giese[93] reported significant mechanical reinforcing effects of CNT compared with CB in NBR due to good dispersion and effective interaction. Influence of ACN content on the mechanical properties of NBR/MWCNT nanocomposites has been investigated[95]. The lower volume fraction of MWCNTs produced significant increase in tensile strength and energy at break compared with carbon black due to high degree of dispersion. In another work, mechanical properties of nitrile rubber) reinforced with 0 to 15 phr of MWCNT, conductive (CB, CB), and

precipitated silica prepared by two roll mill method and corresponding data recorded in **Table 8**[97]. It is clearly seen that tensile strength, modulus (100 %) and hardness enhanced with increasing with loading of filler. Interestingly, MWCNT gives the highest level of reinforcement compared to other conventional reinforcing fillers. However, except for the MWCNT filled system, the elongation at break appears to increase with increasing filler loading. Such increase is believed to be due to the slippage of un-cross-linked rubber molecules around filler particles which increases the specimen volume under high extension. Compared to the unfilled system, the abrasion loss of the filled systems deceased and heat buildup values decrease with increasing filler loading, Ryu *et al.*,[98] studied stress-strain curves of NBR (matrix) and its composites filled with CNT and CB. This study showed that tensile strength and modulus increase with an increase of CNT content compared with the matrix and rubbers. Tensile strength and modulus of the composite on adding 9 phr of CNT increased to 31% and 91%, respectively. Likozar and Blaz[100] investigated effects of acrylonitrile content on both properties of NBR. **Figure 11** shows typical tensile stress–strain curves of the vulcanizates (NBR and HNBR of 0.0–39.0 wt% of acrylonitrile content) filled with 30 phr of MWCNT. It was concluded that, tensile strength of HNBR nanocomposites increases substantially with acrylonitrile content in the range 21.0–36.2 wt%. Also, the stress at small strain (under 20%) increases more remarkably with increasing acrylonitrile content, when compared to NBR/MWCNT composites. It is also inferred that HNBR/MWCNT (36.2 wt% AN content) nanocomposite exhibits highest tensile strength and elongation at break compared to those of other reinforced composites due to high aspect ratio and large surface areas of carbon nanotubes. MWCNTs (1, 3, and 5 wt %)-filled thermoplastic polyurethane–urea (TPU)/XNBR blend nanocomposites showed significantly improved mechanical properties compared to the neat blend[110]. It was seen concluded that 5 wt % CNTs filled XNBR:TPUU

blend the tensile modulus increased from 9.9 to 45 MPa, and the tensile strength at break was increased from 25 to 33 MPa. It was suggested that well-dispersed CNTs in the blend effectively absorb the applied stress and to improve the mechanical stiffness of the corresponding nanocomposite. Salehi and coworkers[107] observed that tensile strength, elongation at break, stress at different elongation and hardness of pure NBR are enhanced on adding MWCNT or silica as reinforcing fillers. Further, properties of the composites are further enhanced in presence of combination of silica and CNT fillers in NBR. Thus, tensile strength increases to 71% on adding 3 phr CNT to the NBR sample containing 25 phr silica compared to tensile strength value of the silica(25 phr) filled NBR due to synergistic effect.

NBR/EG (5,10phr) nanocomposites were prepared by mechanical blending (microcomposites) and latex compounding technique (nanocomposites) and compared their mechanical properties[101]. These findings reflected superior tensile properties at the same graphite loading of nanocomposites to that of micro-composites. This suggested that nano-size dispersed graphite can be dispersed more uniformly and reinforce rubber more effectively than micro-size graphite. Liu and coworkers [102] investigated variation of tensile strength and elongation at break with EG content in the NBR/EG nanocomposites. It was noted that tensile strength increased by 78%for those nanocomposites containing only 5 phr expanded graphite. They believed nanoscale dispersion of the EG nano sheets within NBR matrix account for such enhancement. The drop in tensile strength of the composites at next higher loadings was probably due to the aggregation of the EG. The elongation at break decreased only slightly with increasing EG content. Mechanical properties of NBR/EG/CB nanocomposites with different graphite (1,3,5phr) show that elongation at break rise significantly even for a small increase in the amount of graphite[103]. Interestingly, tensile stress

Peer-reviewed version available at *Nanomaterials* **2018**, *8*, 945; doi:10.3390/nano8110945

(modulus) at 100% elongation is the highest corresponding to 1 phr graphite in the composites. It is believed that at very low loading amount, graphite could be dispersed better in the matrix. Further, it was noted that hardness and tear strength of the NBR/EG/CB nanocomposites increase only to a very small extent.

Manna and Srivastava[104] fabricated hexadecyl amine functionalized graphene (GNS-HAD) filled carboxylated nitrile rubber nanocomposites as flexible dielectric materials. The variation of tensile strength, elongation at break and toughness of neat XNBR and GNS–HAD/XNBR are displayed in **Figure 12** and **13**. It is noted that XNBR filled with 2 phr of GNS- exhibited a significant improvement in tensile strength (60%) and elongation at break (62%) compared to neat XNBR. The toughness of the GNS-HDA/XNBR composites also increases significantly with filler loading. Such an enhancement in the mechanical properties of XNBR/GNS–HAD nanocomposites could be attributed to the interfacial interaction between GNS-HDA and the XNBR matrix and effective load transfer from the filler to the polymer matrix. Alternatively, role of molecular level dispersion of GNS–HDA and its wrinkled shape leading to mechanical interlocking and transmitting the applied stress to XNBR also cannot be ruled out. It is inferred also that the Young's modulus of the composites is remarkably reduced (13%) in 2 phr of GNS–HDA loaded XNBR. This clearly indicates the reduced stiffness and enhanced flexibility of fabricated XNBR/GNS–HDA nanocomposites. Mechanical properties of graphene filled NBR rubber nanocomposites have also been reported by other workers[105,106]. The tensile modulus NBR-reduced grapheme oxide (rGO) composites prepared by solution mixing method at a 0.1-phr rGO loading greatly increased above 83, 114, and 116% at strain levels of 50, 100, and 200%, respectively compared to the 0.1-phr GO loaded sample[195]. The observed enhancement was highly attributed to a

homogeneous dispersion of rGO within the NBR matrix. RGO/HNBR composites exhibits enhanced mechanical properties compared with HNBR[196].

Thermoplastic polyurethane (TPU) with NBR find appreciations in the field of automotive gaskets, gaskets/co-extrusion, protective covers, tubing pipes, and grips etc.[12]. The presence of TPU in the blend accounts for the improvement in tensile strength, fuel/oil, weather, ozone and oxygen resistance, and NBR promotes the solvent resistance and thermal stability. Desai *et al.*,[109] observed co-continuous phase in TPU:NBR (50:50) blend owing to uniformly dispersed phases. However, there exists limited work only on the carbon based hybrid fillers reinforced Polyamide 6/NBR/SWCNT.[91] NBR/PVC/SWCNT,[92] TPPU/XNBR/MWCNT,[110] EPDM/NBR/MWCNT[111] and hybrid filled TPU/NBR blend nanocomposites[112-114] MWCNTs filled thermoplastic polyurethane–urea (TPUU) and carboxylated acrylonitrile butadiene rubber (XNBR) blend nanocomposites exhibited increased tensile modulus from about 9.90 to 45.3 MPa, at 3 wt% loading of CNT[110]. Hoikkanen *et al.*,[111] prepared MWCNT/NBR/EPDM blends nanocomposites by a melt mixing methods and studied their mechanical properties. They concluded that mechanical properties of these blend nanocomposites are controlled by the degree of dispersion of the nanotubes.

Srivastava and his group[112] reported variation of tensile strength (TS) and elongation at break (EB) of TN nanocomposites with respect to SFCNT-LDH and SFCNF-LDH hybrid filler content in **Figure 14.** It is also noted that 0.50 wt% SFCNT-LDH loaded TN nanocomposites exhibit improvement in tensile strength (126 %) and EB (1.50 times) compared to neat TN. On the other hand, with respect to neat TN, 0.50 wt% SFCNF-LDH hybrid filled TN nanocomposites also show

Peer-reviewed version available at *Nanomaterials* **2018**, *8*, 945; doi:10.3390/nano8110945

122 % and 1.43 times improvements in tensile strength and EB respectively. The enhanced mechanical properties of TN nanocomposites clearly suggest the reinforcing effect of both the SFCNTLDH and SFCNF-LDH hybrid fillers in TN. They ascribed such superior mechanical properties of TN due to the synergistic effect of SFCNT (or SFCNF) and LDH. Further, at higher filler loadings tensile strength and elongation at break slightly decrease due to the tendency of the hybrid fillers to agglomerate, giving rise to initiating sites for crack propagation. In another work,[113] carbon nanofiber (CNF)-layered double hydroxide (LDH) hybrid through a noncovalent assembly using sodium dodecyl sulfate as bridging linker between magnesium–aluminum LDH and CNF and used as nanofiller in TPU/NBR (50:50) blend. **Figure 15** shows variation of the tensile strength and elongation at break of the TN nanocomposites with respect to the SFCNF–LDH hybrid filler. The enhancement in the mechanical properties clearly indicated the reinforcing effect of SFCNF-LDH in the TN matrix. It was also noted that mechanical measurements of 0.50 wt % hybrid loaded TN blend exhibited maximum improvements in the elongation at break, tensile strength, and storage modulus of 1.51 times and 167 and 261% respectively. Their findings also confirmed the synergistic effect of SFCNF and LDH in the mechanical properties of the TN nanocomposites. Scheme 1 was proposed to explain mechanical properties of TN blend in the presence of the SFCNF–LDH hybrid filler, Srivastava and workers[114] also applied their approach to assemble MgAl layered double hydroxide onto pristine carbon nanotubes using sodium dodecylsulfate and used as hybrid nanofiller in the development of high-performance TPU/NBR (1:1 w/w) blend nanocomposites. The tensile strength of TPU/NBR filled with 0, 0.25, 0.50, 0.75 and 1 wt% SFCNT–LDH hybrid is 5.09, 11.7, 13.8, 10.6 and 9.78 MPa, respectively. The respective elongation at break values is293, 530, 513, 436 and 413%. It is observed from the data that the 0.50 wt% SFCNT–LDH hybrid loaded

Peer-reviewed version available at Nanomaterials 2018, 8, 945; doi:10.3390/nano8110945

TPU/NBR exhibits the maximum enhancement in tensile strength (171%) and elongation at break (1.8 times) compared to pure TPU/NBR due to the optimum dispersion of SFCNT–LDH hybrid filler that causes enhanced interaction between matrix and nanofiller.

3.4. Mechanical Properties of Carbon Filler incorporated SR and its Blend Nanocomposites

SR are one of the most important functional polymers, which have received considerable interest owing to their unique properties, e.g., excellent physical, chemical, and thermally stability, low glass transition temperature, clarity; biocompatibility, nonreactivity, and low surface energy[18]. Poly(dimethylsiloxane) also referred as PDMS, is a silicon-based organic polymer composed of a repeating $[SiO(CH_3)_2]$ unit and exist in rubber state at room temperature as its glass transition temperature is less than $-120\ ^0C$. It is useful in casting moulds, micro-fluidic devices, automotive and aerospace industry, cables for appliances and telecommunications, cooking, baking and food storage products, medical implants and in electrical insulation products etc. Despite several advantages, the vulcanized neat silicone rubber usually has poor mechanical properties and low thermal/electrical conductivity restricting its use in many industrial applications. Therefore, silicon rubber filled with carbon based nanofillers have been reported[115-143, 197-200].

Room temperature vulcanized (RTV) vulcanizates on adding 2 phr of CNTs increased Young's modulus by 272% and reached as high as ~706% at 8 phr[116]. In another work, RTV reinforced by MWCNTs attained its tensile strength, tear strength and elongation achieved 2.0 MPa, 11.7 kN/m and 238% compared to the composite with untreated MWCNTs having respective values as 1.1 MPa, 7.0 kN/m and 83%[117].

Peer-reviewed version available at *Nanomaterials* **2018**, *8*, 945; doi:10.3390/nano8110945

Shang *et al.*,[118] fabricated series of high temperature vulcanized silicone rubber (HTVSR)/MWCNTs nanocomposites with different CNT contents. In this, MWCNTs was pretreated by the chitosan salt before being incorporated into the HTVSR. **Table 9** show that tensile properties of the HTVSR nanocomposites are significantly increased due to the uniform dispersion of chitosan salt pretreated MWCNTs in HTVSR matrix. It is noted that tensile stress, elongation at break and modulus increased with the increasing MWCNTs (below 8 wt%) contents in HTVSR. At further higher filler loading (11 wt% of MWCNT), tensile stress and modulus still increased while the elongation at break decreased, which meant more MWCNTs made the HTVSR more brittle but tougher. The increasing of the tensile strength of the nanocomposites indicated that chitosan salt treated MWCNTs and HTVSR had very strong interfacial adhesions, and the MWCNTs helped to transfer some tensile force when the HTVSR/MWCNTs nanocomposite was stretched.SR filled with ball mill prepared hybrid filler consisting of 2.5 phr CB and 1.0 phr MWCNT shows improvement in tensile strength and strain to failure due to good dispersion and synergistic effects of MWNT and CB[119].

Cha *et al.*,[122] studied effect of incorporating individual MWCNTs and continuous MWCNT bucky paper on the mechanical properties of the PDMS composite films. The tensile strengths of the composite films filled with the bucky paper and as-received MWCNTs were improved by 2268% and 531% compared to that of the pure PDMS film. The tensile strength of the composite film was found to be superior that that obtained by filling with a commercially available buckypaper fabricated under the same processing. Wu and others[123] investigated the static and dynamic mechanical properties of PDMS and its MWCNT filled nanocomposites. The elastic modulus of pure PDMS (1.65 MPa) was increased in 1.0 wt.%, 2.0 wt.% and 4.0 wt.% CNT loaded

Peer-reviewed version available at *Nanomaterials* **2018**, *8*, 945; doi:10.3390/nano8110945

in PDMS to 1.71, 1.91 and 2.34 MPa respectively. The fracture surface analysis established that superior elastic modulus of PDMS at 4 wt% CNT was due to good bonding between CNTs and PDMS matrix. Katihabwa *et al.*,[125]also studied mechanical properties MWCNTs reinforced SR nanocomposites prepared through a high-shear mechanical mixing technique using DCP as a curing agent. The tensile stress of the SR increased with CNT contents and become four times higher for 20% filler content due to well-dispersed CNTs in the rubber matrix. In contrast, elongation at break of the nanocomposites decreases linearly with the increase of CNT content, probably due to poor filler-polymer interaction. Mazlan *et al.*,[127] reported effects of ultrasonic and mini extruder compounding processing techniques on Modulus at 100% elongation and elongation at break (%) of SR filled with 0.5, 1.0 and 1.5 vol% MWCNT. The reinforcing effect of MWCNT in the PDMS is clearly evident from this. Modulus of silicone rubber (0.6735 MPa) maximum increased in nanocomposites MWCNT/PDMS (1.5 vol%) prepared ultrasonically and MWCNT/PDMS (2.0vol%) fabricated by mini extruder to 1.4061 and 1.6081 MPa respectively. The elongation at break also showed maximum improvements of 140.48 and 149.34 % in corresponding composites compared to neat PDMS (129.67 %). Mechanical properties of PDMS/ MWCNT (covalently functionalized) were synthesized via nitrene chemistry[128]. This study showed significant improvements in tensile modulus (~2 times) and tensile strength (~1.2 times) compared to PDMS. Such enhancements in mechanical properties of the nanocomposites are attributed to the homogeneous dispersion of silicone-g-MWCNTs in the silicone elastomer matrix. In addition, graphene [135-137,139,140,197] and graphene oxide [198-200] has been incorporated to enhance the mechanical properties of the silicone rubber. Mechanical property measurements of liquid silicone rubber/GO functionalized with triethoxyvinylsilane composites (0.3 wt %) revealed displayed a 2.3-fold increase in tensile strength, 2.79-fold enhancement in tear strength,

Peer-reviewed version available at Nanomaterials 2018, 8, 945; doi:10.3390/nano8110945

and a 1.97-fold reinforcement in shear strength compared with the neat liquid silicone rubber[199]. Gan *et al.*,[198] studied effect of vinyl concentration of the silicone rubber on the mechanical properties of the SR/GO composites. It was found that the uniformly dispersed GO sheets within the SR matrix increase mechanical properties of the SR. The 3-aminopropyltriethoxysilane (APTES) graphite oxide (3.0 wt%) reinforced PDMS showed ~71% enhancement of Young's modulus[200].

The study of Bai *et al.*,[120] on tensile testing of SR/RGO nanocomposites revealed that improvement in mechanical properties enhanced with increasing the reduction degree of GO simultaneously. The vulcanized SR/chemically reduced graphene (rGE)/SiO_2 (referred as rGES), addition of 30 wt.% rGE)/SiO_2 (3 wt.% rGE) yielded a tensile strength of 6.13 MPa (up to 25 times), tear strength of 18.08 KN/m, and elongation at break of 267%, several times higher than those of rGE/SR nanocomposite.[197]Functionalized graphene (FG) room-temperature-vulcanized silicone rubber (RTVSR) nanocomposites were also prepared by in-situ reduction of graphene oxide[132]. This was noted that 0.5 wt % loading in RTVSR led maximum improvement in tensile strength (175 %) compared to neat RTVSR. This is ascribed to homogeneous dispersion of FG in the matrix silicone rubber and strong interfacial adhesion between FG/RTVSR ensuring efficient load transfer at the interface. Similarly, elongation at break was also enhanced in 0.5 wt% FG filled RTV by 67% higher compared to neat RTVSR. Zong and coworkers[133] prepared functionalized graphene (FG) by reduction of graphite oxide by hydrazine hydrate and subsequently used in development of silicone rubber nanocomposites. These silicone rubber nanocomposites exhibited significant improvements in tensile strength (198.39%) and elongation at break (268.25%) compared to neat silicone rubber. It was found that tensile stress and Young’s

Peer-reviewed version available at Nanomaterials 2018, 8, 945; doi:10.3390/nano8110945

modulus of neat SR increased on adding 2.0 wt% of graphene by 67% and 93% respectively. Interestingly, tensile strain of SR increased upto 1.0 wt % filled SR then declined. Mechanical properties of graphene nanoribbon (GNR) incorporated SR were significantly enhanced[135]. **Figure 16** show typical stress-strain behaviors of the pristine SR and SR/GNR nanocomposites. It is inferred that tensile stress and Young's modulus of SR filled with 2.0 wt% of GNR content enhanced by 67% and 93% respectively. In addition, elongation at break of the SR/GNR (0/.4 wt%) increased by 64% compared to SR. When the GNR amount reached to 2.0 wt%, although the tensile strain decreased to some extent due to stronger molecular interactions between the SR and the GNR, the tensile stress and Young's modulus increased by 67% and 93% respectively. Such improvements in the mechanical properties of SR nanocomposites is ascribed to good dispersion of the GNR and good interfacial interactions between the GNR and the SR account for observed.

The effect of functionalization of grapheme nanoplatelets by aminopropyltriethoxysilane (APTES), vinyltrimethoxysilane (VTMS), and Triton X-100 on the mechanical properties of SR composites prepared by a solution blending method[137]. **Figure 17** show considerable improvement in the mechanical properties of SR after incorporating surface modified graphene nanoplatelets. The silane treated graphene-based SR composites showed superior mechanical properties. It was observed that composites reinforced with modified grapheme nanoplatelets showed better tensile strength, elongation at break, and thermal conductivity properties compared with the pristine grapheme nanoplatelets /SR composite. The mechanical properties of the VTMS-graphene nanoplatelets based composite were found to be superior than that of the APTES treated counterpart. They ascribed it to the stronger interfacial interactions between VTMS-graphene

Peer-reviewed version available at *Nanomaterials* **2018**, *8*, 945; doi:10.3390/nano8110945

nanoplatelets and silicone chain resulting from the formation of chemical bonds. Bhowmick and Roy[138] prepared polydimethylsiloxane (PDMS)-amine modified CNF based nanocomposites by in situ and conventional ex situ methods. **Figure 18** shows a combined plot of tensile strength and tensile modulus with increasing filler concentration for in situ prepared amine modified CNF/hydroxyl PDMS nanocomposites. It is noted that tensile strength increases by 45, 92, 137, 370%, while modulus increases by 48, 90, 223, 515% corresponding to 1, 2, 4, and 8 phr filler loadings respectively. They suggested that mechanical properties thrive at their maximum for this filler–matrix combination since dispersion is improved by chemical functionalization.

Hu *et al.*,[139] first time reported a novel and simple approach to disperse CNTs completely in silicone rubber by the addition of graphene. Motivated by this, Srivastava and his group made several studies on a different combinations 1D and 2D fillers together referred as 3D hybrid fillers in fabrication of SR nanocomposites[140-142]. First time, they reported fabrication of MWCNT–graphene (G) hybrid (1:1 wt ratio) as nanofiller in enhancing the mechanical properties of high-performance silicone rubber (VMQ).[140] **Table 10** record mechanical property data of neat VMQ, MWCNT(0.375 wt%)/VMQ, G (0.375 wt%)/VMQ, MWCNT–G (0.75 wt%)/VMQ,MWCNT–G (1.0 wt%)/VMQ and MWCNT–G (1.5 wt%)/VMQ. It is noted that TS of MWCNT–G (0.75 wt%)/VMQ is higher than that of the corresponding MWCNT or graphene nanocomposites. The modulus at 50 and 100% strain is increased in VMQ nanocomposites compared to neat VMQ. It attains a maximum value for MWCNT–G/VMQ nanocomposites in all probability due to the development of shear zones in the nanocomposites under stress and strain conditions, or better dispersion of MWCNT-G leading to its enhanced interaction with VMQ. In addition, EB of VMQ is considerably reduced when filled with 0.375 wt% MWCNTs or graphene.

Peer-reviewed version available at Nanomaterials 2018, 8, 945; doi:10.3390/nano8110945

Interestingly, such loss in flexibility of nanocomposites of VMQ individually filled with MWCNTs or graphene is recovered in case of MWCNT-G (0.75 wt%)/VMQ nanocomposite. All these findings clearly demonstrate the synergistic effect of MWCNT–G hybrid on TS as well as EB of VMQ composites. This could be mainly attributed to the homogeneous dispersion of 3D MWCNT-G hybrid filler in VMQ matrix or due to better interaction between MWCNT-G and VMQ.

Srivastava and his group also extended their work on MWCNT and montmorillonite clay (MMT) in reinforcing properties of silicone rubber nanocomposites[141]. They recorded stress–strain plots for SR, SR/MWCNT (0.5 wt %), SR/MMT (0.5wt %), and SR/MMT (0.5 wt %)/MWCNT(0.5 wt %) were found that TS values with respect to SR are found to be 46, 25, and 215%, which confirmed the synergistic effect of MMT and MWCNT on SR. They observed that Young's modulus and tensile strength are found to be maximum improved in SR loaded with 1 wt % MMT/MWCNT (1:1) to 215 and 133% compared to SR. This was ascribed to the homogeneous dispersion and strong interfacial interaction between SR and MMT/MWCNT hybrid. In addition, the larger aspect ratio of MWCNT and the higher surface area of MMT could lead to the formation of network in the SR due to these 1D and 2D fillers. Elongation at break (EB) of SR gradually increases in the presence of MMT/MWCNT (1:1) hybrids and attains maximum value (260%) at its 1 wt % filler loading. This is in all probability due to the entanglement of polymer chain/synergistic effect of chain slippage, platelet orientation of MMT, and deformation of the MWCNT. However, TS and EB of SR decrease at higher filler loadings due to the aggregation tendency of the MMT/MWCNT. Motivated by their earlier work, Srivastava and workers[142] also investigated mechanical properties of nanocomposites of SR filled by 3D hybrids consisting

of MWCNT-Li-Al-LDH, MWCNT-Mg-Al-LDH and MWCNT-Co–Al-LDH fillers in SR. It is noted that tensile strength is maximum improved by 134%, 100% and 125% compared to neat SR corresponding to 1 wt.% of Mg–Al-LDH/MWCNT, Li–Al-LDH/MWCNT and Co–Al-LDH/MWCNT respectively. The role of synergistic effect of 1D MWCNT and 2D LDH was established based on stress-strain plots neat SR Mg–Al-LDH (0.5 wt.%)/SR, MWCNT (0.5 wt.%)/SR and Mg–Al-LDH/MWCNT (1.0 wt.%)/SR and similarly for SR composites of other fillers (MWCNT-Li-Al-LDH, and MWCNT-Co–Al-LDH). However, EB of the composites is always less compared to neat SR. It is also evident that EB of SR gradually increases in presence of LDH/MWCNT hybrids and attains maximum value at 1 wt.% filler loading. This is in all probability due to the entanglement of polymer chain/synergistic effect of chain slippage, platelet orientation of LDH and deformation of the MWCNT. However, TS and EB of SR decreases at higher filler loadings due to the aggregation tendency of the LDH/MWCNT. In addition to 3 D hybrid fillers, few other combinations of individual fillers have also been used in reinforcing of SR. SR composite, filled with hybrid fillers consisting of 5 phr CB and 1.0 phr CNT shows improvement in tensile strength and strain to failure due to good dispersion and synergistic effects. Witt and others[119] prepared SR composites filled by MWCNTs, CB and MWCNT/CB and subsequently studied mechanical properties of neat SR, SR/3.0CB, SR/4.0CNT and SR/2.5 CB/1.0 CNT composites. It was noted that SR/ SR/2.5 CB/1.0 CNT composite exhibited have higher tensile strength and strain to failure values than those of SR with single CB or CNT nanofiller of similar concentrations (SR/3.0 CB or SR/4.0 CNT). Norlin and Hazizan[143] synthesized MWCNT-Al_2O_3 (0.5 and 1.5 wt%) hybrid in reinforcing of PDMS nanocomposites by solvent casting method and examined their mechanical properties. The results showed that lower tensile properties are observed for the greater contents of MWCNT-Al_2O_3 hybrid in PDMS.

3.5 Mechanical Properties of Carbon Filler incorporated EPDM and its Blend Nanocomposites

Ethylene-propylene-dieneterpolymer (EPDM) is one of the most widel y used and fastest growing synthetic rubbers because of its excellent resistance to heat, oxidation, ozone, weathering, and microbial attack, attributed to the stable and saturated polymer backbone and seals, radiator, electrical insulation, roofing membrane, tubing, belts, and other general-purpose applications, which dominate its impact with regard to various industrial aspects. However, EPDM filled with carbon containing fillers has received relatively lesser attention[144-157]. Enhanced mechanical properties have also been observed in EPDM/ MWCNT rubber composites prepared by solution blending using sonication process[173]. The nanocomposites of EPDM filled with 0.5–5 wt.% MWNTs exhibited improved mechanical properties as compared to the pure EPDM matrix[144]. Young's modulus significantly enhanced with the increase in concentration of MWNTs. In another study, Molavi *et al.*,[145] found that tensile strength and elongation-at-break of compatibilized EPDM/MWCNT (0-7 phr) higher than those of uncompatibilized nanocomposites. Mechanical property investigations on different polymer blends filled with CNT are also reported. EPDM grafted with maleicanhydride on filling with CNF showed in mechanical strength with little compromise of higher density[147]. Dubey and others[148] studied radiation effect on mechanical properties of SBR/EPDM (50:50) blend containing MWNT (0.5–5%). The elastic modulus, tensile strength increased with the radiation dose, while elongation at break exhibited downward trend. The extent of reinforcement as assessed using Kraus equation suggested high reinforcement of blend on MWNT addition. They also extended work on effect of radiations on PCR/EPDM/MWCNT nanocomposites[149]. It was noted that mechanical properties are improved due to synergistic effect of MWCNT induced reinforcement and high energy radiation induced crosslinking of the blend. The extent of reinforcement, as assessed using the Kraus

equation suggested high reinforcement of the blend on MWNT addition. The elastic modulus increased with the radiation dose as well as with the increase in MWNT content. The incorporation of silane treated multiwalled carbon nanotubes in EPDM show increase in ultimate tensile strength and hardness.[154] The formation of simultaneously strengthened and toughened nanocomposites based on polypropylene/EPDM matrix achieved through enhanced adhesion between MWNTs and polymer matrix by using PP grafted MWNTs[155].

Tensile properties of PA-6/EPDM-g-MA (65:35) blend nanocomposites increased on incorporation of the SWNT[152] The tensile modulus of PP/EPDM was enhanced by increasing SWCNTs contents in EPDM[153]. Narimani *et al.*,[156] studied effect of SWNT on mechanical properties of thermoplastic elastomer based polypropylene (PP)/EPDM (80/20) is reported. The addition of SWNT increased the storage modulus. The impact strength and tensile strength improved when 0.5% of SWNT was used. Furthermore, the tensile modulus increased remarkably by increasing the SWNT content, but the elongation at break of the material decreased. Mechanical properties of EPDM filled phenol formaldehyde resin coated carbon nanotube has also been studied[157].

Allahbakhsh and Mazinani[201] investigated influences of sodium dodecyl sulfate on the mechanical performance of EPDM/GO nanocomposites. The maximum strength of the nanocomposite was about 137% more in the presence of SDS than the mechanical strength of the EPDM/GO nanocomposite. Furthermore, EPDM/GO nanocomposite was elongated up to 700% in the presence of sodium dodecyl sulfate. Valentini *et al.*,[150] prepared EPDM based nanocomposites containing CB, graphite nanoplatelets (GNPs), and mixtures of CB/GNP and

Peer-reviewed version available at Nanomaterials 2018, 8, 945; doi:10.3390/nano8110945

studied mechanical properties. It is noted that addition of filler to EPDM increase of the stiffness of the material as evident from improvement of the modulus at different strains. EPDM filled with 2 wt.% of GNPs and 24wt.% of CB showed a higher increment of the maximum strength. It was concluded that carbon black and graphite nanoplatelets synergistically account for the superior reinforcement in mechanical properties of the rubber composites Valentini *et al.*,[151] also used platelets GNPs to prepare EPDM nanocomposites and studied its mechanical properties. Their study has shown in the composite with high filler contents give rise to an increase of the stiffness of the material.

3.6 Mechanical Properties of EVA Rubber Nanocomposites

EVA copolymers are typically used for electrical insulation, cable jacketing and repair, component encapsulation and water proofing, corrosion protection, and packaging of components. However, available literature reveals that not much work is reported on the mechanical properties of carbon based nanofiller nanocomposites[158,159]. Bhowmick and George[158] made comparative study of mechanical properties of EVA (40-70% VA content) filled with EG, MWCNT and CNF. They concluded that EVA sample with lowest vinyl acetate content exhibits highest mechanical properties. However, the enhancement in mechanical properties of nanocomposites is the highest for EVA with high VA content. The variation of tensile strength and elongation at break versus EG content (in EVM/Ammonium Polyphosphate/Dipentaerythritol/EG system) decreased gradually with the increase of EG content[159].

Bhiyan *et al.*, [208] observed remarkably improved mechanical properties of neat EVA with HMM content up to 3 wt% followed by reversion. The tensile strength, elongation at break, and toughness

Peer-reviewed version available at Nanomaterials 2018, 8, 945; doi:10.3390/nano8110945

showed maximum improvements corresponding to 424, 109, and 1122 %, respectively. In another study, EVA)/MWCNTs/Hectorite (4 wt.%) nanocomposites showed significant improvement in tensile strength (243%), elongation at break (105%) and toughness (426%) without significant change in Young's modulus [209].

4. Dynamical Mechanical Properties of Carbon Nanofillers containing Rubber Nanocomposites

The storage modulus reflects the elastic modulus of the rubber materials which measures the recoverable strain energy in a deformed specimen, and the loss factor is related to the energy damped due to energy dissipation as heat. Therefore, dynamic mechanical property of different rubbers containing carbon nanofillers has been studied. The storage modulus, loss modulus and glass transition temperature increased for all MWCNTs reinforced NR[24]. In another work, addition of CNT at a very low loading could enhance the storage modulus of NR/SBR and NR/XSBR blend nanocomposites prepared by latex compounding[61].

Boonmahitthisud and Chuayjuljit[61] studied variation of storage modulus and loss tan δ as a function of temperature for neat NR/SBR and NR/XSBR blends and its nanocomposites filled with varying amount of CNT. These findings indicated that dose-dependent increase in the *E'* in CNT added rubber blend nanocomposites compared to the neat rubber blends and ascribed this to the high stiffness of CNT that constrains the rubber chain motion. Further, *T*g of each rubber in NR/SBR and NR/XSBR nanocomposites Tg increased with the increase in CNT loadings. Thomas *et al.*,[62] showed shifting of Tg to higher temp in the case of NR/phenol functionalized CNT nanocomposites. Loss tangent showed a decrease in the presence of CNT, and the effect is more

Peer-reviewed version available at *Nanomaterials* **2018**, *8*, 945; doi:10.3390/nano8110945

pronounced in the case of phenol functionalized CNT. Sui and others[47] observed that storage modulus of the CNT/NR nanocomposites greatly exceeds that of neat NR and CB/NR composites under all temperature. region). The glass transition temperature of natural rubber/ethylene propylene diene monomer nanocomposites slowly enhanced with increasing contents on MWCNT[56]. Xu *et al.*,[32] performed dynamic mechanical measurements on NR/CB composite and NR/CB/MWCNTs composites with different MWCNTs loadings. Thermoplastic PP-NR blend filled with acid-treated MWCNTs has the highest storage modulus (-90 ^{0}C) while the TPNR containing untreated MWCNTs has the lowest[61].This could be in all probability due to the fine dispersion of the acid treated MWCNTs in the TPNR matrix. Bhattacharya and Bhowmick [65] observed superior dynamic mechanical properties of NR/CNF nanocomposites compared with those to either NR/clay or NR/CNF nanocomposites or the NR/black control microcomposite. Natural rubber/graphene nanocomposites prepared by direct mech. mixing showed improved dynamic properties[48]. The dynamic mechanical properties of natural rubber-based composites comprising multiwall carbon nanotubes and graphene nanoplatelets have also been reported[49]. The elastic modulus of NR at room temperature increases and the maximum loss tangent and the corresponding glass transition temperature of composites decrease with increasing content of MWCNT[160,161]. The storage modulus of the NR/graphene oxide and nanocomposites significantly increased with the GO contents, indicating GO had a strong reinforcing tendency on NR[202]. Compared with neat NR, modulus at 300% for NR composites containing 0.9 phr graphene were increased by 154.9%[204]. The improvements in dynamic mech. properties were achieved at small substitution content of GO or reduced grapheme nanosheets for carbon black in NR[205].

The rolling resistance and wet traction properties of SBR are very valuable for their applications, especially in tire trade. In view of this, dynamical mechanical analysis of SBR filled with carbon-based nanomaterials received attention[15]. Peddini *et al.*,[68] carried on cured 12.3 wt.% MWCNT master batch and the various dilutions with SBR. They noted that storage modulus gradually increases with filler contents in SBR and is greatest above the Tg of SBR (-20- to 60 ^{0}C) due to the reinforcing effect. Loss modulus of SBR increases with addition of MWCNT in the composite. Tg of cured plaques by DMTA was shown to increase 4.5 ^{0}C with dilution of the SBR masterbatch containing 12.3 wt.% MWCNT. Pedroni *et al.*,[70] compared DMA findings of SBR/MWCNTs nanocomposites made by the solution casting and melt mixing methods. Storage modulus increases with the amount of filler in SBR in either method due to its reinforcing effect, though effect being more evident for composites prepared by casting method. The Tg of the polybutadiene blocks (PB) in the composites prepared by the casting method shifts from -88 to -80 ^{0}C with increasing MWCNT content. In contrast, no significant change in the Tg was observed for PB blocks of the composites prepared by extrusion. The addition of CNTs in SBR/BR (50:50) blend affects the glass transition behavior[73]. Adohi *et al.*,[82] observed that storage modulus of the SBR filled with carbon black- and carbon nanotubes composites is close to the modulus value of the neat styrene-butadiene rubber (f<0.1).Dynamic mechanical properties of modified expanded graphite/emulsion styrene butadiene rubber nanocompositesdemonstrated improvement than the respective control [86] Zhang *et al.*,[87] reported dynamical mechanical properties of SBR/CB and SBR/CB-RG hybrid filled nanocomposites, Tg is shifted slightly to higher temperature on adding CB from 10 phr to 13 phr in SBR. In contrast, Tg shifted to higher temperature by increasing the RG loading in RG-CB hybrid filled SBR blend nanocomposites. The comparison of two blends with the same total filler loading in SBR suggested that SBR/CB-RG (100/10:3)

exhibited higher Tg than that of SBR/CB (100/13). Tang and coworkers[89] noted that tubular clay (HNT)-tannic acid functionalized graphene (TAG) hybrid (22 phr) showed relatively higher modulus with respect to individually filled 20 and 2 phr of HNT and TAG respectively. The corresponding value of Tg were found to be -34.3, -37.9 and -32.2 ^{0}C respectively. Dynamical mechanical analysis indicated that the storage modulus of the composites was improved with the CNTs addition, especially CNTs. exceeding 30 phr in SBR[163,164]. Liquid polyisoprene and MgO affected the dynamical mech. properties of SBR/CNT vulcanizate, increasing the elastic modulus, glass transition temperature and tan δ value at 0 °C[165]. Another study showed reduction in T_g and enhanced the storage modulus of SBR matrix in the presence of PVP-modified GO [206]. Recently, Bhuyan *et al.*, [207] observed no significant enhancement in dynamic mechanical properties of SBR/MWCNT/Hectorite nanocomposites.

The significant increase in storage modulus of NBR was observed relatively in presence of relatively much lower volume fraction of CNTs compared to carbon black[95]. Likozar and Major[100] reported that storage modulus (25 ^{0}C) is enhanced by 6.0–8.3 times in NBR/MWCNT compared to HNBR/MWCNT, but the enhancement for 34.0 wt% AN content nanocomposite is only 3.3-4.8 times. Mahmood *et al.*, [110] studied effect of CNTs loading on the loss tangent (tan d) of TPUU:XNBR blend system as a function of temperature.(-60 to 100^{0}C,10 Hz). It is noted that intensity of the tan δ peak decreases with increasing the amount of the CNTs in the TPUU/XNBR. These findings also shown no significant shift of the tan d peak at about 25.8 ^{0}C on adding of the CNTs. The observed changes in the shape and intensity of the tan δ peaks in TPUU:XNBR/CNT blend nanocomposites in all probability due to extent of interaction/distribution of the CNTs. Salehi *et al.*,[107] observed improvements in the dynamic

storage modulus, E' (25 ^{0}C) and decrease of the magnitude of the loss angle (tan δ), of SBR/CNT/SiO_2 25/3 phr (E'=8.2 MPa, Tg = -1 ^{0}C) and NBR/CNT/SiO_2 (25/5 phr) (E'=9.6 MPa, Tg= 0 ^{0}C) compared to neat NBR (E'=1.6 MPa, Tg= -1.4 ^{0}C) due good polymer-filler interaction including synergistic effect. Storage modulus PVC/NBR filled with cylindrical SWNT exhibited improved storage modulus[110]. Srivastava and his group[112] observed significant improvements in dynamical mechanical properties of NBR/TPU blend in presence of Zn-LDH/surfactant modified CNT (referred as (SFCNT) and surfactant modified CNF hybrid filler. The storage modulus and loss modulus of hybrid filled NBR/TPU nanocomposites were found to be always higher compared to neat blend and blend filled with 0.50 wt% hybrid loading exhibited maximum improvements. They also extended their dynamical thermal analysis on SF CNF)/Mg-Al-LDH filled neat NBR/TPU nanocomposites[113]. It is noted that 0.50 wt % SFCNF–LDH filled NBR/TPU achieved maximum E' (276% at-60 ^{0}C, 261% at 25 ^{0}C) and loss modulus (254 %, at -30 ^{0}C) including maximum positive shift in Tg (~3 ^{0}C) compared to the neat sample. Dynamical mechanical properties of TPU/NBR/SFCNT/Mg-Al-LDH blend nanocomposites were also carried out in the range −80 to 80 ^{0}C[114]. The storage modulus of the 0.50wt% hybrid filled TPU/NBR matrix is significantly increased in both the glassy region (by 243% at −60 ^{0}C) and rubbery state (by 241% at 25 ^{0}C) compared to pure TPU/NBR. Such enhancement in storage modulus is attributed to the homogeneous dispersion of the SFCNT–LDH nanofiller within the matrix along with strong interaction between SFCNT–LDH hybrid filler and polymer matrix, which accounts for stress transfer from the TPU/NBR matrix to the hybrid filler resulting in strong reinforcement. The loss modulus (at −30 ^{0}C) also maximum improved by 254 % for TPU/NBR nanocomposites filled with 0.50 wt% hybrid, compared to pure TPU/NBR.

The dynamic storage modulus of NBR/EG composites is found to be significantly higher than that of pure NBR rubber about one order of magnitude above the glass transition temperature [101]. This is ascribed to the good reinforcing effect of nano-size graphite and restricted chain mobility of the NBR chain segments. Liu and others [102] observed higher storage modulus and lower glass transition temperature in NBR/EG NBR/EG composites. The storage modulus and loss factor (tan δ) of the NBR/EG/CB nanocomposite exhibited relatively higher than that NBR/EG/ and NBR/CB[103].

PDMS/silane molecules onto diphenyl-carbinol-functionalized MWCNT nanocomposites showed enhanced dynamic mechanical properties compared to those containing unmodified MWNTs and diphenyl-carbinol-functionalized MWNTs[115]. Saji and others[129] studied effect of MWCNT loadings on loss tangent, storage modulus and loss modulus, the corresponding findings are showed in **Figure 19**. It is noted that the location of maximum value of loss tangent ($\tan\delta_{max}$) is not significantly affected by the extent of MWCNT loading. The glass transition of all the samples lies in the range of −10 °C to−5 °C. This can be explained on the basis of relaxation dynamics of the polymer matrix. The variation in storage modulus (E′) as a function of temperature show characteristics sigmoidal variation. The temperature dependence of the loss modulus (E”) showed appearance of a distinct peak (α transition) at ~ −50 °C for all filled compositions. This could be ascribed to conformational transitions occurring in the silicone elastomer backbone caused by micro-Brownian motion. Roy and Bhowmick[138] observed no prominent shift in glass transition temperature shift of PDMS (-116 ^{0}C) and its amine modified CNF filled PDMS nanocomposites. The effects of the incorporation of single-walled carbon nanotubes (SWNTs) on dynamical mechanical properties of on blends of isotactic polypropylene (iPP) and EPDM are

Peer-reviewed version available at Nanomaterials 2018, 8, 945; doi:10.3390/nano8110945

investigated[166]. The effect of the incorporation of SWNT increased storage modulus of PP/EPDM (80/20) thermoplastic blend[167].

5. Payne and Mullin Effects in Carbon Nano Fillers incorporated Rubber Nanocomposite

It is also well-known that elastomeric nanocomposites exhibit high performance under such conditions. According to Payne, storage modulus (G0) of filled rubber compounds decreases rapidly with increasing applied dynamic strain amplitudes (Payne effect)[168]. Don *et al.*,[35] studied variation of storage modulus as a function of dynamic strain amplitudes at 0,13,5 phr loadings of carbon nanotube bundles (CNTB) in NR. It is noted that CNTB-5 exhibiting the highest storage modulus and magnitude of the Payne effect. Galimberti *et al.*,[36] observed that Payne effect increased with the CB-CNT and G-CNT nanofiller contents in synthetic poly(1,4-cis-isoprene). Ivanoska-Dacikj *et al.*,[44] made dynamic mechanical properties hybrid NR nanocomposites containing 2 phr MWCNT and different quantities (from 0 to 20 phr) of expanded organically modified montmorillonite (EOMt). **Figure 20** show strain sweep measurements by applying cyclic deformations in the tension mode to determine E′ (storage) and E″ (loss) moduli respectively. The dependence of E′, measured at low strain (so called Payne effect), on the hybrid filler content was studied to investigate the existence of a percolation threshold in the NR matrix. It showed a significant increase of the loss factor tan δ for the nanocomposites with filler concentrations above the mechanical percolation threshold (16 phr). This percolation threshold was found to be much higher compared to NR/EOMt system without MWCNT. This study also indicated pronounced non-linear dependence called Payne effect and could be explained in terms of a filler–filler network in the polymer matrix above the filler percolation threshold. Tan δ versus temperature plots in **Figure 20** also indicated a remarkable increase of the loss factor tan for the

Peer-reviewed version available at *Nanomaterials* **2018**, *8*, 945; doi:10.3390/nano8110945

nanocomposites NR/MWNT (2 phr)/EDMt (16 phr) and NR/MWNT (2 phr)/EOMt (20 phr) at higher dynamic strains. This effect could be attributed to the filler–filler network breaks down. Nah *et al.*,[170] investigated variation of storage modulus of NR filled with varying loadings of CNT and CB (1, 3, 7, 20 phr) as a function of dynamic strain amplitude and findings are displayed in **Figure 21**. It is noted that storage modulus of filled rubber compounds decreases significantly in contrast to little changes displayed in unfilled rubbers. This nonlinear behavior at small strains in NR/CNT nanocomposites is known as Payne effect. It is more pronounced at higher filler loadings and significantly higher in the CNT-filled compounds. **Figure 21** also show Hysteresis loops of NR/CNT and NR/CB compounds with 1 phr of filler content. This clearly demonstrates tress softening phenomenon at large strains (Mullins effect). It is concluded that Payne effect and Mullins effects are more predominant in CNT filled NR than CB-filled NR. Strain dependence of the storage modulus of NR and NR–MWCNTR has also been reported by George *et al.*,[171] where Payne effect was not observable below 0.3 phr MWCNTR. Above that, effect increases with increase in the amount of MWCNTR in NR. Yang and others [172] studied strain dependence of storage modulus (shear mode) of carboxylated CNT/NR and CB/NR rubber compounds and vulcanizates as displayed in **Figure 22**. It is inferred that storage modulus decreases with strain increasing in CNT/NR as well as CB/NR due to Payne effect. This effect is also more inevitable with increasing in SR. They observed constant storage modulus corresponding to 3 phr of CNT or CB 3-9 phr of CB in NR. However, storage modulus increased remarkably for CNT content of 9, 12 phr and CB content of 30, 50 phr in CNT/NR and CB/NR respectively.

Kang and others[173] carried out strain sweep measurements of graphene/NR nanocomposites prepared by direct mechanical mixing. The variation of storage of these filled compounds shows

non-linear behavior and high sensitivity to strain (Payne effect). Further, it is noted that storage modulus greatly increased with the addition of graphene due to the formation of filler network. Aziz *et al.*,[175] investigated variation of storage modulus versus strain amplitude of MRE filled with different types of MWCNT at different magnetic fields (0, 156, 331, 508, 638 and 747 mT). These findings showed that storage modulus gradually dropped as the strain amplitude increases. Such non-linear behavior of filled rubber, i.e. Payne effect, can be explained in terms of filler network in the rubber matrix above the percolation threshold.

Araby *et al.*,[174] studied variation of shear storage modulus versus strain (%) of SBR filled GNP nanocomposites and findings are displayed in **Figure 23**. It showed decrease of shear storage modulus with increase in the applied strain amplitude. Inset of the **Figure 23** clearly indicate overall proportional increase of Payne effect with GNP fractions. This is ascribed to the formation of filler–filler network in an elastomer matrix provides a good interpretation for Payne effect. In another study, storage modulus of SBR-HG compounds decreases dramatically upon increasing strain (Payne effect)[89].

Katihabwathe *et al.*,[125] studied dynamical mechanical behavior of uncured CNT/SR (1,5,10 and 20 wt%) nanocomposites. They observed that storage modulus decreases in the filled rubbers with increasing strain amplitude, i.e. characteristic of the phenomenon, known as the Payne effect. Further, this effect decreases with decreasing amount of filler and is not observed for CNT < 5 wt%. However, Payne effect is pronounced for SR filled with 20 wt% or more as evidenced by significant changes in storage modulus with increasing strain amplitude. Li and Sun[130] studied dynamic strain sweep all specimens from 0.1% to 10% at 5% pre-strain and frequency of 10 Hz.

The decrease in storage modulus of nanocomposites is noted with increasing dynamic strain amplitude, while silicone rubber showed very small change. This effect is more pronounced at high MWCNT loading exhibiting a non-linear behavior. The dependence on dynamic strain amplitude of dynamic mechanical properties of SR filled with CNT (1, 2, 3. 5 and 5 wt%) at 10 Hz showed decrease in storage modulus of nanocomposites with increasing dynamic strain amplitude [130]. This effect is more pronounced at high MWCNT loading, showing a non-linear behavior (Payne effect). Hoikkanen *et al.*,[111] observed that MWCNT filled EPDM/NBR blend nanocomposites prepared directly mixed method showed higher Payne effects than that prepared by masterbatch dilution method.

Another effect known as Mullins effect is also observed in the rubber nanocomposites subjected to a cyclic loading and unloading process. The Mullins effect is closely related to the structural changes during the tensile cycles. The most commonly accepted model to explain Payne effect arises from the breakdown of a filler network formed by filler–filler interactions. Room temperature variation of storage modulus versus strain amplitude (%) of the NR filled with 1 and 5.4 wt% carboxylated MWCNT[169]. It is noted that storage modulus of NR nanocomposite decreases when the strain amplitude increases. Loading–unloading cycles in cyclic tensile tests showed a strong stress-softening (Mullins) effect especially at 8.3 wt% CNT filling. The observed strong Payne effect and strong Mullins effect are ascribed to the mechanical behavior of the nanotube network.

Peer-reviewed version available at Nanomaterials 2018, 8, 945; doi:10.3390/nano8110945

Summary and Outlook

This review article has addressed recent research carried out on elastomers filled with carbon nanomaterials. The melt mixing and solution methods are most widely used methods to prepare polymer nanocomposites. The state of dispersion of fillers account for the enhanced mechanical and dynamical mechanical performances of individual carbon based fillers, such as fillers, such as CNT, CNF, graphene, expanded graphite, graphene oxide. In addition, improvement is also pronounced with the hybrid fillers consisting MWCNT (or CNF)-MMT, MWCNT-Hectorite, MWCNT (or CNF)-LDH, MWCNT-Graphene in variety of rubbers matrix. It is also inferred that introduction of these carbon based fillers in NR,SBR,NBR and SR nanocomposites led significant improvements in tensile strength, impact strength, elongation at break, Young's modulus, stand loss modulus, storage modulus etc. However, more contemporary work is still to be focused on development of corresponding EPDM and EVA nanocomposites. Payne and Mullin effects in rubber- carbon fillers nanocomposites are also reviewed. Thus unique properties of carbon based fillers make them superior compared to conventional fillers such as carbon blacks and silica requiring higher filler loading to enhance the mechanical properties of polymers. However, clear inference is not possible to compare mechanical and dynamical properties of different nanostructural carbon filled individual rubbers due to their dependency on state of filler dispersion. Shape of nanostructured fillers plays very important role on the overall properties of the composite materials especially, complex one with tetrapod and multipod morphology. The recently developed carbon based complex hierarchical filled and hollow nanostructures [210-215] could play very important roles as filler materials towards development of advanced rubber composites with engineered properties.

Acknowledgement

Author is very much thankful to Indrajit Srivastava and Mili Srivastava for providing necessary facilities during my stay in USA and Canada respectively.

References

1. Bokobza, L. Multiwall carbon nanotube elastomeric composites: A review. *Polymer (Guildf).***2007**, *48*, 4907–4920, doi:10.1016/J.POLYMER.2007.06.046.
2. Thomas, S.; Stephen, R. *Rubber nanocomposites : preparation, properties, and applications*; John Wiley & Sons, 2010; ISBN 9780470823453.
3. Sathish kumar, M.; Manonmani, K.; Parasuram, B.; Karthikeyan, S. Composites reinforced with carbon nanotubes A Review. *J. Environ. Nanotechnol.* **2013**, *2*, 67–80, doi:10.13074/jent.2013.09.132032.
4. Hussain, F.; Hojjati, M.; Okamoto, M.; Gorga, R. E. Review article: Polymer-matrix nanocomposites, processing, manufacturing, and application: An overview. *J. Compos. Mater.***2006**, *40*, 1511–1575, doi:10.1177/0021998306067321.
5. Srivastava, S.K.; Pionteck, J. *Recent advances on preparation, structure, properties and application of graphite oxid*e, J. Nanosci. Nanotechnol. **2000**, *15*, 1984-2000, doi: 10.1166/jnn.2015.10047.
6. Coleman, J. N.; Khan, U.; Blau, W. J. Small but strong: A review of the mechanical properties of carbon nanotube–polymer composites, Carbon **2006**, *44*, 1624-1652, doi:10.1155/2011/746029.
7. Moniruzzaman. M.; Winey, K. I. Polymer nanocomposites containing carbon nanotubes. *Macromolecules* **2006**, *39*, 5194–5205, doi:10.1021/MA060733P.
8. Ismail, R.; Ibrahim, A.; Hamid, H. A.; Mahmood, M. R.; Adnan, A. Performance of carbon nanotubes (CNT) based natural rubber composites: A review. In *InCIEC 2014*; Springer Singapore: Singapore, **2015**; pp. 821–829.
9. Feng, L.; Xie, N.; Zhong, J. Carbon nanofibers and their composites: A review of

synthesizing, properties and applications. *Mater.* **2014**, *7*, 3919–3945, doi:10.3390/ma7053919.

10. Liu, Y.; Kumar, S. Polymer/carbon nanotube nano composite fibers–A review. *ACS Appl. Mater. Interfaces* **2014**, *6*, 6069–6087, doi:10.1021/am405136s.
11. Al-Saleh, M. H.; Sundararaj, U. Review of the mechanical properties of carbon nanofiber/polymer composites. *Compos. Part A Appl. Sci. Manuf.* **2011**, *42*, 2126–2142, doi:10.1016/J.COMPOSITESA.2011.08.005.
12. Srivastava, S.K.; Kotal, M. R*ecent advances on preparation, properties and applications of polyurethane nanocomposites*, in Nanocomposites Series: Advanced composites materials, manufacturing and engineering, J Paulo Davim, Constantinos A. Charitdis (Eds.), DE Gruyter, Germany, **2013**, 33-93.
13. Srivastava, S.K.; Mittal, V. Recent developments on elastomer/hybrid filler nanocomposites, in Hybrid nanomaterials: Developments in energy, environments and polymer nanocomposites, S.K. Srivastava, V. Mittal (Eds.), Wiley-Scrivener Publishing, USA, **2017**, 423-490.
14. Srivastava, S. K. CHAPTER 18. Metal oxide filled micro and nano natural rubber composites, **2014**; pp. 504–549.
15. Srivastava, S.K.; Bhuyan, B. Rubber nanocomposites for tire tread application in rubber nano composites and nano textiles in automobiles, Bireswar Banerjee (Ed.), Rapra Publication, **2018**, 37-78.
16. Srivastava, S. K.; Kuila, T. Fire retardancy of elastomers and elastomer nanocomposites. *Polym. Green Flame Retard.* **2014**, 597–651, doi:10.1016/B978-0-444-53808-6.00018-4.
17. Srivastava, S. K.; Acharya, H. Aging and Degradation Behavior of Rubber

Nanocomposites. **2010**, 551–593, doi:10.1002/9780470823477.CH20

18. Srivastava, S. K.; Pradhan, B. Developments and properties of reinforced silicone rubber nanocomposites. In *Concise Encyclopedia of High Performance Silicones*; John Wiley & Sons, Inc.: Hoboken, NJ, USA, **2014**; pp. 85–109.
19. Maiti, M.; Bhattacharya, M.; Bhowmick, A. K. Elastomer Nanocomposites. *Rubber Chem. Technol.***2008**, *81*, 384–469, doi:10.5254/1.3548215.
20. Fritzsche, J.; Lorenz, H.; Klüppel, M. CNT based elastomer-hybrid-nanocomposites with promising mechanical and electrical properties. *Macromol. Mater. Eng.* **2009**, *294*, 551–560, doi:10.1002/mame.200900131.
21. Xu, J.; He, Y. Thermal analysis of NR composite with MWCNTs aligned in a magnetic field. *Int. J. Polym. Sci.* **2015**, *2015*, 1–6, doi:10.1155/2015/305317.
22. Tarawneh, M. A.; Ahmad, S. H.; Yahya, S. Y.; Rasid, R.; Se Yong Eh Noum, S. Y. E. Mechanical properties of thermoplastic natural rubber reinforced with multi-walled carbon nanotubes. *J. Reinf. Plast. Compos.***2011**, *30*, 363–368, doi:10.1177/0731684410397407.
23. Ponnamma, D.; Ramachandran, R.; Hussain, S.; Rajaraman, R.; Amarendra, G.; Varughese, K. T.; Thomas, S. Free-volume correlation with mechanical and dielectric properties of natural rubber/multi walled carbon nanotubes composites. *Compos. Part A Appl. Sci. Manuf.* **2015**, *77*, 164–171, doi:10.1016/J.COMPOSITESA.2015.06.023.
24. Tarawneh, M. A.; Ahmad, S. H.; EhNoum, S.; Lau, K. Sonication effect on the mechanical properties of MWCNTs reinforced natural rubber. *J. Compos. Mater.* **2013**, *47*, 579–585, doi:10.1177/0021998312443394.
25. Le, H. H.; Abhijeet, S.; Ilisch, S.; Klehm, J.; Henning, S.; Beiner, M.; Sarkawi, S. S.; Dierkes, W.; Das, A.; Fischer, D.; Stöckelhuber, K.-W.; Wiessner, S.; Khatiwada, S. P.;

Adhikari, R.; Pham, T.; Heinrich, G.; Radusch, H.-J. The role of linked phospholipids in the rubber-filler interaction in carbon nanotube (CNT) filled natural rubber (NR) composites. *Polymer* **2014**, *55*, 4738–4747, doi:10.1016/J.POLYMER.2014.07.043.

26. Nakaramontri, Y.; Kummerlöwe, C.; Nakason, C.; Vennemann, N. The effect of surface functionalization of carbon nanotubes on properties of natural rubber/carbon nanotube composites. *Polym. Compos.* **2015**, *36*, 2113–2122, doi:10.1002/pc.23122.

27. Ali, A. M.; Ahmad, S. H. Mechanical characterization and morphology of polylactic acid /liquid natural rubber filled with multi walled carbon nanotubes. In *AIP Conference Proceedings*; American Institute of Physics, **2013**; *1571*, pp. 83–89.

28. Lorenz, H.; Fritzsche, J.; Das, A.; Stöckelhuber, K. W.; Jurk, R.; Heinrich, G.; Klüppel, M. Advanced elastomer nano-composites based on CNT-hybrid filler systems. *Compos. Sci. Technol.* **2009**, *69*, 2135–2143, doi:10.1016/J.COMPSCITECH.2009.05.014.

29. Atieh, M.A.; Girun, N.; Ahmadun, F.R.; Guan,C.T.; Mahdi, E.;Baik, D. R. Multi-Wall Carbon Nanotubes/Natural Rubber Nanocomposite. *J. Nanotechnol.* **2005**, DOI : 10.2240/azojono0106.

30. Anand K., A.; Jose T., S.; Alex, R.; Joseph, R. Natural rubber-carbon nanotube composites through Latex compounding. *Int. J. Polym. Mater.* **2009**, *59*, 33–44, doi:10.1080/00914030903172916.

31. Choi, J.; Isayev, A. I. Natural rubber/carbon composites preapred by ultrasonically aided Extrusion. *Rubber Chem. Technol.***2013**, *86*, 109–131, doi:10.5254/rct.13.88919.

32. Xu, J.; Li, S.; Li, Y.; Ta, X. Preparation, morphology and properties of natural rubber/carbon black/multi-walled carbon nanotubes conductive composites. *J. Mater. Sci. Mater. Electron.* **2016**, *27*, 9531–9540, doi:10.1007/s10854-016-5005-4.

33. Deng, F.; Ito, M.; Noguchi,T.; Wang, L.; Ueki, H.; Niihar, K.; Kim, Y.A.; Endo, M.; Zheng, Q-S. Elucidation of the reinforcing mechanism in carbon nanotube/Rubber nanocomposites, *ACS Nano* **2011**, *5* , 3858–3866, doi: 10.1021/nn200201u.

34. Ismail, H.; Ramly, A. F.; Othman, N. Effects of silica/multiwall carbon nanotube hybrid fillers on the properties of natural rubber nanocomposites. *J. Appl. Polym. Sci.***2013**, *128*, 2433–2438, doi:10.1002/app.38298.

35. Dong, B.; Liu, C.; Lu, Y.; Wu, Y. Synergistic effects of carbon nanotubes and carbon black on the fracture and fatigue resistance of natural rubber composites. *J. Appl. Polym. Sci.***2015**, *132*, 42075, doi:10.1002/app.42075.

36. Galimberti, M.; Cipolletti, V.; Musto, S.; Cioppa, S.; Peli, G.; Mauro, M.; Gaetano, G.; Agnelli, S.; Theonis, R.; Kumar, V. Recent Advancements in rubber Nanocomposites, *Rubber Chem. Technol.***2014**, *87*, 417–442, doi:10.5254/rct.14.86919.

37. Tarawneh, M.A.; Ahmad S.H.; Zarin, K.A.K.; Hassan, I.N.; Jiun, Y.L.; Flaifel, M.H.; Bahri, S. *Properties enhancement of TPNR-MWNTs-OMMT hybrid nanocomposites by using ultrasonic treatment*, SainsMalaysiana **2013**, *42*, 503-507.

38. Tarawneh, M. A.; Ahmad, S. H.; Shamsul Bahri, A. R.; Jiun, Y. L. Mechanical properties of TPNR-MWNTs-OMMT hybrid nanocomposites. *Adv. Mater. Res.***2012**, *501*, 194–198, doi:10.4028/www.scientific.net/AMR.501.194.

39 . Li, H.; Yang, L.; Weng, G.; Xing, W.; Wu, J.; Huang, G. Toughening rubbers with a hybrid filler network of graphene and carbon nanotubes. *J. Mater. Chem. A***2015**, *3*, 22385–22392, doi:10.1039/C5TA05836H.

40. Nakaramontri, Y.; Nakason, C.; Kummerlöwe, C.; Vennemann, N. E nhancement of electrical conductivity and other related properties of epoxidized natural rubber/carbon

nanotube composites by optimizing concentration of 3-aminopropyltriethoxy silane. *Polym. Eng. Sci.***2017**, *57*, 381–391, doi:10.1002/pen.24433.

41. Nakaramontri, Y.; Nakason, C.; Kummerlöwe, C.; Vennemann, N. Effects of *in-situ* functionalization of carbon nanotubes with bis(triethoxysilylpropyl) tetrasulfide (TESPT) and 3-aminopropyltriethoxysilane (APTES) on properties of epoxidized natural rubber-carbon nanotube composites. *Polym. Eng. Sci.* **2015**, *55*, 2500–2510, doi:10.1002/pen.24140.

42. Azira, A. A.; Hassim, D. H. A. I.; Verasamy, D.; Suriani, A. B.; Rusop, M. Properties of natural rubber nanocomposites reinforced with carbon nanotubes. *Adv. Mater. Res.***2015**, *1109*, 195–199, doi:10.4028/www.scientific.net/AMR.1109.195.

43. Jiang, H.-X.; Ni, Q.-Q.; Natsuki, T. Tensile properties and reinforcement mechanisms of natural rubber/vapor-grown carbon nanofiber composite. *Polym. Compos.***2009**, *31*, 1099–1104, doi:10.1002/pc.20897.

44. Ivanoska-Dacikj, A.; Bogoeva-Gaceva, G.; Rooj, S.; Wießner, S.; Heinrich, G. Fine tuning of the dynamic mechanical properties of natural rubber/carbon nanotube nanocomposites by organically modified montmorillonite: A first step in obtaining high-performance damping material suitable for seismic application. *Appl. Clay Sci.***2015**, *118*, 99–106, doi:10.1016/J.CLAY.2015.09.009.

45. Peng, Z.; Feng, C.; Luo, Y.; Li, Y.; Yi, Z.; Kong, L. X. Natural rubber/multiwalled carbon nanotube composites developed with a combined self-assembly and latex compounding technique. *J. Appl. Polym. Sci.***2012**, *125*, 3920–3928, doi:10.1002/app.36389.

46. Jiang, H. X.; Ni, Q. Q.; Natsuki, T. Mechanical properties of carbon nanotubes reinforced natural rubber composites. *Adv. Mater. Res.***2009**, *79–82*, 417–420,

doi:10.4028/www.scientific.net/AMR.79-82.417.

47. Sui, G.; Zhong, W. H.; Yang, X. P.; Yu, Y. H.; Zhao, S. H. Preparation and properties of natural rubber composites reinforced with pretreated carbon nanotubes. *Polym. Adv. Technol.***2008**, *19*, 1543–1549, doi:10.1002/pat.1163.

48. Al-Hartomy, O.; Al-Ghamdi, A.; Said, S. F. Al; Dishovsky, N.; Mihaylov, M.; Ivanov, M.; Zaimova, D. Comparison of the dielectric thermal properties and dynamic mechanical thermal properties of natural rubber-based composites comprising multiwall carbon nanotubes and graphene nanoplatelets. *Fullerenes, Nanotub. Carbon Nanostructures***2015**, *23*, 1001–1007, doi:10.1080/1536383X.2015.1004572.

49. Kang, H.; Tang, Y.; Yao, L.; Yang, F.; Fang, Q.; Hui, D. Fabrication of graphene/natural rubber nanocomposites with high dynamic properties through convenient mechanical mixing. *Compos. Part B Eng.***2017**, *112*, 1–7, doi:10.1016/j.compositesb.2016.12.035.

50. Matchawet, S.; Kaesaman, A.; Bomlai, P.; Nakason, C. Effects of multi-walled carbon nanotubes and conductive carbon black on electrical, dielectric, and mechanical properties of epoxidized natural rubber composites. *Polym. Compos.***2017**, *38*, 1031–1042, doi:10.1002/pc.23666.

51. Saravari, O.; Boonmahitthisud, A.; Satitnaithum, W.; Chuayjuljit, S. Mechanical and electrical properties of natural rubber/carbon nanotube nanocomposites prepared by Latex compounding. *Adv. Mater. Res.* **2013**, *664*, 543–546, doi:10.4028/www.scientific.net/AMR.664.543.

52. Bokobza, L. Multiwall carbon nanotube-filled natural rubber: electrical and mechanical properties, *EXPRESS Polym. Lett.* 2012, 6, 213-223, doi: 10.3144/expresspolymlett.2012.24.

53 Shanmugharaj, A.M.; Ryu, S.H. Influence of aminosilane-functionalized carbon nanotubes on the rheometric, mechanical, electrical and thermal degradation properties of epoxidized natural rubber nanocomposites, *Polym. Internat.* **2013**, *62*, 1433-1441, doi:10.1002/pi.4437

54 Ismail, H.; Raml, A.F.; Othman, N. The effect of carbon black/multiwall Carbon nanotube hybrid fillers on the properties of natural rubber nanocomposites, *Polym. Plast. Technol. Eng.* **2011**, *50*, 660-666.

55 Li, M.;Tu, W.; Chen, X.; Wang, H.; Chen, J. NR/SBR composites reinforced with organically functionalized MWCNTs: simultaneous improvement of tensile strength and elongation and enhanced thermal stability, *J. Polym. Engg.* **2016**, *36*, 813-818, doi:10.1515/polyeng-2015-0136.

56 Jahed, M.; Naderi, G.; Mir, H.R.G. Microstructure, mechanical, and rheological properties of natural rubber/ethylene propylene diene monomer nanocomposites reinforced by multi-wall carbon nanotube, *Polym. Compos.* **2016**, *39*, E745-E753, doi:10.1002/pc.24153

57. Li, R.; Sun, L. Z. Dynamic viscoelastic behavior of multiwalled carbon nanotube–reinforced magnetorheological (MR) nanocomposites. *J. Nanomechanics Micromechanics***2014**, *4*, A4013014, doi:10.1061/(ASCE)NM.2153-5477.0000065.

58. Boonmahitthisud, A.; Chuayjuljit, S. NR/XSBR Nanocomposites with carbon clack and carbon nanotube prepared by Latex compounding. *Met. Mater. Miner.***2012**, *22*, 77–85.

59. Nakason, C.; Wannavilai, P.; Kaesaman, A. Effect of vulcanization system on properties of thermoplastic vulcanizates based on epoxidized natural rubber/polypropylene blends. *Polym Test* **2005**; *25*, 34–41.

60. Kong, I.; Shanks, R.; Ahmad, S.; Yu, L.-J. Multiwalled carbon nanotubes-magnetite

reinforced thermoplastic polypropylene-natural rubber blends. *World J. Eng.***2012**, *9*, 463–468, doi:10.1260/1708-5284.9.6.463.

61. Boonmahitthisud, A.; Chuayjuljit, S. Effects of Carbon Nanotube on Tensile and Dynamic Mechanical Properties of NR/SBR and NR/XSBR Nanocomposites Prepared by Latex Compounding. *Adv. Mater. Res.* **2012**, *488–489*, 612–616, doi:10.4028/www.scientific.net/AMR.488-489.612.

62. Thomas, P. S.; Abdullateef, A. A.; Al-Harthi, M. A.; Basfar, A. A.; Bandyopadhyay, S.; Atieh, M. A.; De, S. K. Effect of phenol functionalization of carbon nanotubes on properties of natural rubber nanocomposites. *J. Appl. Polym. Sci.* **2012**, *124*, 2370–2376, doi:10.1002/app.35274.

63. Bokobza, L. Enhanced electrical and mechanical properties of multiwall carbon nanotube rubber composites. *Polym. Adv. Technol.***2012**, *23*, 1543–1549, doi:10.1002/pat.3027.

64. Abraham, J.; P., M. A.; Kailas, L.; Kalarikkal, N.; George, S. C.; Thomas, S. Developing highly conducting and mechanically durable styrene butadiene rubber composites with tailored microstructural properties by a green approach using ionic liquid modified MWCNTs. *RSC Adv.***2016**, *6*, 32493–32504, doi:10.1039/C6RA01886F.

65. Bhattacharya, M.; Maiti, M.; Bhowmick, A. K,Synergy in carbon black filled natural rubber nanocomposites. Part I: Mechanical dynamical properties, and morphology, *J. Mater. Sci.* **2010**, *45*, 6126-6138..

66. De Falco, A.; Goyanes, S.; Rubiolo, G. H.; Mondragon, I.; Marzocca, A. Carbon nanotubes as reinforcement of styrene–butadiene rubber. *Appl. Surf. Sci.* **2007**, *254*, 262–265, doi:10.1016/J.APSUSC.2007.07.049.

67. Girun, N.; Ahmadun, F.; Rashid, S. A.; Ali Atieh, M. Multi-Wall Carbon

Nanotubes/Styrene Butadiene Rubber (SBR) Nanocomposite. *Fullerenes, Nanotub. Carbon Nanostructures* **2007**, *15*, 207–214, doi:10.1080/15363830701236449.

68. Peddini, S. K.; Bosnyak, C. P.; Henderson, N. M.; Ellison, C. J.; Paul, D. R. Nanocomposites from styrene-butadiene rubber (SBR) and multiwall carbon nanotubes (MWCNT) part 1: Morphology and rheology. *Polymer (Guildf).***2014**, *55*, 258–270, doi:10.1016/J.POLYMER.2013.11.003.

69. Peddini, S. K.; Bosnyak, C. P.; Henderson, N. M.; Ellison, C. J.; Paul, D. R. Nanocomposites from styrene–butadiene rubber (SBR) and multiwall carbon nanotubes (MWCNT) part 2: Mechanical properties. *Polymer* **2015**, *56*, 443–451, doi:10.1016/J.POLYMER.2014.11.006.

70. Pedroni, L. G.; Araujo, J. R.; Felisberti, M. I.; Nogueira, A. F. Nanocomposites based on MWCNT and styrene–butadiene–styrene block copolymers: Effect of the preparation method on dispersion and polymer–filler interactions. *Compos. Sci. Technol.***2012**, *72*, 1487–1492, doi:10.1016/J.COMPSCITECH.2012.06.009.

71. Atieh, M. A. Effect of Functionalized Carbon Nanotubes with Carboxylic Functional Group on the Mechanical and Thermal Properties of Styrene Butadiene Rubber. *Fullerenes, Nanotub. Carbon Nanostructures* **2011**, *19*, 617–627, doi:10.1080/1536383X.2010.504953.

72. Atieh, M. A. Effect of Functionalize Carbon Nanotubes with Amine Functional Group on the Mechanical and Thermal Properties of Styrene Butadiene Rubber. *J. Thermoplast. Compos. Mater.***2011**, *24*, 613–624, doi:10.1177/0892705710397456.

73. Das, A.; Kasaliwal, G. R.; Jurk, R.; Boldt, R.; Fischer, D.; Stöckelhuber, K. W.; Heinrich, G. Rubber composites based on graphene nanoplatelets, expanded graphite, carbon

nanotubes and their combination: A comparative study. *Compos. Sci. Technol.***2012**, *72*, 1961–1967, doi:10.1016/J.COMPSCITECH.2012.09.005.

74. Laoui, T. Mechanical and Thermal Properties of Styrene Butadiene Rubber - Functionalized Carbon Nanotubes Nanocomposites. *Fullerenes, Nanotub. Carbon Nanostructures* **2013**, *21*, 89–101, doi:10.1080/1536383X.2011.574324.

75. Abraham, J.; Maria, H. J.; George, S. C.; Kalarikkal, N.; Thomas, S. Transport characteristics of organic solvents through carbon nanotube filled styrene butadiene rubber nanocomposites: the influence of rubber–filler interaction, the degree of reinforcement and morphology. *Phys. Chem. Chem. Phys.***2015**, *17*, 11217–11228, doi:10.1039/C5CP00719D.

76. Zhou, X.; Zhu, Y.; Liang, J.; Yu, S. New Fabrication and Mechanical Properties of Styrene-Butadiene Rubber/Carbon Nanotubes Nanocomposite. *J. Mater. Sci. Technol.***2010**, *26*, 1127–1132, doi:10.1016/S1005-0302(11)60012-1.

77. Song,S-H.; Kwon, O-S.; Jeong. H-K.; Kang, Y-G. Properties of Styrene- Butadience Rubber Nanocomposites with Carbon Black, Carbon Nanotubes, Graphene and Graphite, *Kor. J. Mater. Res.* **2010**, *20*, 104-110.

78 A. Das, K.W. Sto¨ckelhuber, R. Jurk, M. Saphiannikova, J. Fritzsche, H. Lorenz,M. Klu¨ ppel, G. Heinrich, Modified and unmodified multiwalled carbon nanotubes in high performance solution-styrene–butadiene and butadiene rubber blends, *Polymer* **2008,** *49* 5276–5283.

79. Schopp, S.; Thomann, R.; Ratzsch, K.-F.; Kerling, S.; Altstädt, V.; Mülhaupt, R. Functionalized Graphene and Carbon Materials as Components of Styrene-Butadiene Rubber Nanocomposites Prepared by Aqueous Dispersion Blending. *Macromol. Mater. Eng.***2014**, *299*, 319–329, doi:10.1002/mame.201300127.

80. Alimardani, M.; Abbassi-Sourki, F.; Bakhshandeh, G. R. Preparation and characterization of carboxylated styrene butadiene rubber (XSBR)/multiwall carbon nanotubes (MWCNTs) nanocomposites. *Iran. Polym. J.***2012**, *21*, 809–820, doi:10.1007/s13726-012-0087-1.

81. Bhattacharya, M.; Maiti, M.; Bhowmick, A. K. Tailoring properties of styrene butadiene rubber nanocomposite by various nanofillers and their dispersion. *Polym. Eng. Sci.***2009**, *49*, 81–98, doi:10.1002/pen.21224.

82. Adohi, B. J.-P.; Mdarhri, A.; Prunier, C.; Haidar, B.; Brosseau, C. A comparison between physical properties of carbon black-polymer and carbon nanotubes-polymer composites. *J. Appl. Phys.***2010**, *108*, 074108, doi:10.1063/1.3486491.

83. Xing, W.; Tang, M.; Wu, J.; Huang, G.; Li, H.; Lei, Z.; Fu, X.; Li, H. Multifunctional properties of graphene/rubber nanocomposites fabricated by a modified latex compounding method. *Compos. Sci. Technol.* **2014**, *99*, 67–74, doi:10.1016/J.COMPSCITECH.2014.05.011.

84. Tang, M.; Xing, W.; Wu, J.; Huang, G.; Li, H.; Wu, S. Vulcanization kinetics of graphene/styrene butadiene rubber nanocomposites. *Chinese J. Polym. Sci.***2014**, *32*, 658–666, doi:10.1007/s10118-014-1427-8.

85. Malas, A.; Pal, P.; Das, C. K. Effect of expanded graphite and modified graphite flakes on the physical and thermo-mechanical properties of styrene butadiene rubber/polybutadiene rubber (SBR/BR) blends. *Mater. Des.* **2014**, *55*, 664–673, doi:10.1016/J.MATDES.2013.10.038.

86. Malas, A.; Pal, P.; Giri, S.; Mandal, A.; Das, C. K. Synthesis and characterizations of modified expanded graphite/emulsion styrene butadiene rubber nanocomposites: Mechanical, dynamic mechanical and morphological properties. *Compos. Part B Eng.***2014**,

58, 267–274, doi:10.1016/J.COMPOSITESB.2013.10.028.

87. Zhang, H.; Wang, C.; Zhang, Y. Preparation and properties of styrene-butadiene rubber nanocomposites blended with carbon black-graphene hybrid filler. *J. Appl. Polym. Sci.***2015**, *132*, 41309, doi:10.1002/app.41309.

88. Abraham, J.; Soney, M. M. G.; George, C.; Kalarikkal, N.; Thomas, S. Carbon Nanotube-thermally Reduced Graphene Hybrid/Styrene Butadiene Rubber Nano Composites: Mechanical, Morphological and Dielectric Studies. *Res. Rev. J. Eng. Technol.***2015**, *4*, 1–5.

89. Tang, Z.; Wei, Q.; Lin, T.; Guo, B.; Jia, D. The use of a hybrid consisting of tubular clay and graphene as a reinforcement for elastomers. *RSC Adv.***2013**, *3*, 17057, doi:10.1039/c3ra42568a.

90. Song, S. H. Synergistic Effect of Clay Platelets and Carbon Nanotubes in Styrene-Butadiene Rubber Nanocomposites. *Macromol. Chem. Phys.***2016**, *217*, 2617–2625, doi:10.1002/macp.201600344.

91. Naderi, G.; Ghoreishy, M. H. R.; Moradi, M. Effect of modified single-wall carbon nanotubes on mechanical and morphological properties of thermoplastic elastomer nanocomposites based on (polyamide 6)/(acrylonitrile butadiene rubber). *J. Vinyl Addit. Technol.***2016**, *22*, 336–341, doi:10.1002/vnl.21451.

92. Hajibaba, A.; Naderi, G.; Ghoreishy, M.; Bakhshandeh, G.; Nouri, M. R. Effect of single-walled carbon nanotubes on morphology and mechanical properties of NBR/PVC blends. *Iran. Polym. J.* **2012**, *21*, 505–511, doi:10.1007/s13726-012-0055-9.

93. Chougule, H.; Giese, U. Application of Carbon Nano Tubes in specialty Rubbers – Potential and Properties. *KGK-Kautschuk und Gummi Kunststoffe* **2016**, *69*, 45–52.

94. Yue, D.; Liu, Y.; Shen, Z.; Zhang, L. Study on preparation and properties of carbon

nanotubes/rubber composites. *J. Mater. Sci.* **2006**, *41*, 2541–2544, doi:10.1007/s10853-006-5331-7.

95.Harishkumar, C.; Schuster, R.H. *Influence of ACN content on the properties of NBR/CNT nanocomposites*, KGK, KautschukGummi Kunststoffe,2014, 67, 22-28.

96. Boonbumrung, A.; Sea-Oui, P.; Sirisinha, C. Dispersion Enhancement of Multi-Walled Carbon Nanotube (MWCNT) in Nitrile Rubber (NBR). *Adv. Mater. Res.* **2013**, *747*, 59–62, doi:10.4028/www.scientific.net/AMR.747.59.

97. Boonbumrung, A.; Sae-oui, P.; Sirisinha, C. Reinforcement of multiwalled carbon nanotube in nitrile rubber: In comparison with carbon black, conductive carbon black, and precipitated silica, J. Nanomater. **2016**, http://dx.doi.org/10.1155/2016/6391572.

98. Ryu, S.-R.; Sung, J.-W.; Lee, D.-J. Strain-induced crystallization and mechanical properties of NBR composites with carbon nanotubes and carbon black, *Rubber Chem. Technol.***2012**, *85*, 207–218,

99. Psarras, G. C.; Sofos, G. A.; Vradis, A.; Anastassopoulos, D. L.; Georga, S. N.; Krontiras, C. A.; Karger-Kocsis, J. HNBR and its MWCNT reinforced nanocomposites: Crystalline morphology and electrical response. *Eur. Polym. J.* **2014**, *54*, 190–199, doi:10.1016/j.eurpolymj.2014.03.002.

100 Likozar, B.; Major, Z. Morphology, mechanical, cross-linking, thermal, and tribological properties of nitrile and hydrogenated nitrile rubber/multi-walled carbon nanotubes composites prepared by melt compounding: The effect of acrylonitrile content and hydrogenation. *Appl. Surf. Sci.***2010**, *257*, 565–573, doi:10.1016/J.APSUSC.2010.07.034.

101. Wang, L.; Zhang, L.; Tian, M. Effect of expanded graphite (EG) dispersion on the mechanical and tribological properties of nitrile rubber/EG composites. *Wear* **2012**, *276–277*, 85–93,

doi:10.1016/J.WEAR.2011.12.009.

102. Liu, D. W.; Du, X. S.; Meng, Y. Z. Preparation of NBR/expanded graphite nanocomposites by simple mixing. *Polym. Polym. Compos.***2005**, *13*, 815–821.

103. Wang, L. L.; Zhang, L. Q.; Tian, M. Mechanical and tribological properties of acrylonitrile–butadiene rubber filled with graphite and carbon black. *Mater. Des.***2012**, *39*, 450–457, doi:10.1016/J.MATDES.2012.02.051.

104. Manna, R.; Srivastava, S. K. Fabrication of functionalized graphene filled carboxylated nitrile rubber nanocomposites as flexible dielectric materials. *Mater. Chem. Front.* **2017**, *1*, 780–788, doi:10.1039/C6QM00025H.

105. Kumar, V.; Hanel, T.; Fleck, F.; Moewes, M.; Dilman, T.; Giese, U.; Klueppel, M. *Graphene filled nitrile butadiene rubber nanocomposites*, KGK, KautschukGummiKunststoffe, **2015**, *68*, 69.79.

106. Möwes, M. M.; Fleck, F.; Klüppel, M. Effect of filler surface activity and morphology on mehanical and dielectric properties of NBR/Graphenen nanocomposites, *Rubber Chem. Technol.***2014**, *87*, 70–85, doi:10.5254/rct.13.87930.

107. Salehi, M. M.; Khalkhali, T.; Davoodi, A. A. The physical and mechanical properties and cure characteristics of NBR/silica/MWCNT hybrid composites. *Polym. Sci. Ser. A***2016**, *58*, 567–577, doi:10.1134/S0965545X16040131.

108. Hajibaba, A.; Naderi, G.; Esmizadeh, E.; Ghoreishy, M. H. R. Morphology and dynamic-mechanical properties of PVC/NBR blends reinforced with two types of nanoparticles. *J. Compos. Mater.* **2014**, *48*, 131–141, doi:10.1177/0021998312469242.

109. Desai, S.; Thakore, I. M.; Brennan, A.; Devi, S. Polyurethane-nitrile rubber blends. *J. Macromol. Sci. - Pure Appl. Chem.***2001**, *38A*, 711–729, doi:10.1081/MA-100103875.

110. Mahmood, N.; Khan, A. U.; Stöckelhuber, K. W.; Das, A.; Jehnichen, D.; Heinrich, G. Carbon nanotubes-filled thermoplastic polyurethane-urea and carboxylated acrylonitrile butadiene rubber blend nanocomposites. *J. Appl. Polym. Sci.***2014**, *131*, 40341, doi:10.1002/app.40341.

111. Hoikkanen, M.; Poikelispää, M.; Das, A.; Honkanen, M.; Dierkes, W.; Vuorinen, J. Effect of Multiwalled Carbon Nanotubes on the Properties of EPDM/NBR Dissimilar Elastomer Blends. *Polym. Plast. Technol. Eng.* **2015**, *54*, 402–410, doi:10.1080/03602559.2014.958775.

112. Roy, S.; Srivastava, S. K.; Mittal, V. Facile noncovalent assembly of MWCNT-LDH and CNF-LDH as reinforcing hybrid fillers in thermoplastic polyurethane/nitrile butadiene rubber blends. *J. Polym. Res.***2016**, *23*, 36, doi:10.1007/s10965-016-0926-4.

113. Roy, S.; Srivastava, S. K.; Mittal, V. Noncovalent assembly of carbon nanofiber-layered double hydroxide as a reinforcing hybrid filler in thermoplastic polyurethane-nitrile butadiene rubber blends. *J. Appl. Polym. Sci.***2016**, *133*, 43470, doi:10.1002/app.43470.

114. Roy, S.; Srivastava, S. K.; Pionteck, J.; Mittal, V. Assembly of layered double hydroxide on multi-walled carbon nanotubes as reinforcing hybrid nanofiller in thermoplastic polyurethane/nitrile butadiene rubber blends. *Polym. Int.* **2016**, *65*, 93–101, doi:10.1002/pi.5032.

115. Chua, T. P.; Mariatti, M.; Azizan, A.; Rashid, A. A. Effects of surface-functionalized multi-walled carbon nanotubes on the properties of poly(dimethyl siloxane) nanocomposites. *Compos. Sci. Technol.* **2010**, *70*, 671–677, doi:10.1016/J.COMPSCITECH.2009.12.023.

116. Kumar, V.; Lee, D.-J. Studies of nanocomposites based on carbon nanomaterials and RTV silicone rubber. *J. Appl. Polym. Sci.* **2017**, *134*, doi:10.1002/app.44407.

117. Liu, Y.; Chi, W.; Duan, H.; Zou, H.; Yue, D.; Zhang, L. Property improvement of room temperature vulcanized silicone elastomer by surface-modified multi-walled carbon nanotube inclusion. *J. Alloys Compd.* **2016**, *657*, 472–477, doi:10.1016/J.JALLCOM.2015.10.129.

118. Shang, S.; Gan, L.; Yuen, M. C.; Jiang, S.; Mei Luo, N. Carbon nanotubes based high temperature vulcanized silicone rubber nanocomposite with excellent elasticity and electrical properties. *Compos. Part A Appl. Sci. Manuf.***2014**, *66*, 135–141,

119. Witt, N.; Tang, Y.; Ye, L.; Fang, L. Silicone rubber nanocomposites containing a small amount of hybrid fillers with enhanced electrical sensitivity. *Mater. Des.***2013**, *45*, 548–554, doi:10.1016/J.MATDES.2012.09.029.

120. Bai, Y.; Cai, H.; Qiu, X.; Fang, X.; Zheng, J. Effects of graphene reduction degree on thermal oxidative stability of reduced graphene oxide/silicone rubber nanocomposites. *High Perform. Polym.***2015**, *27*, 997–1006, doi:10.1177/0954008315604205.

121. Sankar, N.; Reddy, M.N.; Prasad, R.K. . Carbon nanotubes dispersed polymer nanocomposites: mechanical, electrical, thermal properties and surface morphology. *Bull. Mater. Sci.***2016**, *39*, 47–55, doi:10.1007/s12034-015-1117-3.

122. Cha, J.; Kim, S.; Lee, S. Effect of Continuous Multi-Walled Carbon Nanotubes on Thermal and Mechanical Properties of Flexible Composite Film. *Nanomaterials* **2016**, *6*, 182, doi:10.3390/nano6100182.

123. Wu, C.-L.; Lin, H.-C.; Hsu, J.-S.; Yip, M.-C.; Fang, W. Static and dynamic mechanical properties of polydimethylsiloxane/carbon nanotube nanocomposites. *Thin Solid Films* **2009**, *517*, 4895–4901, doi:10.1016/J.TSF.2009.03.146.

124. Sagar, S.; Iqbal, N.; Maqsood, A. Dielectric, electric and thermal properties of carboxylic

functionalized multiwalled carbon nanotubes impregnated polydimethylsiloxane nanocomposite. *J. Phys. Conf. Ser.* **2013**, *439*, 012024, doi:10.1088/1742-6596/439/1/012024.

125. Katihabwa, A.; Wencai Wang, W.; Yi Jiang, Y.; Xiuying Zhao, X.; Yonglai Lu, Y.; Liqun Zhang, L. Multi-walled carbon nanotubes/silicone rubber nanocomposites prepared by high shear mechanical mixing. *J. Reinf. Plast. Compos.* **2011**, *30*, 1007–1014,

126. Pradhan, B, Ph.D Thesis, 2D and 3D nanofiller reinforced silicone rubber nanocomposites: Preparation, characterization and propertes, Indian Institute of Technology, Kharagpur, India **2014**.

127. Mazlan, N.; Jaafar, M.; Aziz, A.; Ismail, H.; Busfield, J. J. C. Effects of different processing techniques on multi-walled carbon nanotubes/silicone rubber nanocomposite on tensile strength properties. *IOP Conf. Ser. Mater. Sci. Eng.***2016**, *152*, 012060, doi:10.1088/1757-899X/152/1/012060.

128. Yadav, S. K.; Kim, I. J.; Kim, H. J.; Kim, J.; Hong, S. M.; Koo, C. M. PDMS/MWCNT nanocomposite actuators using silicone functionalized multiwalled carbon nanotubes via nitrene chemistry. *J. Mater. Chem. C* **2013**, *1*, 5463, doi:10.1039/c3tc30888j.

129. Saji, J.; Khare, A.; Choudhary, R. N. P.; Mahapatra, S. P. Visco-elastic and dielectric relaxation behavior of multiwalled carbon-nanotube reinforced silicon elastomer nanocomposites. *J. Polym. Res.* **2014**, *21*, 341, doi:10.1007/s10965-013-0341-z.

130. Li, R.; Sun, L. Z. Dynamic mechanical analysis of silicone rubber reinforced with multi-walled carbon nanotubes. *Interact. multiscale Mech.* **2011**, *4*, 239–245, doi:10.12989/imm.2011.4.3.239.

131. Kumar, V.; Lee, D.-J.; Lee, J.-Y. Studies of RTV silicone rubber nanocomposites based on

graphitic nanofillers. *Polym. Test.* **2016**, *56*, 369–378,doi:10.1016/J.POLYMERTESTING.2016.11.004.

132 Ma, W.; Li, J.; Deng, B.; Lin, X.; Zhao, X. Properties of functionalized graphene/room temperature vulcanized silicone rubber composites prepared by an In-situ reduction method. *J. Wuhan Univ. Technol. Sci. Ed.* **2013**, *28*, 127–131, doi:10.1007/s11595-013-0653-1.

133. Zong, Y.; Gui, D.; Li, S.; Tan, G.; Xiong, W.; Liu, J. Preparation and thermo-mechanical properties of functionalized graphene/silicone rubber nanocomposites. In ***2015*** *16th International Conference on Electronic Packaging Technology (ICEPT)*; IEEE, 2015; pp. 30–34.

134. Dong, J.; Wang, P. H.; Sun, D. B.; Xu, Y. L.; Li, K. P. Preparation and Characterization of Graphene/RTV Silicone Rubber Composites. *Adv. Mater. Res.* **2013**, *652–654*, 11–14, doi:10.4028/www.scientific.net/AMR.652-654.11.

135. Gan, L.; Shang, S.; Yuen, C. W. M.; Jiang, S.; Luo, N. M. Facile preparation of graphene nanoribbon filled silicone rubber nanocomposite with improved thermal and mechanical properties. *Compos. Part B Eng.* **2015**, *69*, 237–242, doi:10.1016/J.COMPOSITESB.2014.10.019.

136. Valentini, L.; Bittolo Bon, S.; Pugno, N. M. Severe graphene nanoplatelets aggregation as building block for the preparation of negative temperature coefficient and healable silicone rubber composites. *Compos. Sci. Technol.* **2016**, *134*, 125–131, doi:10.1016/J.COMPSCITECH.2016.08.005.

137 Zhang, G.; Wang, F.; Dai, J.; Huang, Z. Effect of functionalization of graphene nanoplatelets on the mechanical and thermal properties of silicone rubber composites, Materials, 2016,9, 92/1-92/13.138. Roy, N.; Bhowmick, A. K. Novel in situ carbon

nanofiber/polydimethylsiloxane nanocomposites: Synthesis, morphology, and physico-mechanical properties. *J. Appl. Polym. Sci.***2012**, *123*, 3675–3687, doi:10.1002/app.35037.

139. Hu, H.; Zhao, L.; Liu, J.; Liu, Y.; Cheng, J.; Luo, J.; Liang, Y.; Tao, Y.; Wang, X.; Zhao, J. Enhanced dispersion of carbon nanotube in silicone rubber assisted by graphene. *Polymer* .**2012**, *53*, 3378–3385, doi:10.1016/J.POLYMER.2012.05.039.

140. Pradhan, B.; Srivastava, S. K. Synergistic effect of three-dimensional multi-walled carbon nanotube-graphene nanofiller in enhancing the mechanical and thermal properties of high-performance silicone rubber. *Polym. Int.***2014**, *63*, 1219–1228, doi:10.1002/pi.4627.

141. Pradhan, B.; Roy, S.; Srivastava, S. K.; Saxena, A. Synergistic effect of carbon nanotubes and clay platelets in reinforcing properties of silicone rubber nanocomposites. *J. Appl. Polym. Sci.***2015**, *132*, 41818, doi:10.1002/app.41818.

142. Pradhan, B.; Srivastava, S. K. Layered double hydroxide/multiwalled carbon nanotube hybrids as reinforcing filler in silicone rubber. *Compos. Part A Appl. Sci. Manuf.***2014**, *56*, 290–299, doi:10.1016/J.COMPOSITESA.2013.10.011.

143. Norlin, N.; Hazizan, M. A. Influence of Processing on the Properties of Carbon Nanotubes/Alumina Hybrid Compound Filled PDMS Composites. *Adv. Mater. Res.***2013**, *812*, 198–203, doi:10.4028/www.scientific.net/AMR.812.198.

144. Ciselli, P.; Lu, L.; Busfield, J. J. C.; Peijs, T. Piezoresistive polymer composites based on EPDM and MWNTs for strain sensing applications. *e-Polymers* **2010**, *10*, doi:10.1515/epoly.2010.10.1.125.

145. Fatemeh, K.M.; Rohollah, B.; Ghasem, N., Sedigheh, F.; Copmatibilization of multi-wall carbon nanotubes /EPDM: Studies on the properties of nanocomposites, **201**3, *26*, 115-123.

146. Paran, S.M.R.; Naderi, G.; Babakhani, A. An experimental study of the effect of CNTs on

the mechanical properties of CNTs/NR/EPDM nanocomposite, *Polym. Compos.* **2017**, 2017https://doi.org/10.1002/pc.24467.

147 Singh, S.; Guchhait, P. K.; Singha, N. K.; Chaki, T. K. Carbon nanofibre composite with EPDM and polyimide for high temperature insulation, *Rubber Chem. Technol.***2014**, *87*, 593–605, doi:10.5254/rct.14.86916.

148. Dubey, K. A.; Bhardwaj, Y. K.; Chaudhari, C. V.; Goel, N. K.; Sabharwal, S.; Rajkumar, K.; Chakraborty, S. K. Radiation effects on styrene-butadiene-ethylene-propylene diene monomer-multiple walled carbon nanotube nanocomposites: vulcanization and characterization. *Polym. Adv. Technol.* **2011**, *22*, 1888–1897, doi:10.1002/pat.1688.

149. Dubey, K. A.; Bhardwaj, Y. K.; Rajkumar, K.; Panicker, L.; Chaudhari, C. V.; Chakraborty, S. K.; Sabharwal, S. Polychloroprene rubber/ethylene-propylene diene monomer/multiple walled carbon nanotube nanocomposites: synergistic effects of radiation crosslinking and MWNT addition. *J. Polym. Res.***2012**, *19*, 9876, doi:10.1007/s10965-012-9876-7.

150. Valentini, L.; Bittolo Bon, S.; Lopez-Manchado, M. A.; Verdejo, R.; Pappalardo, L.; Bolognini, A.; Alvino, A.; Borsini, S.; Berardo, A.; Pugno, N. M. Synergistic effect of graphene nanoplatelets and carbon black in multifunctional EPDM nanocomposites. *Compos. Sci. Technol.***2016**, *128*, 123–130, doi:10.1016/j.compscitech.2016.03.024.

151. Valentini, L.; Bolognini, A.; Alvino, A.; Bittolo Bon, S.; Martin-Gallego, M.; Lopez-Manchado, M. A. Pyroshock testing on graphene based EPDM nanocomposites. *Compos. Part B Eng.***2014**, *60*, 479–484, doi:10.1016/J.COMPOSITESB.2013.12.022.

152. Augustine, J. M.; Maiti, S. N.; Gupta, A. K. Mechanical properties and crystallization behavior of toughened polyamide-6/carbon nanotube composites. *J. Appl. Polym. Sci.***2012**, *125*, E478–E485, doi:10.1002/app.33975.

153. Hemmati, M.; Narimani, A.; Shariatpanahi, H.; Fereidoon, A.; Ahangari, M. G. Study on Morphology, Rheology and Mechanical Properties of Thermoplastic Elastomer Polyolefin (TPO)/Carbon Nanotube Nanocomposites with Reference to the Effect of Polypropylene-grafted-Maleic Anhydride (PP-g-MA) as a Compatibilizer. *Int. J. Polym. Mater.***2011**, *60*, 384–397, doi:10.1080/00914037.2010.531810.

154. Iqbal, S. S.; Iqbal, N.; Jamil, T.; Bashir, A.; Khan, Z. M. Tailoring in thermomechanical properties of ethylene propylene diene monomer elastomer with silane functionalized multiwalled carbon nanotubes. *J. Appl. Polym. Sci.***2016**, *133*, 43221, doi:10.1002/app.43221.

155. Li, C.; Deng, H.; Wang, K.; Zhang, Q.; Chen, F.; Fu, Q. Strengthening and toughening of thermoplastic polyolefin elastomer using polypropylene-grafted multiwalled carbon nanotubes. *J. Appl. Polym. Sci.***2011**, *121*, 2104–2112, doi:10.1002/app.33892.

156. Narimani, A.; Hemmati, M. Effect of single-walled carbon nanotube on the physical, rheological and mechanical properties of thermoplastic elastomer based on PP/EPDM. *Sci. Eng. Compos. Mater.***2013**, *21*, 15–21, doi:10.1515/secm-2012-0145.

157. Ma, L. X.; Ma, L.; He, Y. Thermal Conductivities and Mechanical Properties of EPDM Filled with Modified Carbon Nanotubes. *Key Eng. Mater.***2013**, *561*, 169–173, doi:10.4028/www.scientific.net/KEM.561.169.

158. George, J. J.; Bhowmick, A. K. Influence of matrix polarity on the properties of ethylene vinyl acetate-carbon nanofiller nanocomposites. *Nanoscale Res. Lett.***2009**, *4*, 655–664, doi:10.1007/s11671-009-9296-8.

159. Lu, Y.; Zhang, Y.; Xu, W. Flame Retardancy and Mechanical Properties of Ethylene-vinyl Acetate Rubber with Expandable Graphite/Ammonium Polyphosphate/Dipentaerythritol

System. *J. Macromol. Sci. Part B* **2011**, *50*, 1864–1872, doi:10.1080/00222348.2011.553168.

160. Yan, N.; Wu, J. K.; Zhan, Y. H.; Xia, H. S. Carbon nanotubes/carbon black synergistic reinforced natural rubber composites. *Plast. Rubber Compos.***2009**, *38*, 290–296, doi:10.1179/146580109X12473409436580.

161. Zhan, Y. H.; Liu, G. Q.; Xia, H. S.; Yan, N. Natural rubber/carbon black/carbon nanotubes composites prepared through ultrasonic assisted latex mixing process. *Plast. Rubber Compos.***2011**, *40*, 32–39, doi:10.1179/174328911X12940139029284.

162. Xing, W.; Wu, J.; Huang, G.; Li, H.; Tang, M.; Fu, X. Enhanced mechanical properties of graphene/natural rubber nanocomposites at low content. *Polym. Int.***2014**, *63*, 1674–1681, doi:10.1002/pi.4689.

163. Zhou, X.; Zhu, Y.; Gong, Q.; Liang, J. Preparation and properties of the powder SBR composites filled with CNTs by spray drying process. *Mater. Lett.***2006**, *60*, 3769–3775, doi:10.1016/j.matlet.2006.03.147.

164. Zhou, X.-W.; Zhu, Y.-F.; Liang, J. Preparation and properties of powder styrene–butadiene rubber composites filled with carbon black and carbon nanotubes. *Mater. Res. Bull.***2007**, *42*, 456–464, doi:10.1016/j.materresbull.2006.06.027.

165. Wang, C.; Zhang, Y. Effects of liquid polyisoprene and magnesium oxide on the mechanical properties of styrene-butadiene rubber/carbon nanotubes composite. *Polym. Compos.***2018**, *39*, E765–E771, doi:10.1002/pc.24164.

166. Valentini, L.; Biagiotti, J.; Kenny, J. M.; López Manchado, M. A. Physical and mechanical behavior of single-walled carbon nanotube/polypropylene/ethylene-propylene-diene rubber nanocomposites. *J. Appl. Polym. Sci.***2003**, *89*, 2657–2663, doi:10.1002/app.12319.

167. Narimani, A.; Hemmati, M. Effect of single-walled carbon nanotube on the physical, rheological and mechanical properties of thermoplastic elastomer based on PP/EPDM. *Sci. Eng. Compos. Mater.***2014**, *21*, 15–21, doi:10.1515/secm-2012-0145.

168 Payne, A. R. The dynamic properties of carbon black loaded natural rubber vulcanizates. Part II. *J. Appl. Polym. Sci.***1962**, *6*, 368–372, doi:10.1002/app.1962.070062115.

169. Bhattacharyya, S.; Sinturel, C.; Bahloul, O.; Saboungi, M. L.; Thomas, S.; Salvetat, J. P. Improving reinforcement of natural rubber by networking of activated carbon nanotubes. *Carbon N. Y.***2008**, *46*, 1037–1045, doi:10.1016/j.carbon.2008.03.011.

170. Nah, C.; Lim, J. Y.; Cho, B. H.; Hong, C. K.; Gent, A. N. Reinforcing rubber with carbon nanotubes. *J. Appl. Polym. Sci.***2010**, *118*, 1574–1581, doi:10.1002/app.32524.

171. George, N.; C.S., J. C.; Mathiazhagan, A.; Joseph, R. High performance natural rubber composites with conductive segregated network of multiwalled carbon nanotubes. *Compos. Sci. Technol.***2015**, *116*, 33–40, doi:10.1016/j.compscitech.2015.05.008.

172. Yang, K.; Zhang, T.; Zhu, C.; Zhang, P.; Zhao, S.; Guo, L. The reinforcing mechanism study of carbon nanotube in the NR matrix. *Polym. Bull.***2017**, *74*, 949–962, doi:10.1007/s00289-016-1755-7.

173. Kang, H.; Tang, Y.; Yao, L.; Yang, F.; Fang, Q.; Hui, D. Fabrication of graphene/natural rubber nanocomposites with high dynamic properties through convenient mechanical mixing. *Compos. Part B Eng.***2017**, *112*, 1–7,

174. Araby, S.; Meng, Q.; Zhang, L.; Kang, H.; Majewski, P.; Tang, Y.; Ma, J. Electrically and thermally conductive elastomer/graphene nanocomposites by solution mixing. *Polym. (United Kingdom)***2014**, *55*, 201–210, doi:10.1016/j.polymer.2013.11.032.

175. Aziz, S. A. A.; Mazlan, S. A.; Ismail, N. I. N.; Ubaidillah, U.; Choi, S. B.; Khairi, M. H.

A.; Yunus, N. A. Effects of multiwall carbon nanotubes on viscoelastic properties of magnetorheological elastomers. *Smart Mater. Struct.***2016**, *25*,077001/1-077001/10.

176. Mittal, G.; Dhanda, V.; Rheea, K.Y.; Park, S.J.; Lee, W.R. *A review on carbon nanotubes and graphene as fillers in reinforced polymer nanocomposites*, *J. Ind. Eng. Chem.* **2015**, *21*, 11-25, doi: 10.1016/j.jiec.2014.03.022.

177. Wipatkrut, P.; Poompradub, S. Exfoliation approach for preparing high conductive reduced graphite oxide and its application in natural rubber composites. *Mater. Sci. Eng. B Solid-State Mater. Adv. Technol.***2017**, *218*, 74–83, doi:10.1016/j.mseb.2017.02.007.

178. Zhang, X.; Wang, J.; Jia, H.; Yin, B.; Ding, L.; Xu, Z.; Ji, Q. Polyvinyl pyrrolidone modified graphene oxide for improving the mechanical, thermal conductivity and solvent resistance properties of natural rubber. *RSC Adv.***2016**, *6*, 54668–54678, doi:10.1039/c6ra11601a.

179. Zhao, L.; Sun, X.; Liu, Q.; Zhao, J.; Xing, W. Natural rubber/graphene oxide nanocomposites prepared by latex mixing. *J. Macromol. Sci. Part B Phys.***2015**, *54*, 581–592, doi:10.1080/00222348.2015.1019325.

180. Bian, J.; Lan Lin, H.; Xiong He, F.; Wang, L.; Wei Wei, X.; Chang, I.-T.; Lu, Y. Comparative study on the natural rubber nanocomposites reinforced with carbon black nanoparticles and graphite oxide nanosheets: Comparative Study on the Natural Rubber Nanocomposites Reinforced. *Polym. Compos.***2017**, *38*, 1427–1437, doi:10.1002/pc.23710.

181. Wu, X.; Lin, T. F.; Tang, Z. H.; Guo, B. C.; Huang, G. S. Natural rubber/graphene oxide composites: Effect of sheet size on mechanical properties and straininduced crystallization behavior. *Express Polym. Lett.***2015**, *9*, 672–685, doi:10.3144/expresspolymlett.2015.63.

182. Aguilar-Bolados, H.; Lopez-Manchado, M. A.; Brasero, J.; Avilés, F.; Yazdani-Pedram, M. Effect of the morphology of thermally reduced graphite oxide on the mechanical and

electrical properties of natural rubber nanocomposites. *Compos. Part B Eng.***2016**, *87*, 350–356, doi:10.1016/J.COMPOSITESB.2015.08.079.

183. Aguilar-Bolados, H.; Brasero, J.; Lopez-Manchado, M. A.; Yazdani-Pedram, M. High performance natural rubber/thermally reduced graphite oxide nanocomposites by latex technology. *Compos. Part B Eng.***2014**, *67*, 449–454, doi:10.1016/j.compositesb.2014.08.010.

184. Yan, N.; Xia, H.; Wu, J.; Zhan, Y.; Fei, G.; Chen, C. Compatibilization of natural rubber/high density polyethylene thermoplastic vulcanizate with graphene oxide through ultrasonically assisted latex mixing. *J. Appl. Polym. Sci.***2013**, *127*, 933–941, doi:10.1002/app.37861.

185. Li, Y.; Zhang, L.; Hou, Z. Preparation and Properties of Graphene Oxide/Glycidyl Methacrylate Grafted Natural Rubber Nanocomposites. *J. Polym. Environ.***2017**, *25*, 315–322, doi:10.1007/s10924-016-0817-0.

186. Wu, L. mei; Liao, S. quan; Zhang, S. jun; Bai, X. ying; Hou, X. Enhancement of mechanical properties of natural rubber with maleic anhydride grafted liquid polybutadiene functionalized graphene oxide. *Chinese J. Polym. Sci.* **2015**, *33*, 1058–1068, doi:10.1007/s10118-015-1652-9.

187. Wu, L.; Qu, P.; Zhou, R.; Wang, B.; Liao, S. Green synthesis of reduced graphene oxide and its reinforcing effect on natural rubber composites. *High Perform. Polym.***2015**, *27*, 486–496, doi:10.1177/0954008314555530.

188. Lin, Y.; Chen, Y.; Zeng, Z.; Zhu, J.; Wei, Y.; Li, F.; Liu, L. Effect of ZnO nanoparticles doped graphene on static and dynamic mechanical properties of natural rubbercomposites. *Compos. Part A Appl. Sci. Manuf.***2015**, *70*, 35–44.

189 . a) Mittal, V. Functional Polymer Nanocomposites with Graphene: A Review, *Macromol. Mater. Engg.* **2014**, 299, 906-931.190. b)Chen, Y.; Yin, Q.; Zhang, X.; Jia, H.; Ji, Q.; Xu, Z. Impact of various oxidation degrees of graphene oxide on the performance of styrene-butadiene rubber nanocomposites. *Polym. Eng. Sci.***2017**, doi:10.1002/pen.24729.

191. Yin, B.; Zhang, X.; Zhang, X.; Wang, J.; Wen, Y.; Jia, H.; Ji, Q.; Ding, L. Ionic liquid functionalized graphene oxide for enhancement of styrene-butadiene rubber nanocomposites. *Polym. Adv. Technol.***2017**, *28*, 293–302, doi:10.1002/pat.3886.

192. Lin, Y.; Liu, S.; Peng, J.; Liu, L. Constructing a segregated graphene network in rubber composites towards improved electrically conductive and barrier properties. *Compos. Sci. Technol.***2016**, *131*, 40–47, doi:10.1016/j.compscitech.2016.05.012.

193. Zhang, X.; Xue, X.; Yin, Q.; Jia, H.; Wang, J.; Ji, Q.; Xu, Z. Enhanced compatibility and mechanical properties of carboxylated acrylonitrile butadiene rubber/styrene butadiene rubber by using graphene oxide as reinforcing filler. *Compos. Part B Eng.***2017**, *111*, 243–250, doi:10.1016/j.compositesb.2016.12.003.

194. Xue, X.; Yin, Q.; Jia, H.; Zhang, X.; Wen, Y.; Ji, Q.; Xu, Z. Enhancing mechanical and thermal properties of styrene-butadiene rubber/carboxylated acrylonitrile butadiene rubber blend by the usage of graphene oxide with diverse oxidation degrees. *Appl. Surf. Sci.***2017**, *423*, 584–591, doi:10.1016/j.apsusc.2017.06.200.

195. Mensah, B.; Kumar, D.; Lim, D. K.; Kim, S. G.; Jeong, B. H.; Nah, C. Preparation and properties of acrylonitrile-butadiene rubber-graphene nanocomposites. *J. Appl. Polym.S ci.* **2015**, *132*, 42457, doi:10.1002/app.42457.

196. Cao, P.; Huang, C.; Zhang, L.; Yue, D. One-step fabrication of RGO/HNBR composites via selective hydrogenation of NBR with graphene-based catalyst. *RSC Adv.* **2015**, *5*, 41098–

41102, doi:10.1039/c5ra05271h.

197. Wang, H.; Yang, C.; Liu, R.; Gong, K.; Hao, Q.; Wang, X.; Wu, J.; Zhang, G.; Hu, Y.; Jiang, J. Build a Rigid–Flexible Graphene/Silicone Interface by Embedding SiO_2 for Adhesive Application. *ACS Omega* **2017**, *2*, 1063–1073, doi:10.1021/acsomega.7b00017.

198. Gan, L.; Shang, S.; Jiang, S. X. Impact of vinyl concentration of a silicone rubber on the properties of the graphene oxide filled silicone rubber composites. *Compos. Part B Eng.***2016**, *84*, 294–300, doi:10.1016/j.compositesb.2015.08.073.

199. Zhao, X.; Zang, C.; Wen, Y.; Jiao, Q. Thermal and mechanical properties of liquid silicone rubber composites filled with functionalized graphene oxide. *J. Appl. Polym. Sci.***2015**, *132*, n/a-n/a, doi:10.1002/app.42582.

200 Zhang, Y.; Zhu, Y.; Lin, G.; Ruoff, R. S.; Hu, N.; Schaefer, D. W.; Mark, J. E. What factors control the mechanical properties of poly (dimethylsiloxane) reinforced with nanosheets of 3-aminopropyltriethoxysilane modified graphene oxide? *Polym.(United Kingdom)* **2013**, *54*, 3605–3611, doi:10.1016/j.polymer.2013.04.057.

201, Allahbakhsh, A.; Mazinani, S. Influences of sodium dodecyl sulfate on vulcanization kinetics and mechanical performance of EPDM/graphene oxide nanocomposites. *RSC Adv.***2015**, *5*, 46694–46704, doi:10.1039/c5ra00394f.

202. Cecen, V.; Thomann, R.; Mülhaupt, R.; Friedrich, C. Thermal conductivity, morphology and mechanical properties for thermally reduced graphite oxide-filled ethylene vinylacetate copolymers. *Polym. (United Kingdom)* **2017**, *132*, 294–305, doi:10.1016/j.polymer.2017.11.009.

203. Yaragalla, S.; Meera, A.P.; Kalarikkal, N.; Thomas, S. Chemistry associated with natural rubber–graphene nanocomposites and its effect on physical and structural properties, *Industrial Crops and Products* **2015**, *74*, 792–802.

204. Wu, L.; Qu, P.; Zhou, B.; Liao, S. Green synthesis of reduced graphene oxide and its reinforcing effect on natural rubber composites, *High Performance Polymers* **2015**, *27*, 486–496

205. Yang, G.; Liao.; Yang, Z.; Liao, Z.; Tang, Z.; Guo, B. Effects of substitution for carbon black with graphene oxide or graphene on the morphology and performance of natural rubber/carbon black composites, *J. Appl. Polym. Sci.* **2015**, *132*, 41832.

206. Yin, B.; Wang, J.; Jia, H.; Xu, X. Enhanced mechanical properties and thermal conductivity of styrene–butadiene rubber reinforced with polyvinylpyrrolidone-modified graphene oxide, *J. Mater. Sci.* **2016**, *51*, 5724–5737 DOI: 10.1007/s10853-016-9874.

207. Bhiyan, B.; Srivastava, S.K.; Piontecj, J. Multiwalled carbon nanotubes/Hectorite hybrid reinforced styrene butadiene rubber nanocomposite: Preparation and properties, *Polym. Plastics Technol. Engg.* **2018**, 1-8.

208. Bhiyan, B.; Srivastava, S.K.; Mittal, V. Ethylene-co-vinyl acetate/MWCNTs/Hectorite elastomeric nanocomposites: Characterization and electrical properties, *J. Nanosci. Nanotechnol.* **2018**, *18*, 4057-4064.

209. Bhiyan, B.; Srivastava, S.K.; Mittal, Multiwalled carbon nanotube/montmorillonite hybrid filled ethylene-co-vinyl acetate nanocomposites with enhanced mechanical properties, thermal stability, and dielectric response, *Polym. Engg. Sci.* **2018**, *58*, 1155-1165.

210. Muhulet, A.; Miculescu, F.; Voicu, S. I.; Schütt, F.; Thakur, V. K.; Mishra, Y. K. Fundamentals and scopes of doped carbon nanotubes towards energy and biosensing applications, *Materials Today Energy* **2018**, *9*, 154-186, doi:10.1016/j.mtener.2018.05.002.

211. Mishra, Y. K.; Adelung, R. ZnO tetrapod materials for functional applications, *Materials Today* **2018**, *21*, 631-651, doi:10.1016/j.mattod.2017.11.003

212. Plesco, I.; Strobel, J.; Schütt, F.; Himcinschi, C.; Sedrine, N. B.; Monteiro, T.; Correia, M. R.; Gorceac, L.; Cinic, B.; Ursaki, V:, Marx, J.; Fiedler, B.; Mishra, Y. K.; Kienle, L.; Adelung, R.; Tiginyanu, I. Hierarchical Aerographite 3D flexible networks hybridized by InP micro/nanostructures for strain sensor applications, *Sci. Rep.* **2018**, *8*, 13880, doi: 10.1038/s41598-018-32005-0

213. Schütt, F.; Signetti, S.; Krüger, H.; Röder, S.; Smazna, D.; Kaps, S.; Gorb, S. N.; Mishra, Y. K.; Pugno, N. M.; Adelung, R. Hierarchical self-entangled carbon nanotube tube networks, *Nat. Commun.* **2017**, 8, 1215, doi: 10.1038/s41467-017-01324-7.

214. Silva, E. L.; Mishra, Y. K.; Fernandes, A. J. S.; Silva, R. F.; Strobel, J.; Kienle, L.; Adelung, R.; Oliveira, F. J.; Zheludkevich, M. L. Direct Synthesis of Electrowettable carbon nanowall–diamond hybrid materials from sacrificial ceramic templates using HFCVD, *Adv. Mater. Interfaces* **2017**, *4*, 1700019, doi: 10.1002/admi.201700019.

215. Garlof, S.; Mecklenburg, M.; Smazna, D.; Mishra, Y. K.; Adelung, R.; Schulte, K.; Fiedler, B. 3D carbon networks and their polymer composites: Fabrication and electromechanical investigations of neat Aerographite and Aerographite-based PNCs under compressive load, *Carbon* **2017**, *111*, 103-112, doi:10.1016/j.carbon.2016.09.046.

216. Garlof, S.; Fukuda, T.; Mecklenburg, M.; Smazna, D.; Mishra, Y. K.; Adelung, R.; Fiedler, B.; Schulte, K. Electro-mechanical piezoresistive properties of three dimensionally

interconnected carbon aerogel (Aerographite)-epoxy composites, *Composite Sci. Technol.* **2016**, *134*, 226-233, doi: 10.1016/j.compscitech.2016.08.019.

217. Nasajpour, A.; Mandla, S.; Shree, S.; Mostafavi, E.; Sharifi, R.; Khalilpour, A.; Saghazadeh, S.; Hassan, S.; Mitchell, M. J.; Leijten, J.; Hou, X.; Moshaverinia, A.; Annabi, N.; Adelung, R.; Mishra, Y. K.; Shin, S. R.; Tamayol, A.; Khademhosseini, A. Nanostructured fibrous membranes with rose spike-like architecture, *Nano Lett.* **2017**, *25*, 1342-1347, doi: 10.1021/acs.nanolett.7b02929.

218. Hölken, I.; Hoppe, M.; Mishra, Y. K.; Gorb, S. N.; Adelung, R.; Baum, M. J. Complex shaped ZnO nano-and microstructure based polymer composites: mechanically stable and environmentally friendly coatings for potential antifouling applications, *Phys. Chem. Chem. Phys.* **2016**, *18*, 7114-7123, doi:10.1039/C5CP07451G.

219. Mishra, Y. K.; Kaps, S.; Schuchardt, A.; Paulowicz, I.; Jin, X.; Gedamu, D.; Freitag, S.; Claus, M.; Wille, S.; Kovalev, A.; Gorb, S. N.; Adelung, R. Fabrication of macroscopically flexible and highly porous 3D semiconductor networks from interpenetrating nanostructures by a simple flame transport approach, *Part. Part. Syst. Charact.* **2013**, *30*, 775-783, doi: 10.1002/ppsc.201300197.

220. Jin, X.; Götz, M.; Wille, S.; Mishra, Y. K.; Adelung, R.; Zollfrank, C. A novel concept for self-reporting materials: Stress sensitive photoluminescence in ZnO tetrapod filled elastomers, *Adv. Mater.* **2013**, *25*, 1342-1347, doi: 10.1002/adma.201203849.

221. Shree, S:, Schulz-Senft, M.; Alsleben, N. H.; Mishra, Y. K.; Staubitz, A.; Adelung, R. Light, force and heat: A multi-stimuli composite that reveals its violent past, *ACS Appl. Mater. Interfaces* **2017**, *9*, 38000-38007, doi: 10.1021/acsami.7b09598.

222. Mecklenburg, M.; Schuchardt, A.; Mishra, Y. K.; Kaps, S.; Adelung, R.; Lotnyk, A.; Kienle, L.; Schulte, K. Aerographite: ultra lightweight, flexible nanowall, carbon microtube material with outstanding mechanical performance, *Adv. Mater.* **2012**, *24*, 3486-3490, doi: https://doi.org/10.1002/adma.201200491.

Preprints (www.preprints.org) | NOT PEER-REVIEWED | Posted: 24 September 2018 doi:10.20944/preprints201809.0464.v1

Peer-reviewed version available at *Nanomaterials* **2018**, *8*, 945; doi:10.3390/nano8110945

Figures and Captions

Figure 1

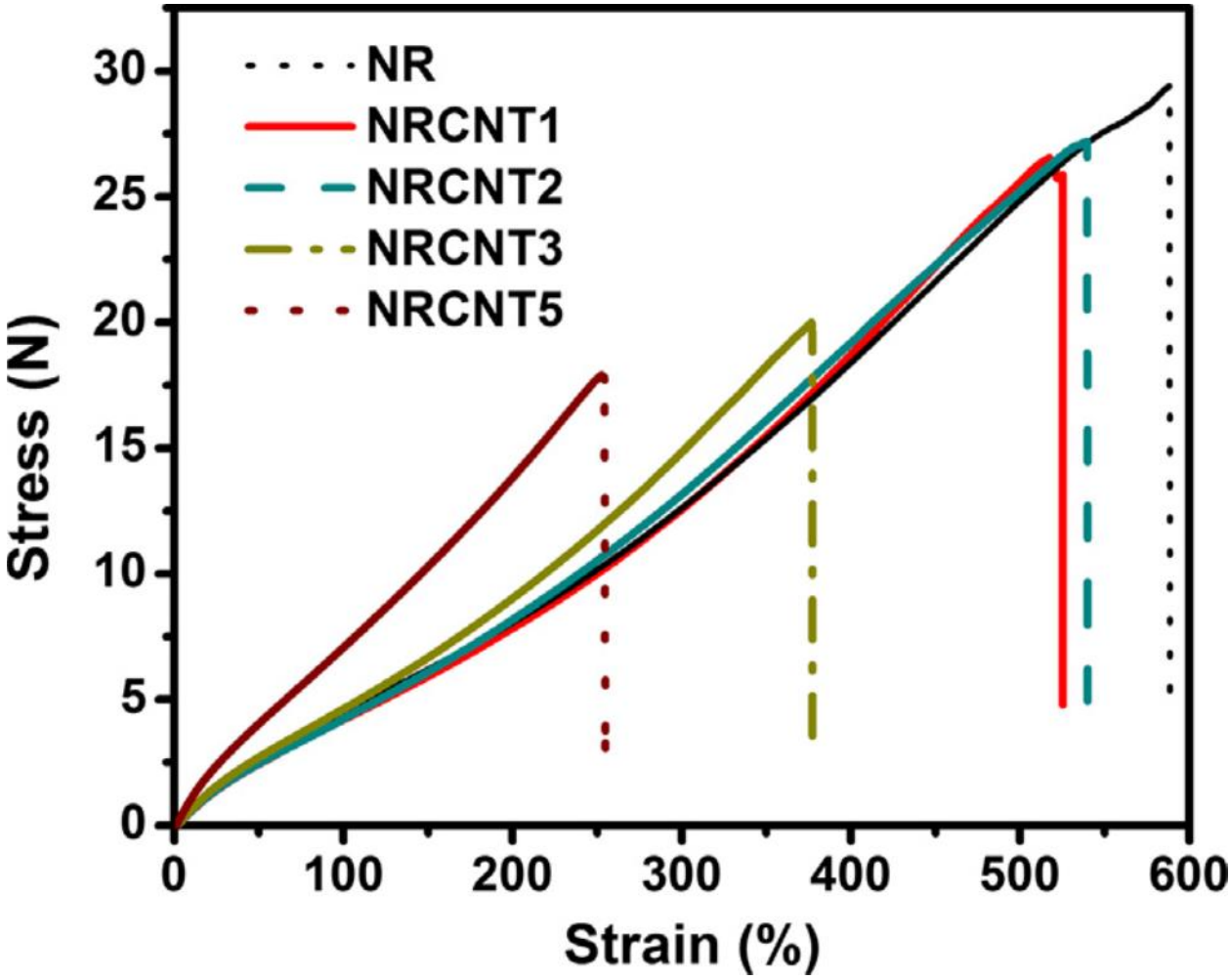

Figure 1: Stress–strain curves for pure NR and NR/MWCNT composites. Reproduced with permission from Elsevier [23].

Figure 2

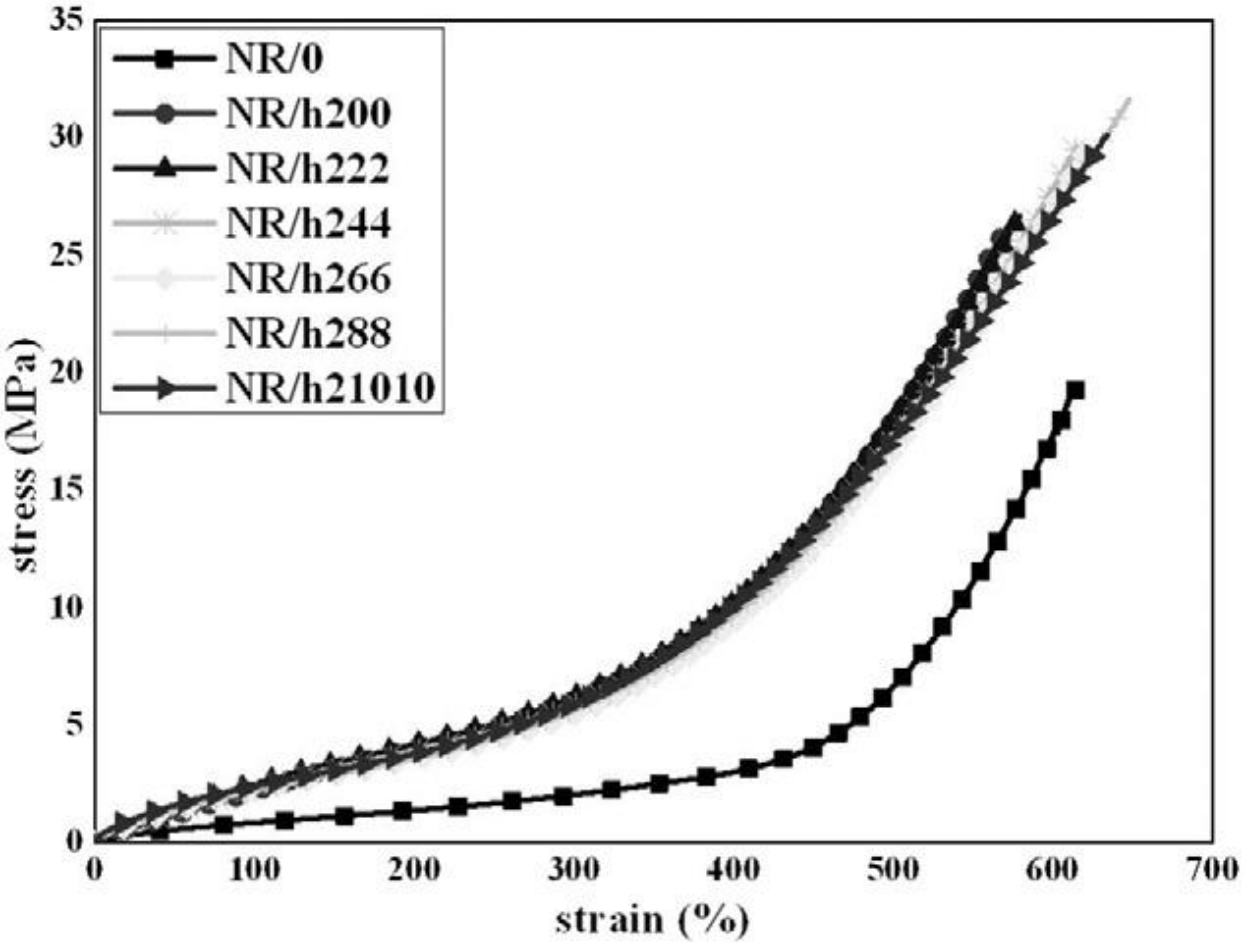

Figure 2: Stress–strain curves of NR/0 and different NR/MWCNT/EOMt nanocomposites. Reproduced with permission from Elsevier [44].

Preprints (www.preprints.org) | NOT PEER-REVIEWED | Posted: 24 September 2018 doi:10.20944/preprints201809.0464.v1

Peer-reviewed version available at Nanomaterials 2018, 8, 945; doi:10.3390/nano8110945

Figure 3

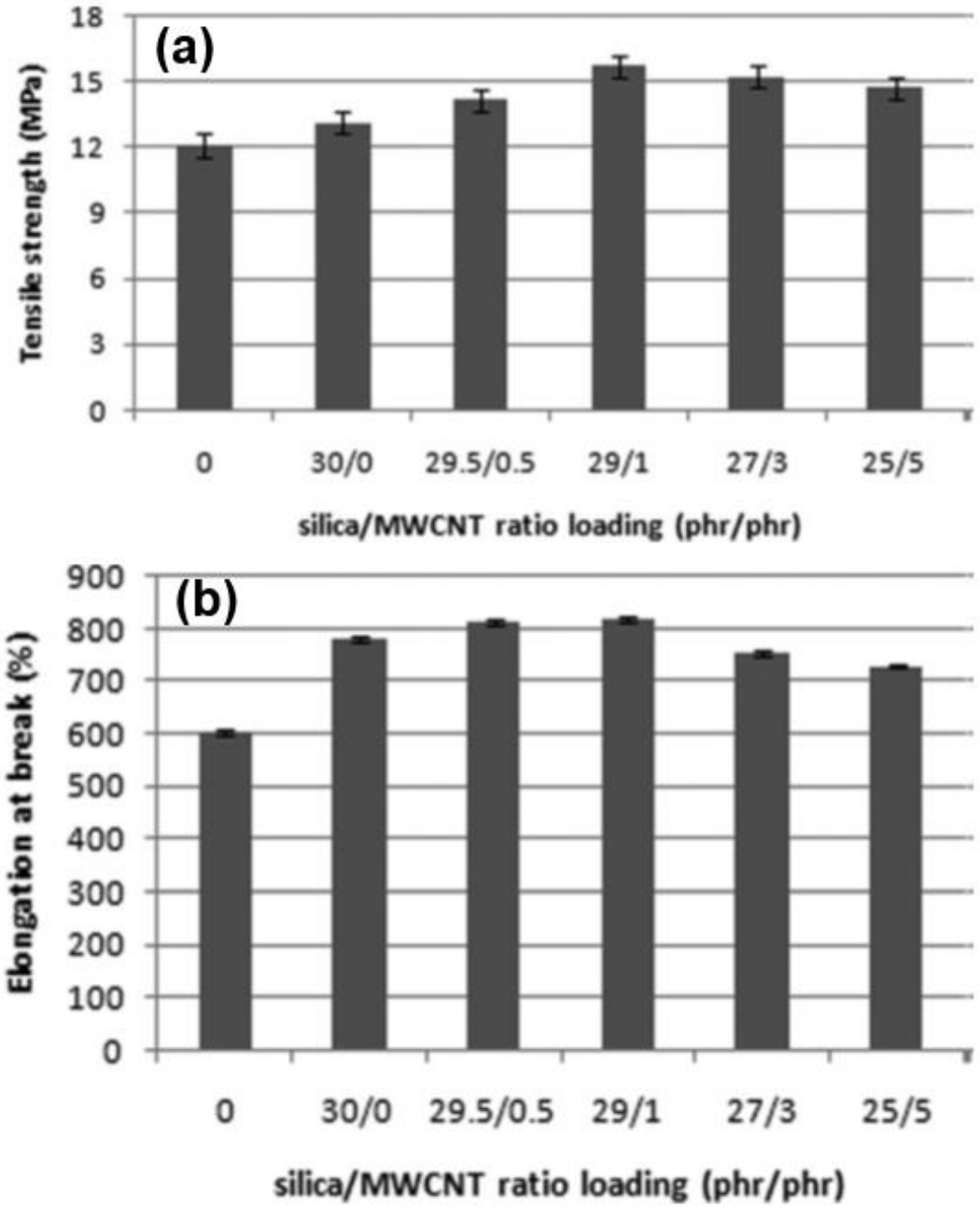

Figure 3: (a) Effect of the silica/MWCNT hybrid loading ratio on the tensile strength of the NR/silica/MWCNT hybrid nanocomposites. **(b)** Effect of the silica/NWCNT hybrid loading ratio on the EB of the NR/silica/MWCNT hybrid nanocomposites. Reproduced with permission from Wiley [34].

Preprints (www.preprints.org) | NOT PEER-REVIEWED | Posted: 24 September 2018 doi:10.20944/preprints201809.0464.v1

Peer-reviewed version available at Nanomaterials 2018, 8, 945; doi:10.3390/nano8110945

Figure 4

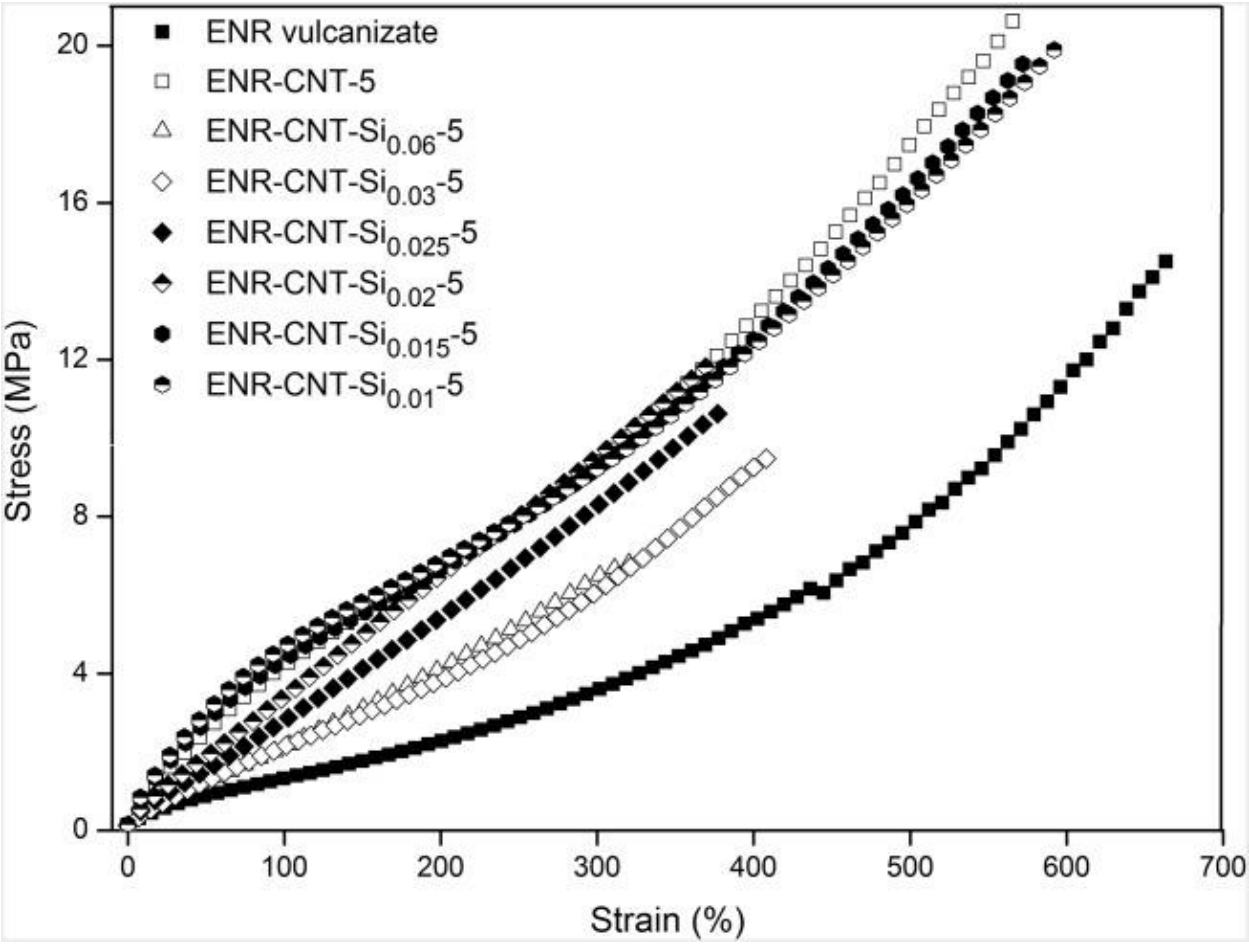

Figure 4: Stress–strain curves of ENR vulcanizate and ENR-CNT composites without and with APTES at concentrations from 0.06 to 0.01 mL/ (g of CNTs). Reproduced with permission from Wiley [40].

Preprints (www.preprints.org) | NOT PEER-REVIEWED | Posted: 24 September 2018 doi:10.20944/preprints201809.0464.v1

Peer-reviewed version available at *Nanomaterials* **2018**, *8*, 945; doi:10.3390/nano8110945

Figure 5

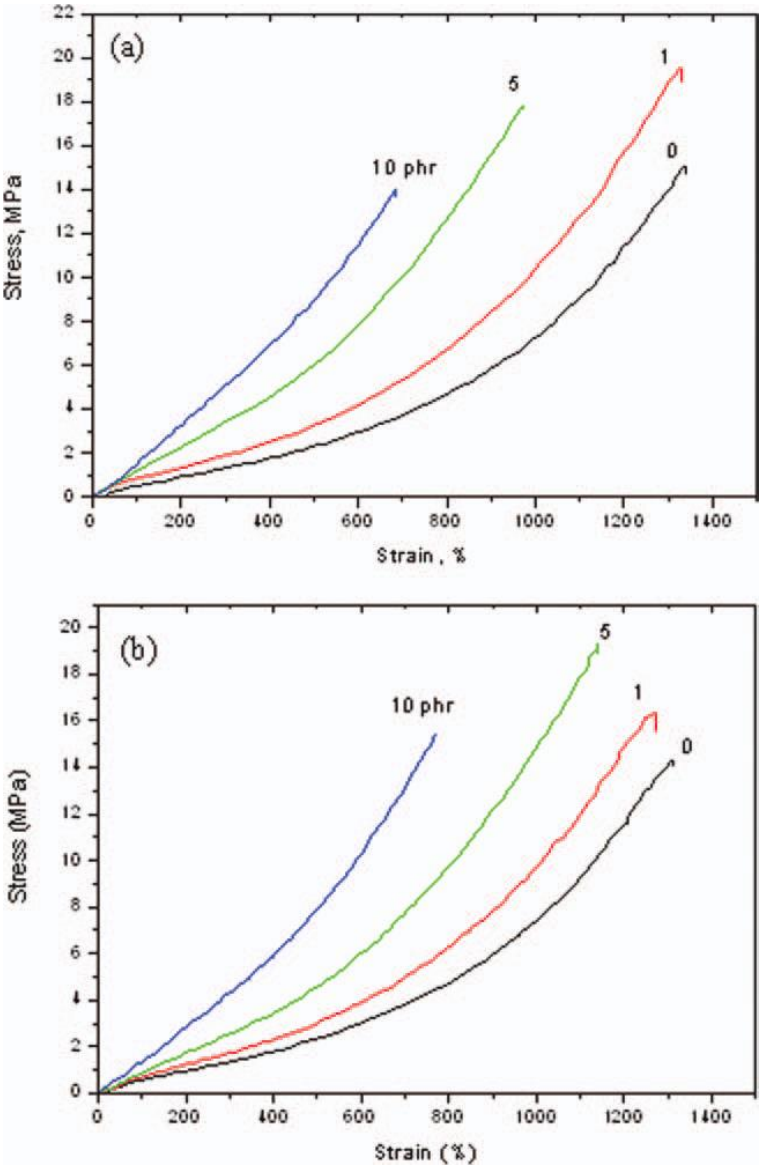

Figure 5: Stress-strain curves of NR composites with **(a)** CNT and **(b)** phenol functionalized CNT. Reproduced with permission from Wiley [62].

Preprints (www.preprints.org) | NOT PEER-REVIEWED | Posted: 24 September 2018 doi:10.20944/preprints201809.0464.v1

Peer-reviewed version available at Nanomaterials 2018, 8, 945; doi:10.3390/nano8110945

Figure 6

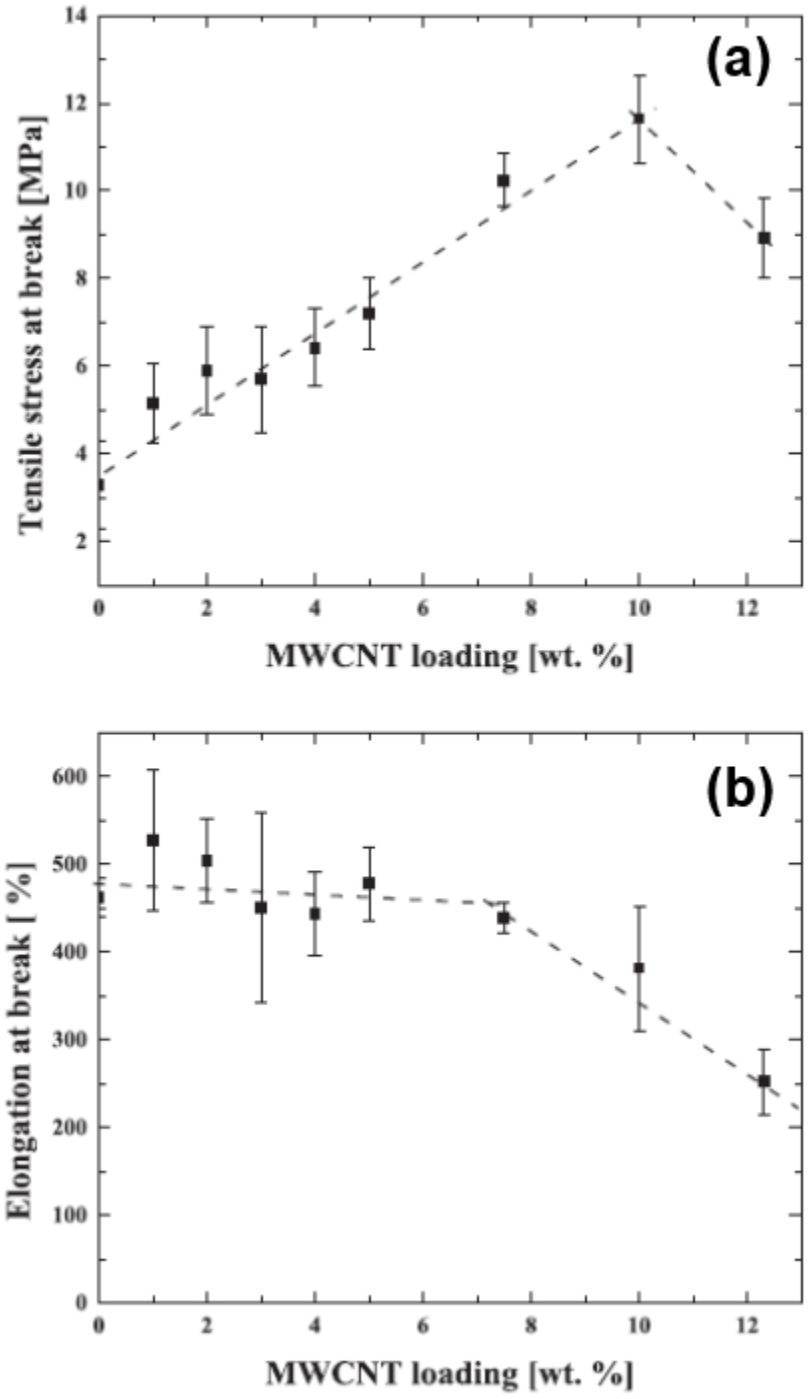

Figure 6: (a) Tensile stress at break, **(b)** elongation at break as a function of MWCNT loading. Reproduced with permission from Elsevier [69].

Figure 7

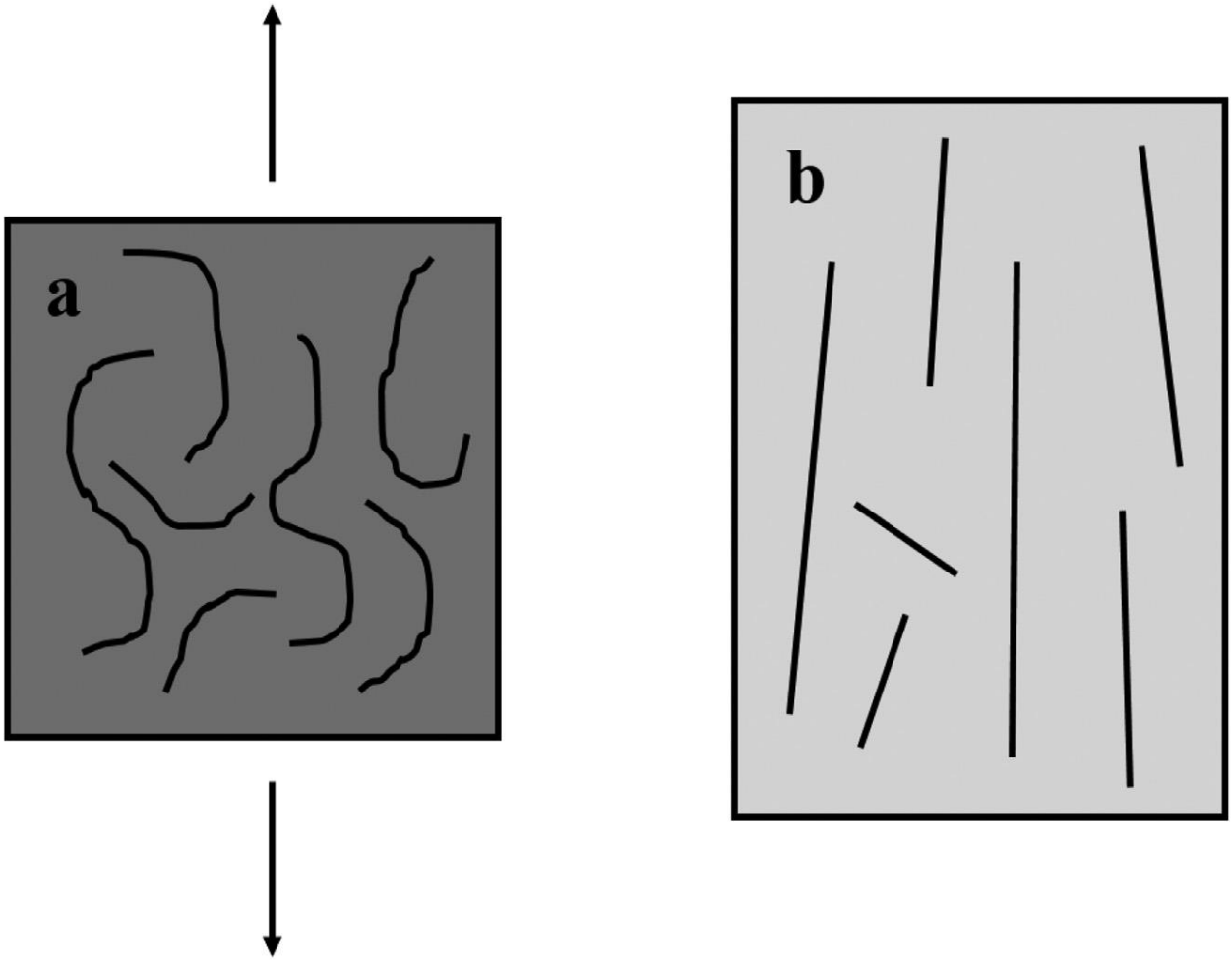

Figure 7: (a) Composite sample with coiled MWCNTs before stretching. **(b)** Stretched sample with straight MWCNTs. Reproduced with permission from Elsevier [69].

Preprints (www.preprints.org) | NOT PEER-REVIEWED | Posted: 24 September 2018 doi:10.20944/preprints201809.0464.v1

Peer-reviewed version available at Nanomaterials 2018, 8, 945; doi:10.3390/nano8110945

Figure 8

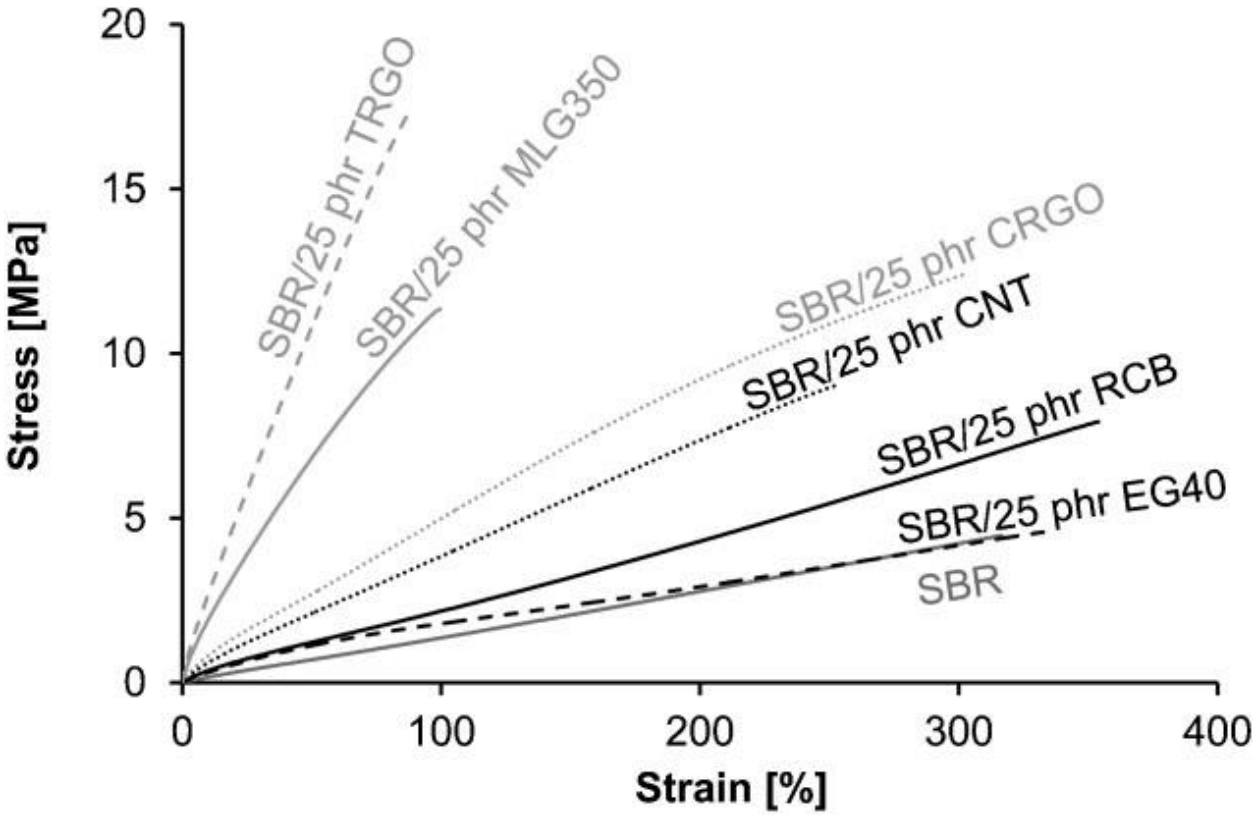

Figure 8: Stress/strain curves of SBR with 25 phr of different carbon fillers. Reproduced with permission from Wiley [79].

Preprints (www.preprints.org) | NOT PEER-REVIEWED | Posted: 24 September 2018 doi:10.20944/preprints201809.0464.v1

Peer-reviewed version available at Nanomaterials 2018, 8, 945; doi:10.3390/nano8110945

Figure 9

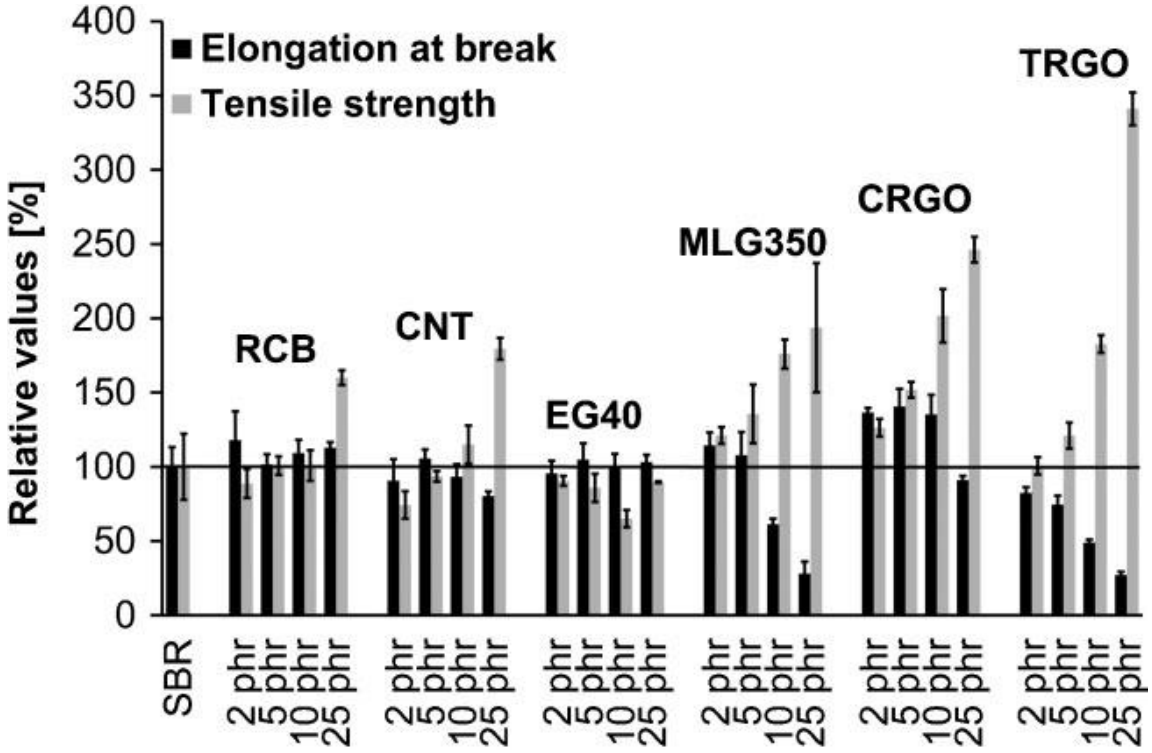

Figure 9: Elongation at break and tensile strength for SBR/C filler composites relative to neat SBR. Reproduced with permission from Wiley [79].

Preprints (www.preprints.org) | NOT PEER-REVIEWED | Posted: 24 September 2018 doi:10.20944/preprints201809.0464.v1

Peer-reviewed version available at Nanomaterials 2018, 8, 945; doi:10.3390/nano8110945

Figure 10

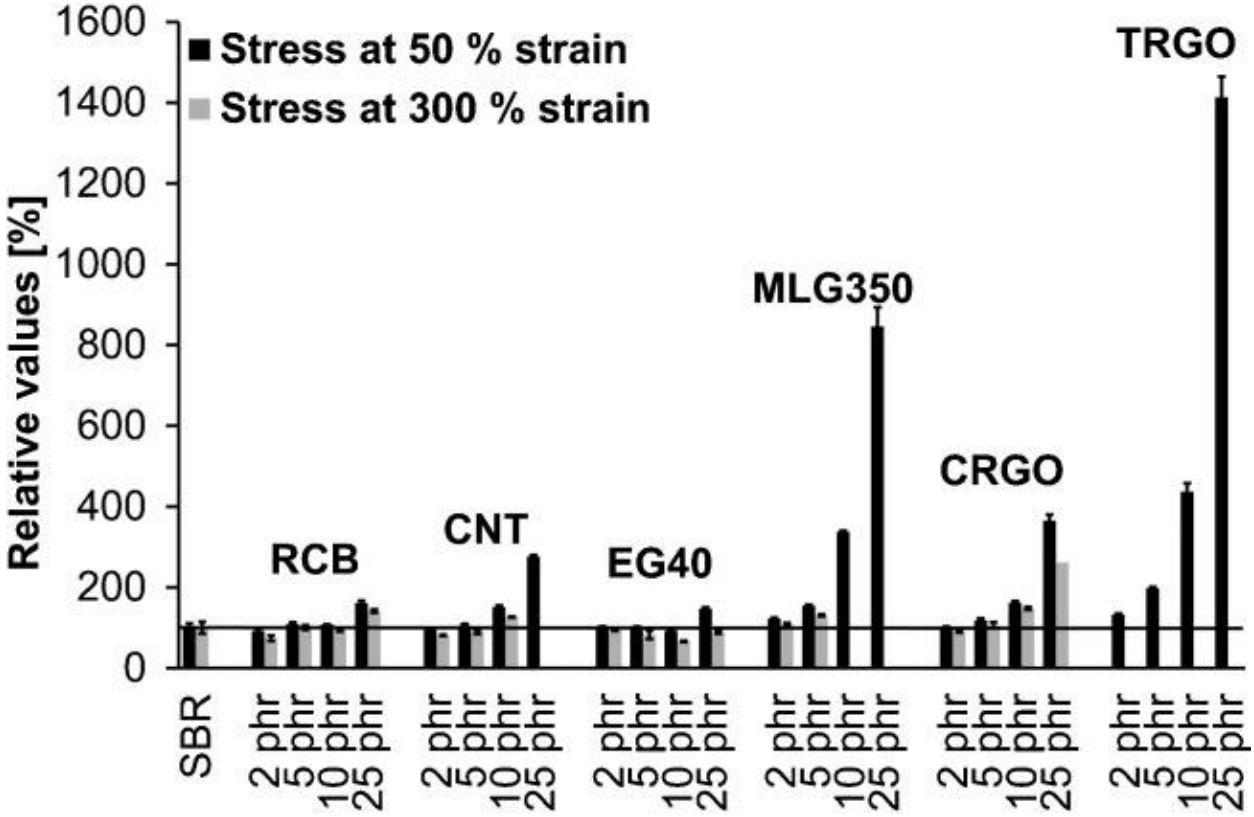

Figure 10: Stress at 50 and 300% strain of SBR/C based fillers as relative values compared to neat SBR. Reproduced with permission from Wiley [79].

Figure 11

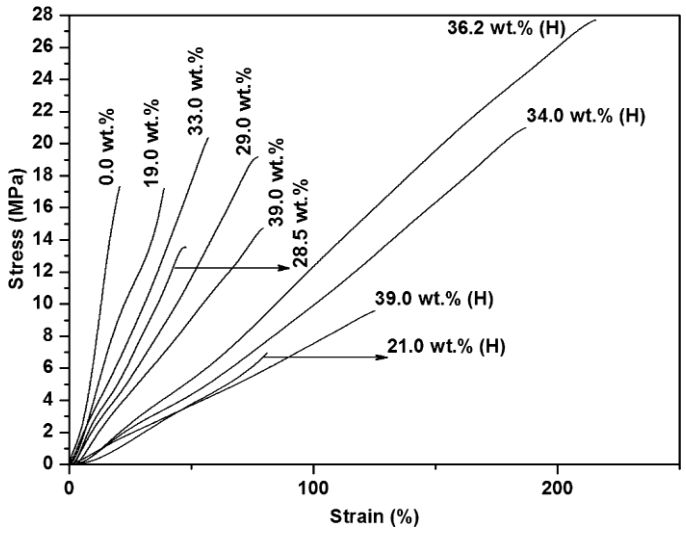

Figure 11: Characterization of mechanical properties–tensile properties (stress vs. strain) of (H)NBR/MWCNT nanocomposites with different AN contents prepared by MC. Reproduced with permission from Elsevier [100].

Preprints (www.preprints.org) | NOT PEER-REVIEWED | Posted: 24 September 2018 doi:10.20944/preprints201809.0464.v1

Peer-reviewed version available at Nanomaterials 2018, 8, 945; doi:10.3390/nano8110945

Figure 12

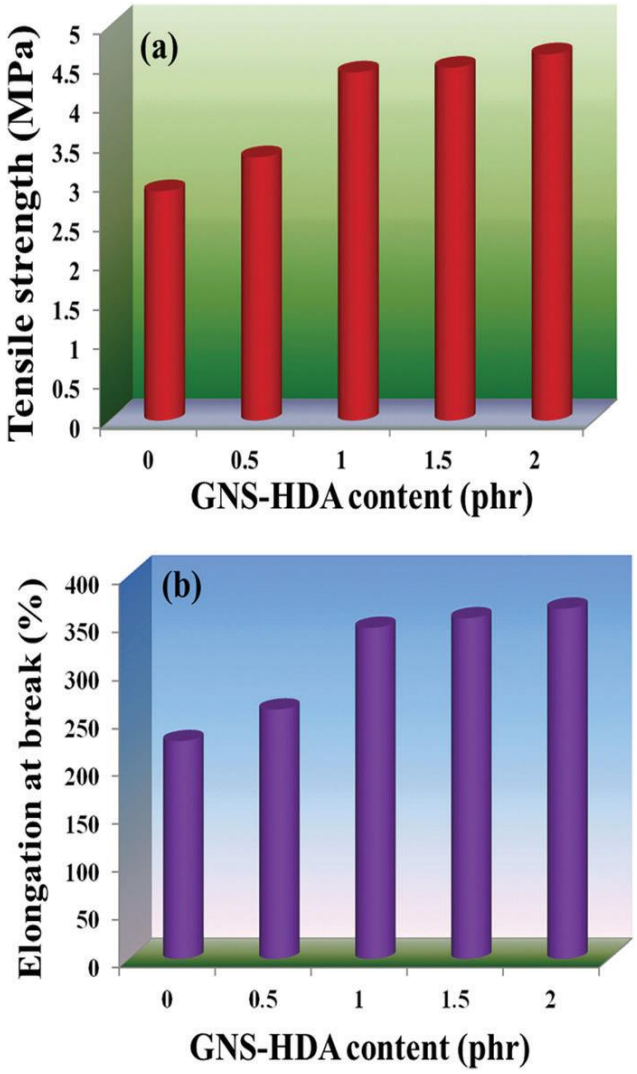

Figure 12: **(a)** Tensile strength and **(b)** elongation at break of neat XNBR and various GNS–HDA/XNBR composites. Reproduced with permission from RSC [104].

Preprints (www.preprints.org) | NOT PEER-REVIEWED | Posted: 24 September 2018 doi:10.20944/preprints201809.0464.v1

Peer-reviewed version available at Nanomaterials 2018, 8, 945; doi:10.3390/nano8110945

Figure 13

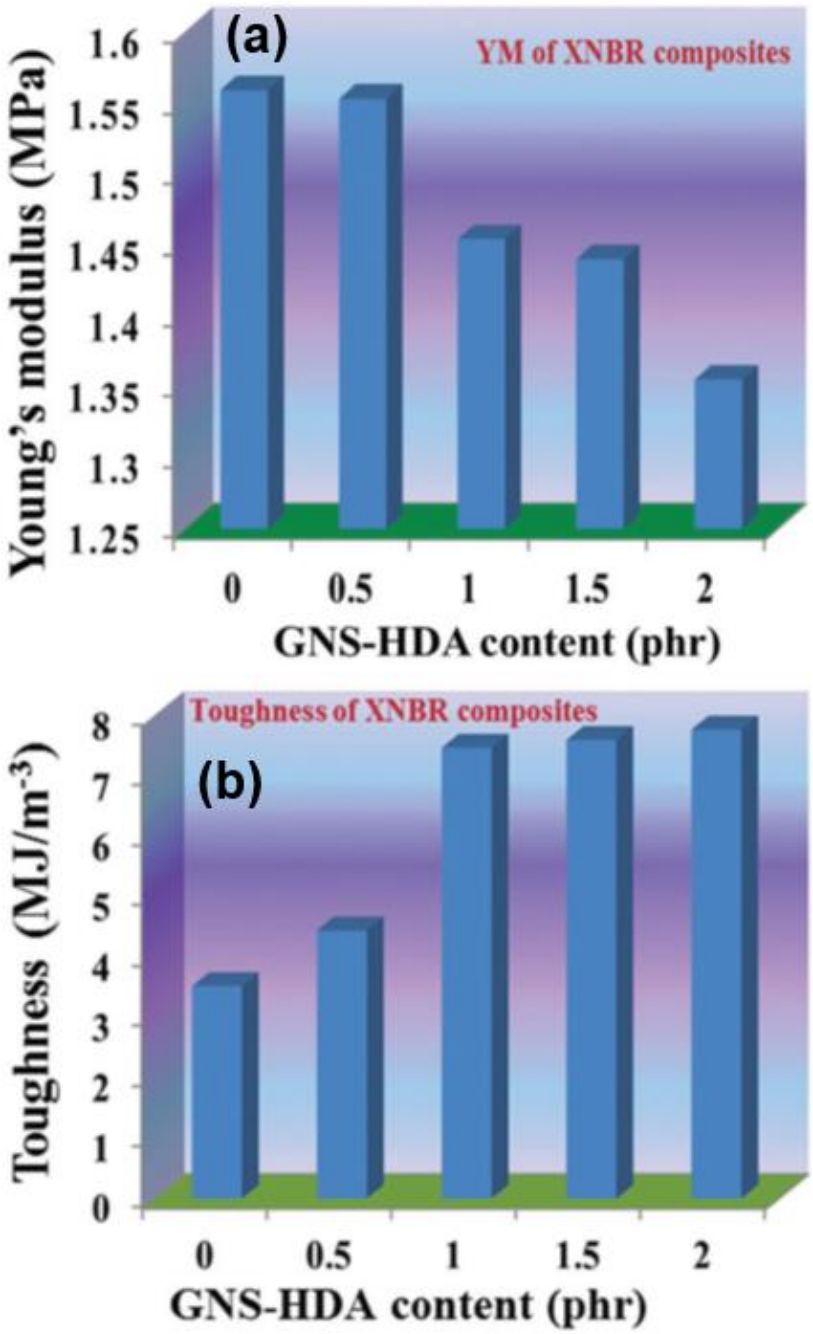

Figure 13: (a) Young's modulus of neat XNBR and various GNS–HDA/XNBR composites. **(b)** Toughness of neat XNBR and various GNS–HDA/XNBR composites. Reproduced with permission from RSC [104].

Figure 14

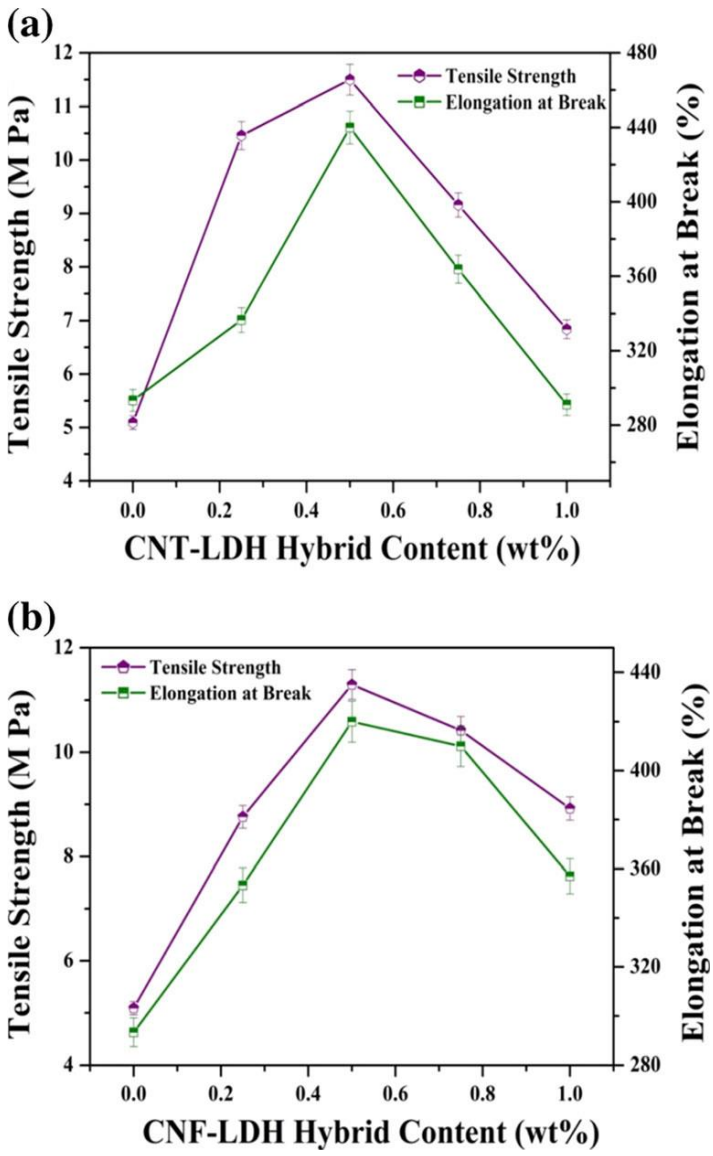

Figure 14: (a) Variation of tensile strength and elongation at break of TN nanocomposites with SFCNT-LDH hybrid content. (b) Variation of tensile strength and elongation at break of TN nanocomposites with SFCNFLDH hybrid content. Reproduced with permission from Springer [112].

Preprints (www.preprints.org) | NOT PEER-REVIEWED | Posted: 24 September 2018 doi:10.20944/preprints201809.0464.v1

Peer-reviewed version available at Nanomaterials 2018, 8, 945; doi:10.3390/nano8110945

Figure 15

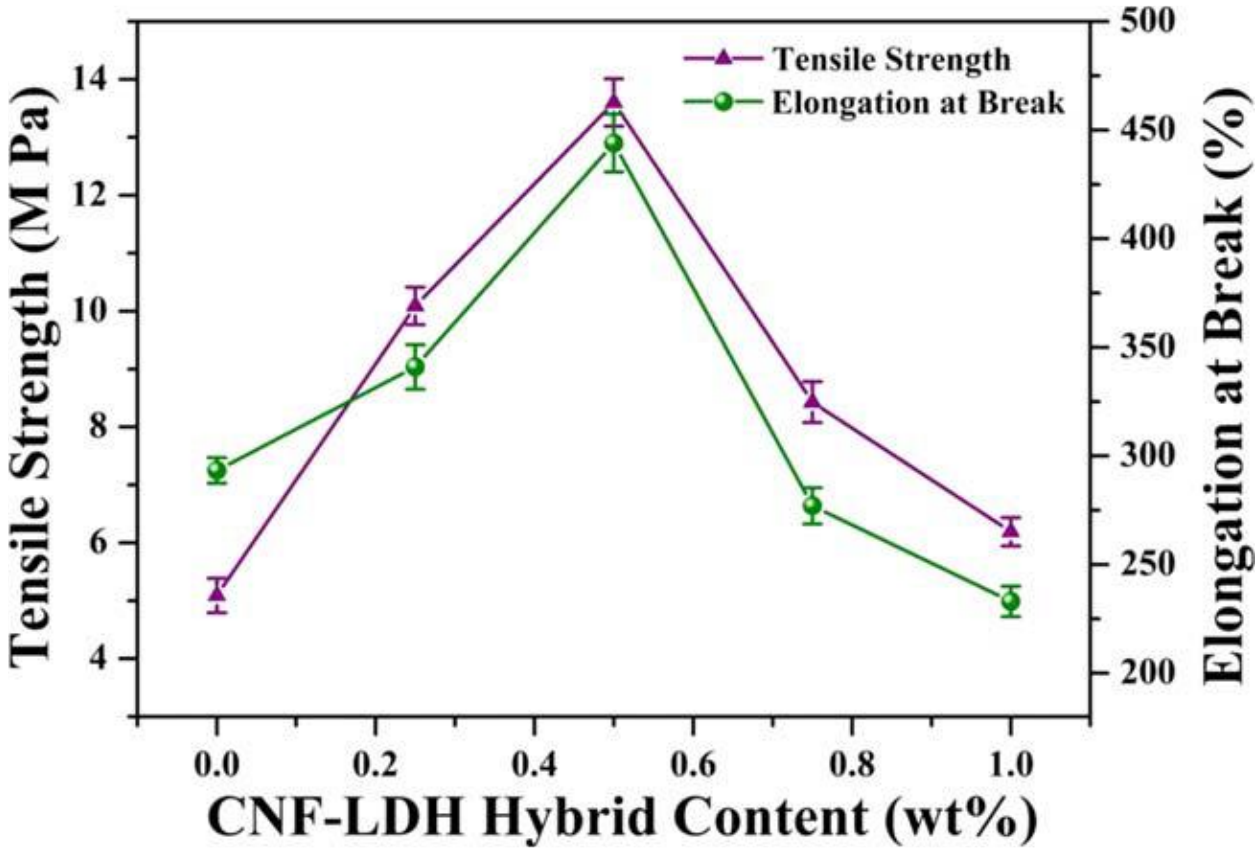

Figure 15: Variation of the tensile strength and elongation at break of the TN nanocomposites versus the SFCNF–LDH hybrid content. Reproduced with permission from Wiley [113].

Preprints (www.preprints.org) | NOT PEER-REVIEWED | Posted: 24 September 2018 doi:10.20944/preprints201809.0464.v1

Peer-reviewed version available at Nanomaterials 2018, 8, 945; doi:10.3390/nano8110945

Figure 16

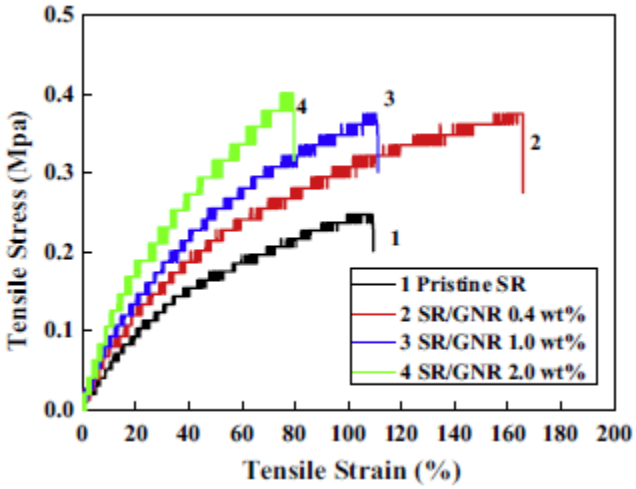

Figure 16: Typical stress–strain behaviors of the pristine SR and the SR/GNR nanocomposites. Reproduced with permission from Elsevier [135].

Preprints (www.preprints.org) | NOT PEER-REVIEWED | Posted: 24 September 2018 doi:10.20944/preprints201809.0464.v1

Peer-reviewed version available at Nanomaterials 2018, 8, 945; doi:10.3390/nano8110945

Figure 17

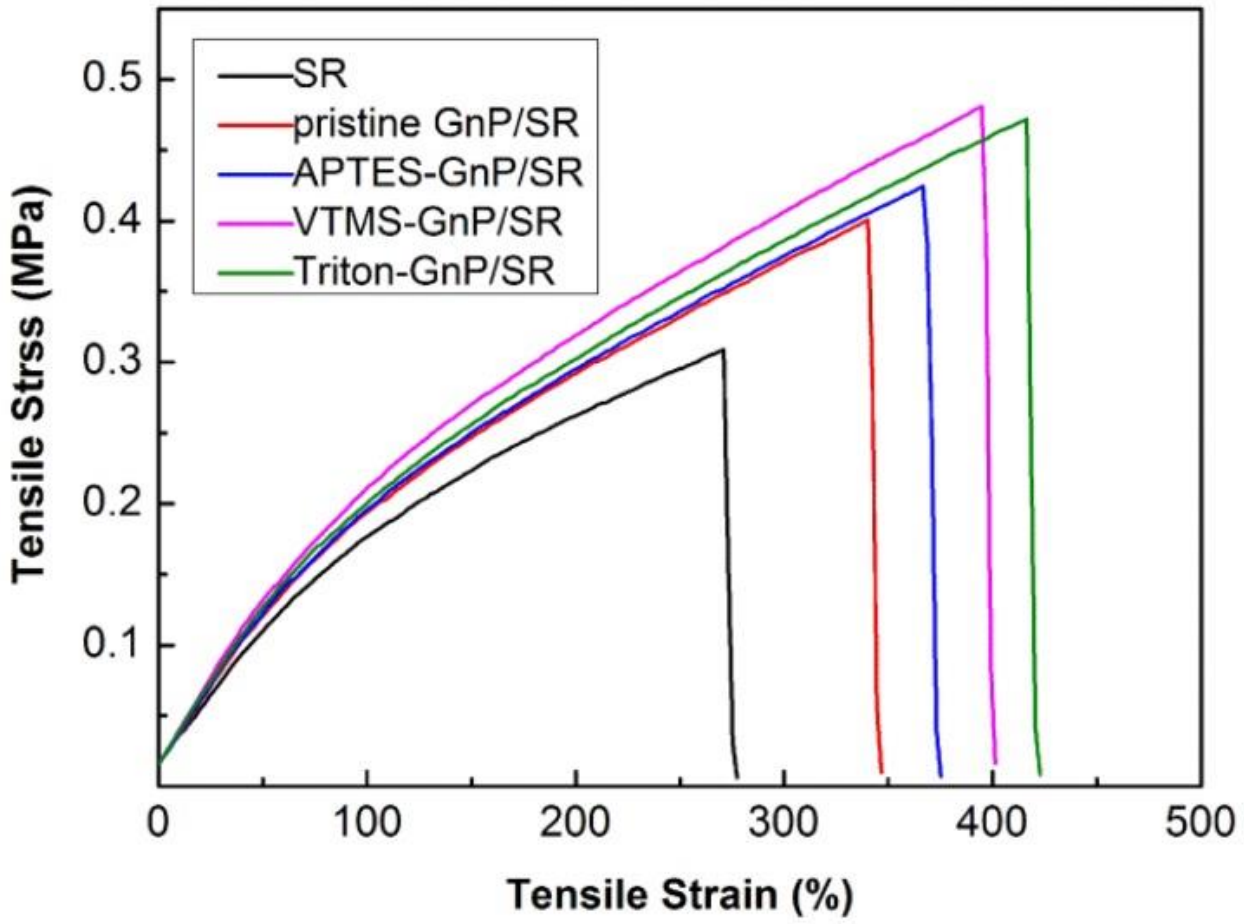

Figure 17. Typical stress–strain curves of neat silicone rubber (SR) and the composites filled with various GNP. Reproduced with permission from Wiley [137]

Preprints (www.preprints.org) | NOT PEER-REVIEWED | Posted: 24 September 2018 doi:10.20944/preprints201809.0464.v1

Peer-reviewed version available at Nanomaterials 2018, 8, 945; doi:10.3390/nano8110945

Figure 18

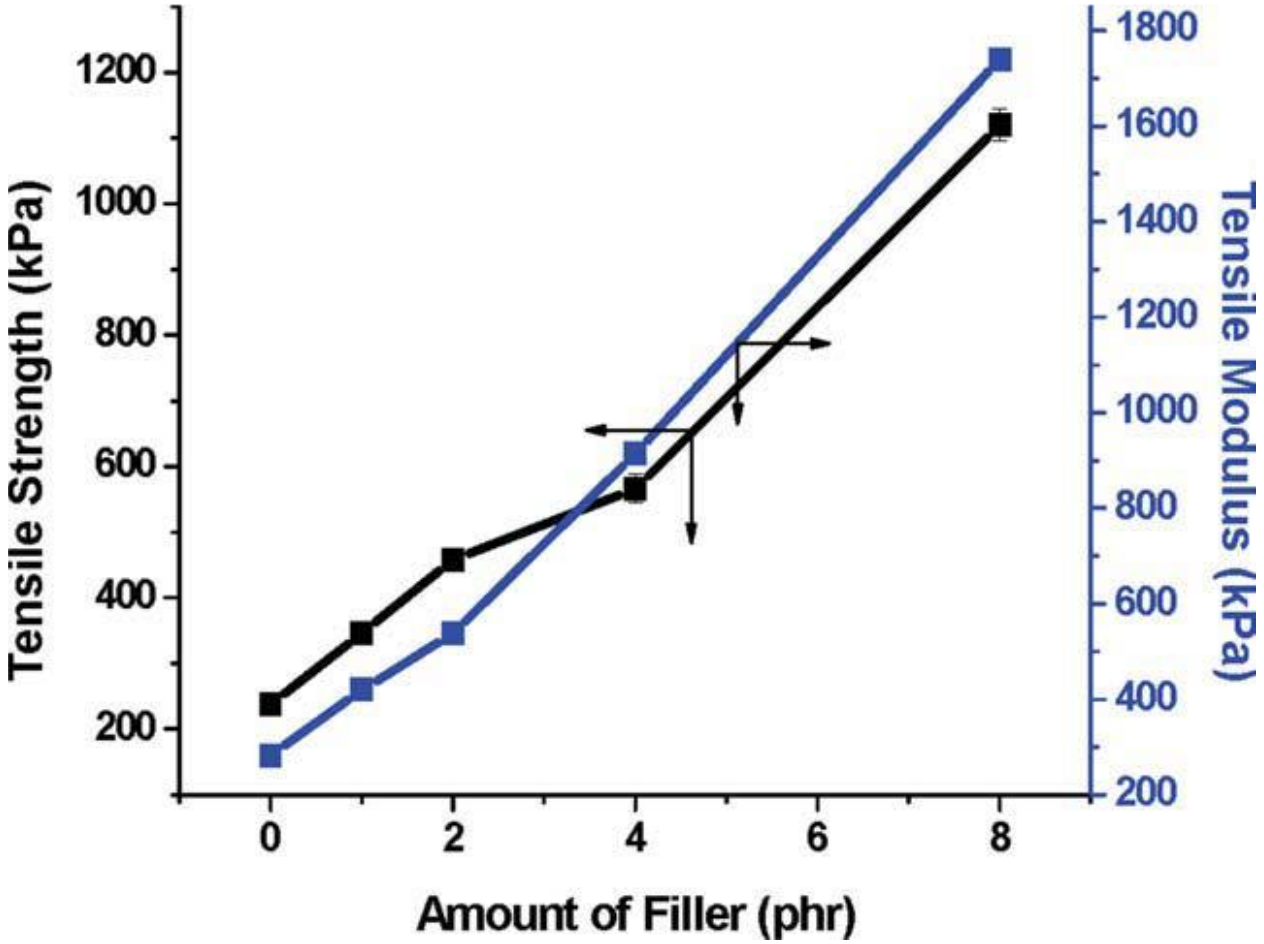

Figure 18: Plot of tensile strength and tensile modulus for in situ prepared amine modified CNF-hydroxyl PDMS nanocomposites as a function of filler loading. [138].

Preprints (www.preprints.org) | NOT PEER-REVIEWED | Posted: 24 September 2018 doi:10.20944/preprints201809.0464.v1

Peer-reviewed version available at Nanomaterials 2018, 8, 945; doi:10.3390/nano8110945

Figure 19

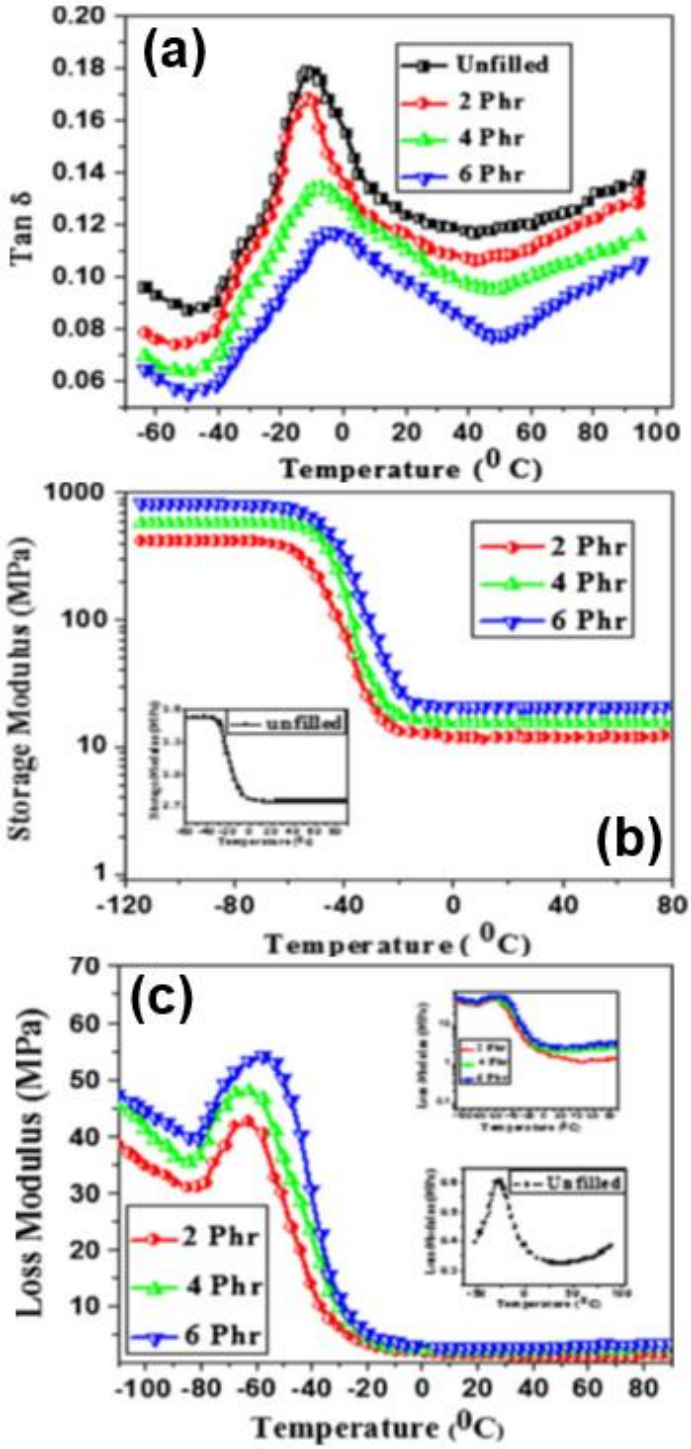

Figure 19: (a) Variation of loss tangent (Tan δ) with temperature as a function of MWCNT loading in silicone elastomer nanocomposites. **(b)**Variation of storage modulus with temperature as a function of MWCNT loading in silicone elastomer nanocomposites. **(c)** Variation of loss modulus with temperature as a function of MWCNT loading in silicone elastomer nanocomposites. Reproduced with permission from Springer [129].

Preprints (www.preprints.org) | NOT PEER-REVIEWED | Posted: 24 September 2018 doi:10.20944/preprints201809.0464.v1

Peer-reviewed version available at Nanomaterials 2018, 8, 945; doi:10.3390/nano8110945

Figure 20

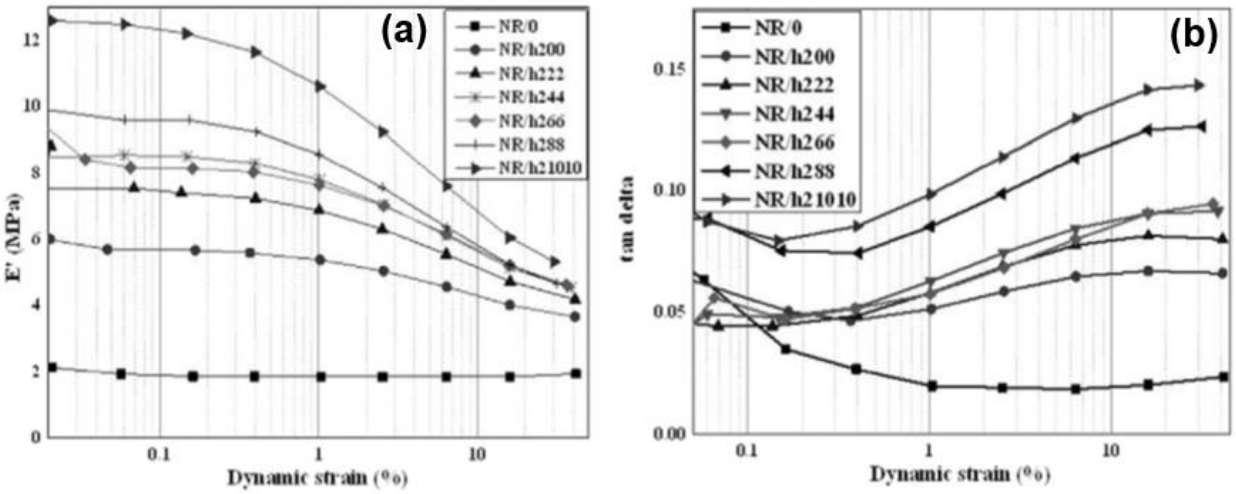

Figure 20: Strain dependence of E′ (a) and tan δ (b) for the NR/0 and NR/MWCNT/EOMt nanocomposites. Reproduced with permission from Elsevier [44].

Figure 21

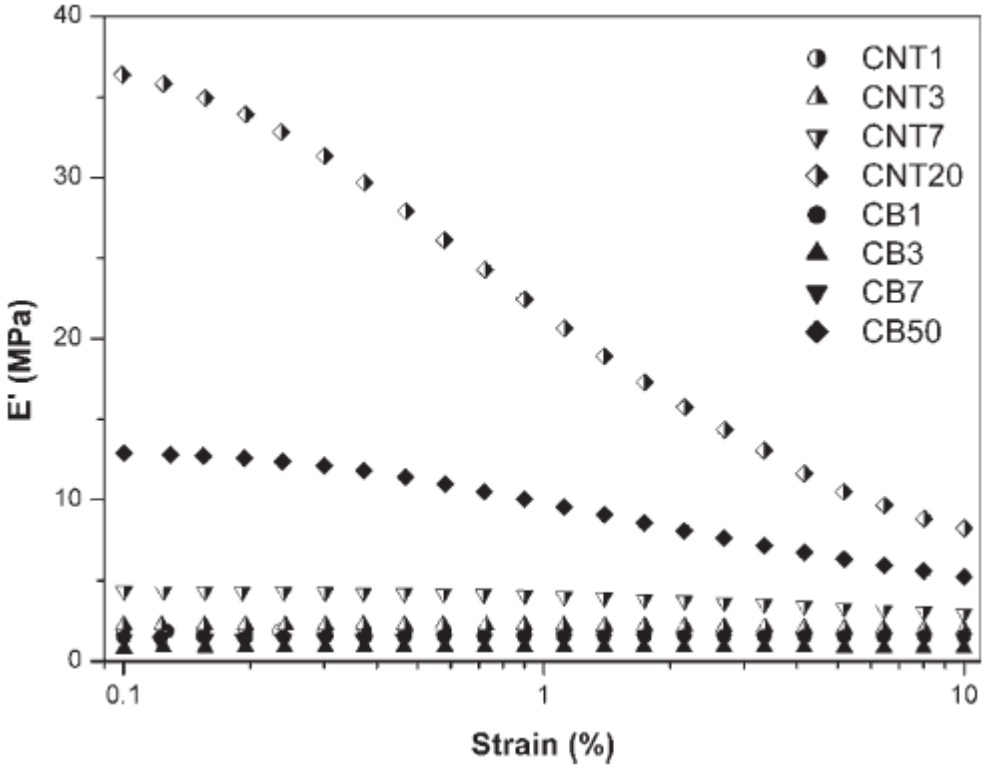

Figure 21: Storage modulus of NR/CNT and NR/CB compounds at different filler loadings as a function of dynamic strain amplitude. Reproduced with permission from Wiley [170].

Preprints (www.preprints.org) | NOT PEER-REVIEWED | Posted: 24 September 2018 doi:10.20944/preprints201809.0464.v1

Peer-reviewed version available at Nanomaterials 2018, 8, 945; doi:10.3390/nano8110945

Figure 22

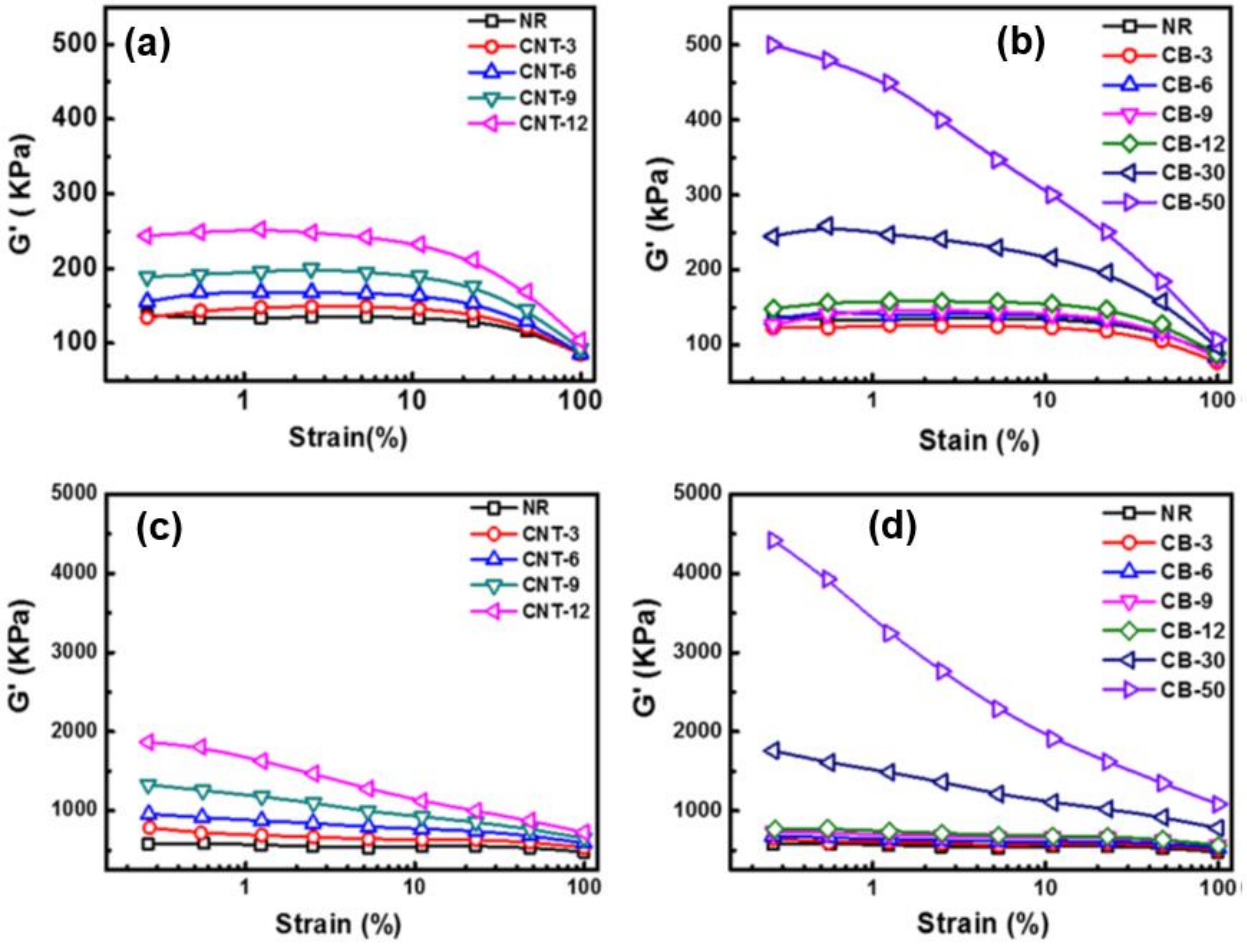

Figure 22: The strain dependence of G' of CNT/NR and CB/NR rubber compounds (a, b) and vulcanizates(c, d). Reproduced with permission from Springer [172].

Preprints (www.preprints.org) | NOT PEER-REVIEWED | Posted: 24 September 2018 doi:10.20944/preprints201809.0464.v1

Peer-reviewed version available at Nanomaterials 2018, 8, 945; doi:10.3390/nano8110945

Figure 23

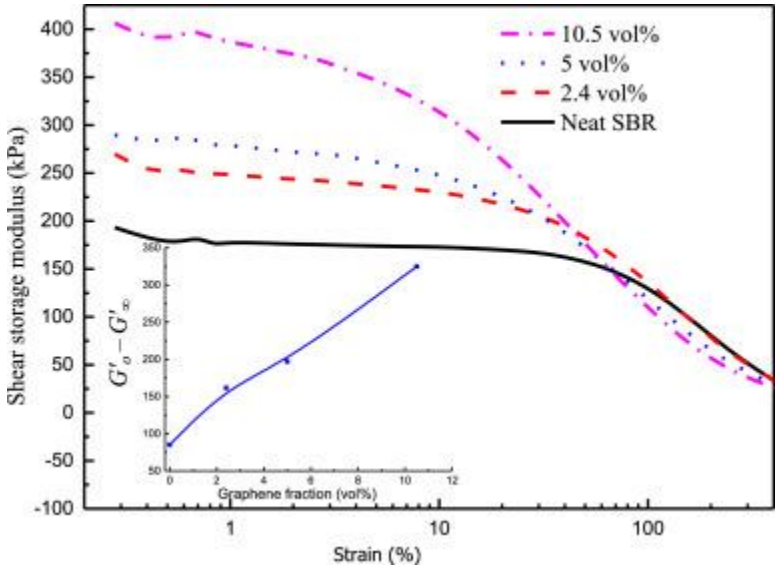

Figure 23: Payne effect of elastomer and its nanocomposites. Reproduced with permission from Elsevier [174].

Scheme 1

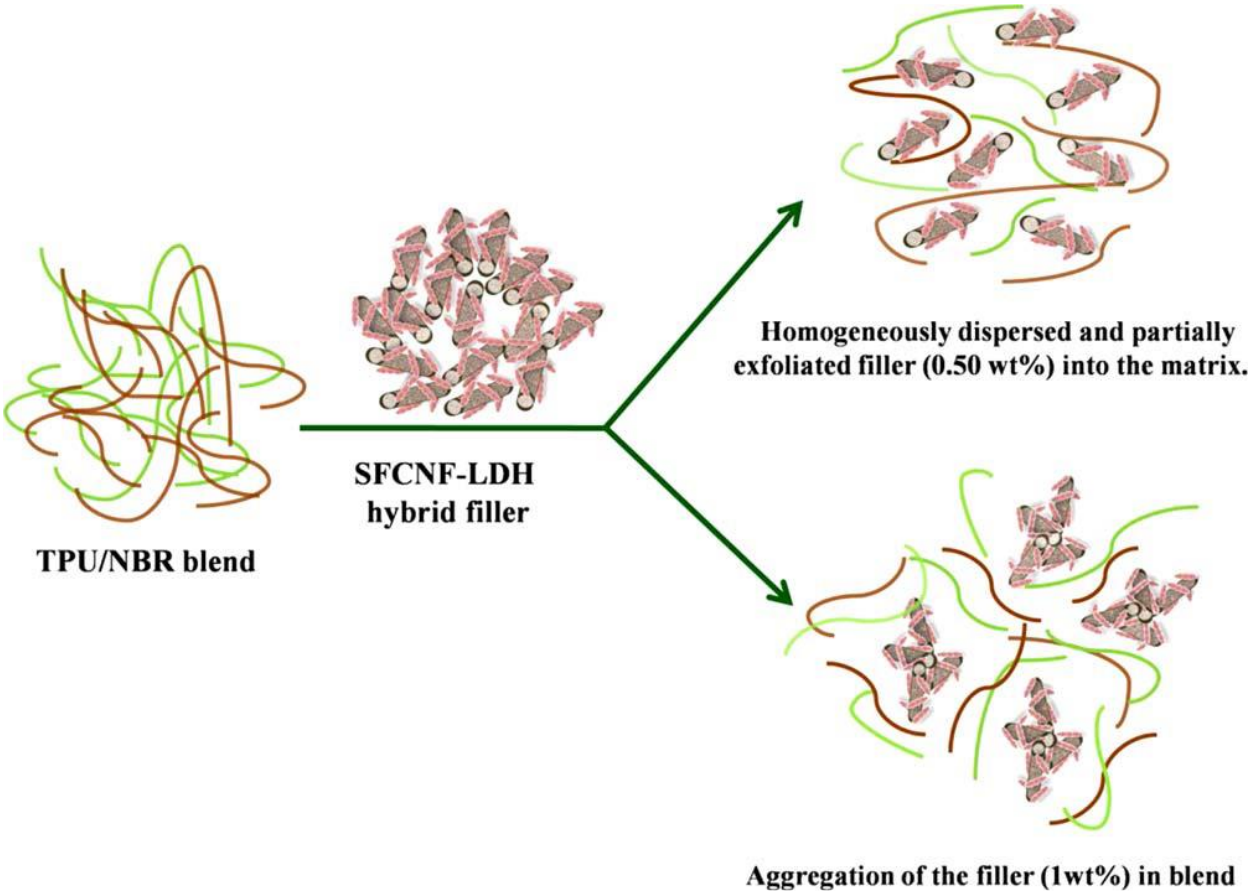

Scheme 1: TN blend without and with the filler to explain the mechanical properties. Reproduced with permission from Wiley [113].

Table 1: Types of carbonaceous nanofillers, preparative methods adopted and morphology of NR nanocomposites.

Rubber	Filler	Preparation Method	Morphology	Ref
NR	MWCNT	Solution method	SEM: Contact between Fe3O4 and MWNTs increases with the increasing filling fraction of particle.	[21]
NR	MWCNT	Orient the CNT by a flow field from mixture latex of NR, MWCNTs and other components.	TEM: Composite containing of MWCNTs (2 vol. % and 6 vol. %) exhibited alignment of in NR matrix.	[22]
NR	MWCNT	Master batch mixing method (open two roll mill)	SEM: CNT bundles totally exfoliated in CNT (1 phr) filled NR, uniform CNT (3 phr) dispersion and agglomeration of CNT (5 phr) bundles.	[23]
TPNR	MWCNT	Melt blending	SEM: Good dispersion of MWNTs in after TPNR/MWCNT being sonicated for 1 h. MWCNTs entangle for the sonication time > 1 h.	[24]
NR	CNT	Mixing method	TEM: Large agglomerates in microscopic level in CNT (5 phr) filled NR (without ethanol).	[25]
NR	Functionalized CNT	Melt blending	_____	[26]
L (Liquid) NR	MWCNT	melt blending	SEM: Good dispersion of MWNTs (3.5wt%) in PLA/LNR; Poor dispersion and agglomeration of MWCNTs (4%) in PLA/LNR.	[27]
NR	CNT	Solvent casting method	TEM: Good dispersion of CNT (3 phr) in SBR/BR (1:10 ethanol).	[28]

NR	MWCNT	Solvent casting method	TEM: 1 wt % of CNTs are homogenously distributed in the NR matrix	[29]
NR	SWNTs	Latex stage mixing method	_____	[30]
NR	MWCNT	Ultrasonically aided extrusion	AFM: Deagglomeration of MWCNT (3.5 phr) at an amplitude of 7.5 μm.	[31]
NR	CB-MWCNT	Latex compounding	SEM: MWNTs uniformly dispersed in NR matrix	[32]
NR	Silica/MWCNT	Two-roll mill	SEM: Good dispersion and better interaction between silica and the MWCNTs with the NR matrix at a 29/1 silica/MWCNT loading ratio	[34]
NR	CNT/CB	Mechanical compounding method	TEM: Homogeneous dispersion of CNT in CNTB (1 phr)/CB (22 phr), CNTB (3phr)/CB (16 phr) and CNTB (5 phr)/CB (10 phr) and formation of hybrid filler network.	[35]
NR	CNT, Graphene, CB-CNT	Melt blending	_____	[36]
TPNR	MWNTs-OMMT	Melt blending	TEM: Good dispersion of OMMT-MWNTs (3 h) in TPNR	[37]
TPNR	MWNTs-OMMT		TEM: Indicated strongly to interfacial adhesion between fillers and the matrix	[38]
NR	Graphene /CNT	Modified latex mixing method	SEM and TEM: Homogeneous dispersion of graphene (5 phr) and CNT (5 phr) in NR matrix.	[39]
ENR	CNT	Mixing in internal mixer, roll milling	SEM: ENR-CNT composites with APTES additions and 0.01 mL/(g of CNTs) at 5 phr CNT loading.	[40]

Preprints (www.preprints.org) | NOT PEER-REVIEWED | Posted: 24 September 2018 doi:10.20944/preprints201809.0464.v1

Peer-reviewed version available at Nanomaterials 2018, 8, 945; doi:10.3390/nano8110945

ENR	Bis(triethoxysilylpropyl) tetrasulfide (TESPT)functionalized MWCNT	Melt blending	SEM: ENR–CNT and the ENR–CNT–TESPT composites confirmed good dispersion of the CNTs in the ENR matrix.	[41]
ENR	CNT	Latex technology	TEM: Good dispersion of CVNT in ENR matrix.	[42]
NR	VGCF	Solvent casting	SEM: VGCFs (1,3 and 10 wt%) dispersed randomly and evenly in NR matrix.	[43]
NR	MWCNT/ organically modified montmorillonite	Internal mixing	TEM: Dispersion of the MWCNT throughout the NR matrix in NR/MWCNT (2 phr); Agglomerates of both MWCNT and EOMt and regions with fully exfoliated structure in NR/MWCNT (2phr)/Modified montmorillonite (20 phr)	[44]
NR latex	MWCNT treated with SDS	Combination of the latex compounding and self-assembly	MWCNT–PDDA prepared with the self-assembly technique was more intimate with the NR matrix	[45]
NR	CNT	Solution casting	SEM: CNTs well distributed into NR	[46]
NR	CNT	Solvent mixing assisted with a two-roll mill	SEM: Dispersion of the CNTs in rubber matrix.	[47]
NR	MWCNT, Graphene nanoplatelets	Roll milling	_____	[48]
NR	Reduced graphene oxide	Two roll mill	SEM: NR/GNR-2 nanocomposite well dispersed.	[49]

Preprints (www.preprints.org) | NOT PEER-REVIEWED | Posted: 24 September 2018 doi:10.20944/preprints201809.0464.v1

Peer-reviewed version available at Nanomaterials 2018, 8, 945; doi:10.3390/nano8110945

ENR	MWCNT	Mixing in an internal mixer,	TEM: More homogeneous dispersion and distribution of S-MWCNTs in the ENR matrix.	[50]
NR	MWCNT	Latex compounding	----------	[51]
NR	MWCNT	Solvent mixing method	TEM: Homogeneous distribution of MWNTs (3 phr) in NR matrix.	[52]
ENR	MWCNT	Roll mill	SEM: Distribution of MWNT (4 phr) are observed in ENR matrix.	[53]
NR	CB/MWCNT	Mixing in laboratory two roll mill	SEM: A good dispersion is seen corresponding to CB/MWCNT (29.5/0.5) loading.	[54]
NR/XSBR	CNT (0.1-0.4 phr)	Latex compounding	_____	[58]
TPPU	(MWCNTs)-magnetite (Fe3O4) hybrid	Internal mixer using melt blending method with ball-milling as a pre-mixed process.	_____	[60]
NR/SBR NR/XSBR	CNT	Latex compounding method	_____	[61]
NR	CNT	Solvent casting method	TEM: Phenol functionalization causes improvement in dispersion of CNT in NR matrix	[62]
NR	MWCNT	Solution blending	TEM: Good levels of dispersion with well-isolated nanotubes in NR/MWNTs (4 phr) composite.	[63]
NR	Carboxylated MWCNT	Mixing, sonicating and casting	AFM: No aggregates of MWCNT (2.8 wt%) observed in NR.	[169]

Preprints (www.preprints.org) | NOT PEER-REVIEWED | Posted: 24 September 2018 doi:10.20944/preprints201809.0464.v1

Peer-reviewed version available at Nanomaterials 2018, 8, 945; doi:10.3390/nano8110945

	dispersed with SDS			
NR	MWCNT	Internal mixer, roll mill	SEM: CNTs well-dispersed (unstretched state) in NR/MWCNT (7 phr).	[170]
NR	MWCNT	Ultrasonication assisted latex mixing and film casting method	TEM: MWCNTs wrapped around NR particles forming a segregated network.	[171]
NR	CNT	Mechanical blending	SEM: CNT (9 phr) are disperses well in NR matrix.	[172]
NR	Graphene	Direct mechanical mixing	SEM: Graphene (2 phr) well dispersed in NR.	[173]
NR	Modified NWCNT	Sonication, mixing roll milling	SEM: COOH-MWCNT and CIP have better compatibility among MRE samples. This leads to the formation of interconnected network in the matrix	[175]
NR	RGOT(Thermally reduced graphene oxide)	Mixing/two roll milling	TEM: NR vulcanizates filled with RGOT at 5 phr exhibited networks of aggregated or agglomerated filler networks with a decreased gap between the filler aggregates or agglomerates.	[177]
NR	Polyvinyl pyrrolidone modified graphene oxide PGO)	PGO aqueous dispersion with NR latex, followed by coagulation and vulcanization	SEM: The fracture surface of GO5 has more irregular tear paths suggesting the greater tear strength while PGO5 show more tears paths with irregular branches.	[178]
NR	Graphene oxide	Latex mixing/two-roll milling	TEM: Uniform dispersion of graphene oxide (1 phr) in NR/GO	[179]
NR	Graphene oxide nanosheets (GON)	Solution blending	SEM: GON (5 wt%) homogeneously dispersed in NR matrix.	[180]

Preprints (www.preprints.org) | NOT PEER-REVIEWED | Posted: 24 September 2018 doi:10.20944/preprints201809.0464.v1

Peer-reviewed version available at Nanomaterials 2018, 8, 945; doi:10.3390/nano8110945

NR	Graphene oxide	Latex mixing	_____	[181]
NR	Thermally reduced graphite oxide(TRGO)	Mixing method	TEM: TRGO prepared by the Brodie's method (TRGO-B) showed more homogeneous dispersion and distribution through the NR matrix.	[182]
NR	Thermally reduced graphite oxide (TRGO)	Latex method	TEM: Graphene sheets in TRGO dispersed in SDS are distributed throughout the NR.	[183]
NR/HDPE	Graphene oxide	Ultrasonically assisted latex mixing process	SEM: Delamination of the GO sheets in NR/HDPE is observed. Mainly GO sheets are dispersed in the NR phase.	[184]
Grafted NR (GMA)	Graphene Oxide	Mechanical mixing method.	SEM: GO (3 and 6 phr) dispersed uniformly in the NR-g-GMA.	[185]
NR	Functionalized graphene oxide grafted by maleic anhydride grafted liquid polybutadiene (MLPB-GO).	Co-coagulation process.	FESEM: GO sheets are dispersed as single layers in NR/MLPB-GO (2.12phr)	[186]
NR latex	Reduced graphene oxide (rGO)	Ultrasonically assisted latex mixing and the co-coagulation	HRTEM: rGO (0.9 phr) show presents a good dispersion and exfoliation in NR.	[187]
NR	ZnO nanoparticles doped graphene	Two roll mill	FESEM: Good dispersion of graphene in the matrix and strong adhesion between graphene and NR in in nanocomposite.	[188]

Table 2: Types of carbonaceous nanofillers, preparative methods adopted and morphology of SBR nanocomposites.

Rubber	Filler	Preparation	Morphology	Ref.
SBR (25% styrene Content)	Ionic liquid modified MWCNT	Two roll mixing mill.	TEM: A substantial dispersion of modified MWCNT with less agglomerates in SBR	[64]
Solution-SBR/BR	MWCNTT	Roll mill	TEM: Smaller magnification show no homogeneous distribution of the MWCNTs (5 phr)	[65]
SBR (23.5 wt% bound Styrene)	MWCNT	Solvent casting method	FE-SEM: MWCNT (0.66 wt%) are dispersed homogeneously in SBR.	[66]
SBR	MWCNT	Solvent casting	----------	[67]
SBR	MWCNT	Coagulation method followed by mastication in a twin-screw extruder	SEM: MWCNT (15 wt%) are well dispersed in the masterbatch.	[68]
SBR	MWCNT	Coagulation process followed by melt mixing	----------	[69]
SBR	Functionalized CNT	Solvent casting	----------	[71]
SBR and butadiene blend	Modified/unmodified MWCNT	Solvent casting	TEM: CNT form percolating networks at 5 phr loading.	[73]
SBR	Functionalized CNT	Solvent casting		[74]

Preprints (www.preprints.org) | NOT PEER-REVIEWED | Posted: 24 September 2018 doi:10.20944/preprints201809.0464.v1

Peer-reviewed version available at Nanomaterials 2018, 8, 945; doi:10.3390/nano8110945

SBR (25 % styrene icntent)	MWCNT	Two roll mixing method	TEM: Good dispersion of MWCNT in SBR matrix	[75]
SBR	MWCNT	Spray drying/ mechanical mixing process.	SEM: Dispersion of MWCNTs (50 phr) in the rubber matrix remarkably improved.	[76]
SBR (23% styrene and 77% butadiene)	CB,CNT, Carbon Graphene, Graphite	In banbury mixer	----------	[77]
SBR Latex (20 wt% styrene, 80 wt% butadiene)	Graphene (MLG350), CRGO, and TRGO	Latex blending techniques	TEM: SBR nanocomposites containing 25 phr MLG350, CRGO, and TRGO homogeneously dispersed in the SBR.	[79]
SBR (styrene content of23.5%)	CNF	Mixing followed by two-roll milling	TEM: Fiber diameter (unmodified) of 78 nm swells to 97 nm in SF6 (unmodified SBR) and 144 nm in TSF6 (modified SBR)	[81]
SBR(23.5 wt % styrene SBR polymer)	CNT	Mechanical mixing	TEM: Fairly good dispersion.	[82]
SBR Latex (21 wt.% of SBR content)	Graphene	Modified latex compounding method	TEM: Exfoliated graphene (7 phr) is homogeneously dispersed in SBR.	[83]
SBR latex (21wt% of SBR content)	Graphene	Mechanical stirring	----------	[84]

Preprints (www.preprints.org) | NOT PEER-REVIEWED | Posted: 24 September 2018 doi:10.20944/preprints201809.0464.v1

Peer-reviewed version available at Nanomaterials 2018, 8, 945; doi:10.3390/nano8110945

XSBR (23% styrene content)	Modified expanded graphite	Solution mixing and melt blending	HR-TEM: MEG nanosheets uniformly dispersed in the XSBR matrix.	[86]
SBR	CB-Graphene	Two roll mixing	Homogeneous dispersion of graphene sheets on the application of hybrid CB-RG filler in SBR matrix.	[87]
SBR	MWCNT/Thermally reduced graphene (TrG)	Two roll mill	SEM of tensile fracture surfaces: Excellent dispersion of CNTs (1 phr)/ TrG (0.25 phr) in SBR matrix	[88]
SBR latex	Tubular clay and (HNT) functionalized graphene(TAG)	Dispersion of HNT and HNT-TAG hybrid filler added into SBR latex.	TEM: HNTs (40 phr) individually dispersed and as aggregates in SBR TAG (4 phr) uniformly dispersed in SBR. Dispersion of HNTs is greatly improved in the presence of TAG (HNT-TAG:44phr) in SBR.	[89]
SBR	Fe-MMT/MWCNT	Mixing method	TEM: MWCNT/MMT (5 phr) filled SBR composite show CTAB-MWCNT networks are disrupted by the well dispersed FE-MMT particles.	[90]
SBR	CNT	spray drying of the suspension of CNTs in SBR latex.	SEM: SBR/CNTs (20 and 50 phr) powder is uniformly spherical (Diameters < 10 μm). On adding more CNTs, powders are more spherical like and the isolation among the spherules is improved as well.	[163]

SBR	Graphene platelets (GNPs)	Solution mixing, melt compounding	TEM: Better dispersion and exfoliation of GNP (2.4 vol %) in the matrix in solution-prepared nanocomposite the show, while GNPs exist as aggregates of stacked in the melt-prepared samples.	[174]
SBR	Ionic liquid functionalized graphene oxide(GO-IL)	Latex hetro-coagulation method	SEM: GO-IL can be well-dispersed in the SBR matrix	[191]
SBR latex	3D segregated graphene	Mixing	TEM: 3D segregated graphene networks throughout SBR matrix.	[192]
SBR	MWCNT/Hectorite	Solution blending	FESEM (fracture surface): Homogenous dispersion in 0.70 wt% MWCNT/ Hectorite.	[207]

Preprints (www.preprints.org) | NOT PEER-REVIEWED | Posted: 24 September 2018 doi:10.20944/preprints201809.0464.v1

Peer-reviewed version available at Nanomaterials 2018, 8, 945; doi:10.3390/nano8110945

Table 3: Types of carbonaceous nano fillers, preparative methods adopted and morphology of NR nanocomposites.

Rubber	Filler	Method of Preparation	Morphology	Ref.
NBR/PA6	Functionalized SWCNT	Melt mixing process in internal mixer	TEM: Homogenous dispersion of SWNT in the PA6 phase	[91]
NBR/PVC blends	SWCNT	Brabender internal mixer	TEM: Fine dispersion of functionalized SWNTs (1.5 phr) is observed NBR/PVC.	[92]
NBR	CNT	Lab mixing	----------	[93]
HNBR	CNT	Roll and mixing solvent methods	TEM: The modified CNTs disperse very well in HNBR when the ultrasonic pre-dispersing technique is utilized to prepare composites.	[94]
NBR	MWCNT	Two roll mill	TEM: Dry mixing process is a quite effective to disperse and distribute CNTs in NBR.	[95]
NBR	MWCNT	Two roll mill	TEM: MWCNT (6 phr)/NBR vulcanizates show enhanced dispersion of filler by increased mixing time.	[96]
NBR	MWCNT, CB, conductive CB.	Two roll mill	----------	[97]
HNBR	MWCNT	Two roll mill method	SEM: Fine dispersion of MWCNT (20 phr) in NBR.	[99]
NBR and HNBR	MWCNT	Melt compounding	TEM/SEM: Exfoliation and intercalation of nanotubes in (H)NBR matrix.	[100]

Preprints (www.preprints.org) | NOT PEER-REVIEWED | Posted: 24 September 2018 doi:10.20944/preprints201809.0464.v1

Peer-reviewed version available at Nanomaterials 2018, 8, 945; doi:10.3390/nano8110945

NBR	Expanded graphite	Mechanical blending (microcomposites) and latex compounding technique	SEM: graphite disperses more uniformly with smaller lamellar agglomerates in composites.	[101]
NB	Expanded graphite	Melt mixing	TEM: Nanoscale dispersion of graphite sheets within NBR matrix.	[102]
SBR/XNBR	Graphene oxide	Two roll mill	SEM: Better dispersion of GO can be found for SBR/XNBR/GO1.5 (1.5 refers denote KMnO4 loading in g)	
Carboxylic NBR	MWCNT	Solution mixing method	HRTEM: Wrinkled and folded sheets of GNS–HAD in 1 phr and 1.5 phr GNS–HDA filled XNBR composites	[104]
NBR	Graphene	Melt mixing	TEM: Composite with 10 Vol.% graphenes (xg-M-5) in NBR with 20 Vol.% softener (DOP) showed exfoliation/breakdown of the graphene nanoplatelets.	[106]
NBR	Silica/MWCNT	Melt mixing	SEM: Good dispersion of silica and CNT fillers in NBR.	[107]
TPPU-XNBR	MWCNT	Laboratory roll mill	TEM: MWCNT (3 wt%) are preferentially distributed in XNBR phase. However, 5 wt% of MWCNTs are present in TPPU phase.	[110]
TPU-NBR	MWCNT/ZnAl-LDH, CNF/ ZnAl-LDH	Solution intercalation	HRTEM: 0.5 wt% SFCNT-LDH and SFCNF-LDH fillers in the blend matrix consist of uniformly distributed interconnected network.	[112]

Preprints (www.preprints.org) | NOT PEER-REVIEWED | Posted: 24 September 2018 doi:10.20944/preprints201809.0464.v1

Peer-reviewed version available at *Nanomaterials* **2018**, *8*, 945; doi:10.3390/nano8110945

TPU-NBR	CNF/MgAl-LDH	Solution intercalation	HRTEM: Interconnected hybrid network spread throughout in TPU/NBR/SFCNF-LDH (0.50 wt%).	[113]
TPU-NBR	MWCNT-LDH	Solution intercalation	TEM: Fine dispersion of 0.50 wt% SFCNF-LDH hybrid filler is observed in TPU/NBR matrix.	[114]
XNBR (75 phr)/SBR(25 phr)	Graphene oxide (GO)	Coagulation/roll mill	TEM: Uniform dispersion of XNBR/SBR/GO blends (GO-0.1 phr, GO-0.3 phr).	[193]
SBR/XNBR	GO	Aqueous-phase mixing (GO/SBR) and a small loading of XNBR latex, followed by co-coagulation	AFM: Full exfoliation of GO nanosheets in GO-15 sample.	[194]
NBR	Reduced graphene oxide (rGO)	Solution mixing method	TEM: rGO0.1–1 phr) appears to be evenly dispersed in the NBR matrix.	[195]

Table 4: Types of carbonaceous nanofillers, preparative methods adopted and morphology of silicone rubber nanocomposites

Rubber	Filler (S)	Preparative method	Morphology	Ref.
SR	CB,CNT	Solution mixing method	AFM: SR vulcanizates containing 3 phr of CNTs and CB show the heterogeneity of the filler and rubber components.	[116]
RTV	MWCNT	Solvent method	SEM: MWCNTs (not higher than 5 phr) is well dispersed in the silicone matrix	[117]
HTVSR	Chitosan salt pretreated MWCNTs	Mixing method	SEM: Uniform distribution of MWCNT (4-11 wt%) in HTVSR.	[118]
SR	CB (2.5 phr)/CNT(1.0 phr)	Ball mixing	TEM: god dispersion	[119]
SR	RGO with different reduction degree	Ball milling	SEM: Graphene sheets were well dispersed in the SR matrix	[120]
SR	MWCNT (0.3 g/50 ml solvent)	Solvent method	SEM: Rough surface texture on nanocomposite with large surface area and nanosized textures.	[121]
SR	MWCNT buckypaper	Two-step process	FESEM (fracture film): PDMS matrix fully impregnated into buckypaper network.	[122]
PDMS	CNT	Mixing method	SEM (Fracture surface) Good bonding between MWCNT (1,2, and 4 wt%) and PDMS apparent.	[123]
SR	F-Graphene	Solvent mixing method	SEM: Uniform dispersion of CNTs (0.3 wt%) in polymer matrix.	[124]
HTVSR	CNTs pretreated by chitosan salt	Mechanical/solvent mixing	CNT (4 to 8 wt%) uniformly distributed.	[118]

Preprints (www.preprints.org) | NOT PEER-REVIEWED | Posted: 24 September 2018 doi:10.20944/preprints201809.0464.v1

Peer-reviewed version available at Nanomaterials 2018, 8, 945; doi:10.3390/nano8110945

PDMS	MWCNT	Twin screw extruder mixer	SEM: Good dispersibility of the tubes in the silicone matrix	[127]
PDMS	MWCNT	By ultrasonication of mixture PDMS and silicone-g-MWCNTs in toluene.	HRTEM: Single strands of MWCNTs (0.1 wt%) disperse in silicone grafted MWCNTs	[128]
SR	MWCNT	Two roll mixing mill	SEM/: Excellent distribution of MWCNT (2,4 and 6 phr)in silicone elastomer:	[129]
SR	MWCNT	Mixing method	SEM: Good dispersion of MWCNT (1 and 3.5 wt%) reinforced SR.	[130]
RTV-SR	Graphitic nanofiller (GR):10 phr	Mixing method	AFM: completely delaminated single graphitic sheets in rubber matrix.	[131]
RTV-SR	Functionalized graphene oxide (FGO)	Solution casting	-------	[132]
SR	F-Graphene	Mixing method	-------	[133]
RTV-SR	Graphene (1.0 wt %)	Solvent method	SEM (Fracture surface): Graphene nanosheets randomly disperse/protrude from the fracture surface in the PDMS.	[134]
SR	Graphene nanoribbon	Solution mixing	SEM: GNR (0.4,1.0, 2.0) distributed randomly without obvious aggregations in SR matrix	[135]
SR	Graphene nanoplatelets	liquid mixing method	FESEM: agglomeration of GNPs in the composite	[136]
SR	Triton-GNP, APTES-GNP and VTMS GNPs	Solution blending	ESM (Tensile fractured surface): VTMS-GNP and Triton-GNP seem to be well embedded in silicone matrix.	[137]

Preprints (www.preprints.org) | NOT PEER-REVIEWED | Posted: 24 September 2018 doi:10.20944/preprints201809.0464.v1

Peer-reviewed version available at Nanomaterials 2018, 8, 945; doi:10.3390/nano8110945

PDMS	CNF	In-situ and ex-situ	TEM: Ex situ prepared nanocomposites feature prominent agglomeration of nanofibers in the form of lumps.	[138]
SR	MWCNT	Solvent casting	TEM/SEM: Graphene was well dispersed in the silicone rubber matrix.	[139]
VMQ	MWCNT/Graphene	Solution method	TEM: VMQ nanocomposite filled with 0.375 and 0.75 wt% MWCNT–G show better dispersion and homogeneity in VMQ matrix	[140]
SR	MWCNT-MMT	Solution blending	TEM: MWCNT/MMT (2 wt %) is well-dispersed and fully exfoliated in SR.	[141]
SR	MWCNT-Mg-Al-LDH	Solution blending	TEM: MWCNT (1 wt%) homogeneously distributed in SR.	[142]
PDMS	MWCNT/ Al_2O_3	Ultrasonic sonication followed by casting	MWCNT-Al_2O_3 was well dispersed in PDMS	[143]
Liquid SR	Graphene oxide	Solution method	TEM/SEM: Random and uniform distribution of GO sheets.	[198]
Liquid silicone rubber (LSR)	Functionalized graphene oxide	Ultrasonic sonication followed by casting	SEM: TEVS-GO exhibited excellent compatibility with the LSR matrix, and formation of strong interfacial interactions between TEVS-GO and the LSR polymeric chain.	[199]
PDMS	Graphite oxide (GO) modified using 3-aminopropyltriethoxysilane (APTES)	Solvent method	----------	[200]

Table 5: Mechanical properties of NR gums and CNT composites of melt and latex–based samples (Modified). Reproduced with permission from Wiley [26].

Sample	**Tensile strength (MPa)**	**Elongation at break (%)**	**100% modulus (MPa)**
NR	14.9 ±0.65	716±52.19	0.9±0.06
NR-R-CNT-5 (CNT content: 5 phr).	12.6±1.48	454±21.45	2.1±0.08
NR-R-CNT-5+S (Silane content was adjusted to 0.1 ml)	16.9±0.78	554±20.27	2.3±0.18
NR-F-CNT-5+S (Functionalized CNT: 5 phr, Silane content: 0.1 ml)	13.0±0.35	476±4.85	2.1±0.11
N (NR latex)	16.3±1.48	746±42.09	0.9±0.05
L-R-CNT-5 (Raw CNT content: 5 phr).	13.9±0.06	525±16.63	1.9±0.04
L-R-CNT-5+S (Raw CNT content: 5 phr; Silane content: 0.1 ml)	18.3±0.72	595±17.72	2.3±0.1

Preprints (www.preprints.org) | NOT PEER-REVIEWED | Posted: 24 September 2018 doi:10.20944/preprints201809.0464.v1

Peer-reviewed version available at *Nanomaterials* **2018**, *8*, 945; doi:10.3390/nano8110945

Table 6: Mechanical properties of CNTB (carbon nanotube bundles) reinforced natural rubber composites (Modified). Reproduced with permission from Wiley [35].

Samples*	Stress at 100% (MPa)	Stress at 300% (MPa)	Tensile strength (MPa)	Elongation at break (%)	Tear strength (kN/m)	Shore A hardness
CNTB-0	2.2	8.7	24.9	659	91.8	71
CNTB-1	2.5	9.9	25.9	640	99.8	73
CNTB-3	2.7	11.2	26.5	620	103.0	74
CNTB-5	3.6	13.7	28.2	596	110.8	75

*Sample CNTB-0, CNTB-1, CNTB-3 and CNTB-5 refer to 0, 1, 3, and 5 phr of CNTB filled NR respectively).

Table 7: Mechanical Properties and Volume Resistivity of SBR/CB-RG(CB) Composites (Modified). Reproduced with permission from Wiley [87].

Rubber	CB-RG(CB) contents (CB/GO)	Tensile strength (MPa)	Elongation at break (%)	M200 (MPa)
SBR (100 phr)	10 phr/0 phr	3.5±0.21	260±10	2.3±0.1
	13 phr/0 phr	3.8±0.4	270±20	2.4±0.2
	10 phr/1 phr	4.9±0.3	300±20	2.8±0.2
	10 phr/2 phr	4.8±0.3	280±20	3.1±0.2
	10 phr/2 phr	4.8±0.3	280±20	3.1±0.2

Table 8: Mechanical properties of NBR vulcanizates. Reproduced with permission from Hindawi Publishing Corporation [97].

Properties	Loading (phr)	MWCNT	CCB	CB	PS
Tensile strength (MPa)	0	2.9±0.37	2.9±0.4	2.9±0.4	2.9±0.4
	5	8.6±0.1	4.3±0.1	4.1±0.2	3.6±0.4
	10	12.9±0.4	9.1±0.2	5.3±0.5	3.8±0.2
	15	17.7±0.5	14.6±0.6	8.5±1.5	5.3±0.3
Elongation at break (%)	0	182±14	182±14	182±14	182±14
	5	176±2	196±3	202±10	210±17
	10	178±3	244±2	217±14	220±1
	15	171±6	277±6	231±14	218±10
Modulus at 100% (MPa)	0	1.73±0.04	1.73±0.04	1.73±0.04	1.73±0.04
	5	5.04±0.09	1.93±0.02	1.82±0.10	1.79±0.06
	10	7.49±0.56	2.47±0.07	1.79±0.05	1.75±0.06
	15	11.28±0.35	3.30±0.27	2.15±0.10	2.30±0.12
Hardness (Shore A)	0	53±0.3	53.±0.3	53.±0.3	53.±0.3
	5	61.8±0.3	56.0±0.0	55.3±0.3	54.8±0.8
	10	69.0±0.5	61.7±0.6	56.5±0.9	56.8±1.0
	15	69.3±0.8	65.5±0.5	58.2±0.3	59.9±0.8
Heat build-up (∘C)	0	7.5±0.7	7.5±0.7	7.5±0.7	7.5±0.7
	5	11.5±0.7	9.0±0.0	8.0±0.0	8.0±0.0
	10	18.5±0.7	14.0±0.0	9.0±0.0	9.0±0.0
	15	29.0±1.4	21.0±0.0	10.5±0.7	10.0±0.0
Abrasion loss (mm^3)	250.7±10	250.7±10.	250.7±10.	250.7±10.	250.7±10.
	5	82.0±12.7	91.4±10.0	188.2±4.7	171.2±25.0
	10	54.2±3.7	54.9±3.1	132.6±12.6	155.7±8.8
	15	48.0±2.6	53.3±1.3	90.8±6.3	127.7±9.9

Table 9: Tensile properties of the HTVSR and the HTVSR/CNT nanocomposites. Reproduced with permission from Elsevier [118].

Sample name	Tensile stress (MPa)	Tensile strain (%)	Modulus (MP)
Pure HTVSR hybrid	0.28	86.7	0.30
HTVSR/CNTs 4.0 wt%	0.61	144.8	0.42
HTVSR/CNTs 6.0 wt%	0.82	243.2	0.55
HTVSR/CNTs 8.0 wt%	1.59	440.	1 0.55
HTVSR/CNTs 11.0 wt%	1.67	241.0	0.95

Table 10: Summary of mechanical properties of VMQ and its nanocomposites. Reproduced with permission from Wiley [140].

Sample	TS (MPa)	EB (%)	50% Modulus (MPa)	100% Modulus (MPa)
Neat VMQ	0.32±0.02	192±8	0.15	0.22
MWCNT (0.375 wt%)/VMQ	0.42±0.03	1137	0.23	0.39
MWCNT (0.75 wt%)/VMQ	0.44±0.03	104±6	0.26	0.40
G (0.375 wt%)/VMQ	0.33±0.01	88±7	0.25	—
G (0.75 wt%)/VMQ	0.37±0.01	90±5	0.27	—
MWCNT–G (0.375wt%)/VMQ	0.48±0.02	144±2	0.26	0.40
MWCNT – G (0.5 wt%)/VMQ	0.53±0.01	158±3	0.28	0.43
MWCNT – G (0.75 wt%)/VMQ	0.67±0.03	194±4	0.28	0.43
MWCNT – G (1.0 wt%)/VMQ	0.61±0.02	165±5	0.29	0.44
MWCNT – G (1.5 wt%)/VMQ	0.50±0.01	123±3	0.30	0.45